UC San Diego

UC San Diego Electronic Theses and Dissertations

Title

Interrogating in vivo Mechanisms of Kupffer Cell Transcriptional Regulation Using Natural Genetic Variation

Permalink

https://escholarship.org/uc/item/0kb7860f

Author

Bennett, Hunter

Publication Date

2022

Peer reviewed|Thesis/dissertation

eScholarship.org Powered by the California Digital Library
University of California

UNIVERSITY OF CALIFORNIA SAN DIEGO

Interrogating *in vivo* Mechanisms of Kupffer Cell Transcriptional Regulation Using Natural Genetic Variation

A dissertation submitted in partial satisfaction of the
requirements for the degree Doctor of Philosophy

in

Biomedical Sciences

by

Hunter Bennett

Committee in Charge:

Professor Christopher K. Glass, Chair
Professor Ronald Evans
Professor Mohit Jain
Professor Bernd Schnabl
Professor Amir Zarrinpar

2021

Copyright
Hunter Bennett, 2021
All rights reserved.

The dissertation of Hunter Bennett is approved, and it is acceptable in quality and form for publication on microfilm and electronically.

University of California San Diego

2021

DEDICATION

This work is dedicated to my parents Tammy and Brad, who taught me how to follow my curiosity and the importance of finding meaning in work, and to my grandmother Huguette, who I miss deeply.

EPIGRAPH

"Virtue is a capacity. It can always be lost or gained", Atul Gawande

TABLE OF CONTENTS

LIST OF ABBREVIATIONS

KC	Kupffer cell
BM-MΦ	Bone marrow macrophage
BM-KC	Bone marrow derived KC
SAMac	Scar associated macrophage
ER	Endoplasmic reticulum
LXR	Liver X receptor
LSEC	Liver sinusoidal endothelial cells.
PPAR	Peroxisome proliferator-activated receptor
SREBP	Sterol responsive element binding protein
IRF	Interferon response factor
TLR	Toll-like receptor
H3K27Ac	Histone Lysine 27 Acetylation
H3K27me3	Histone Lysine 27 Trimethylation
TF	Transcription factor.
LDTF	Lineage determining transcription factor.
SDTF	Signal dependent transcription factor.
ATAC-seq	Assay for transposase accessible chromatin followed by next generation sequencing.
ChIP-seq	Chromatin immunoprecipitation followed by next generation sequencing
TNF	Tumor necrosis factor
BMP	Bone morphogenic protein
LPS	Lipopolysaccharide
DT	Diptheria toxin
DTR	Diptheria toxin receptor
NAFLD	Non-alcoholic fatty liver disease
NASH	Non-alcoholic steatohepatitis

LIST OF FIGURES

ACKNOWLEDGEMENTS

I would like to acknowledge Professor Christopher K. Glass for his mentorship over the last four years, for his open door, both literal and metaphorical, that allowed for engaging scientific discussions, and for empowering me to work creatively and independently at this stage of my career.

I would also like thank my undergraduate mentor Dr. Kim Woodrow, who sparked my early interest in biological sciences and encouraged me to pursue an academic career. I am grateful for the team members at the National Cancer Institute Division of Cancer Epidemiology and Genetics, including Neil Caporaso, Lynn Goldin, Rose Yang, Lisa Mirabello, and Paula Hyland, who gave me the freedom to begin work in genomics as a post-baccalaureate researcher.

A special thank you goes to the many members of the Glass Laboratory for their expertise and support throughout the last four years. I'd like to thank Ty Troutman, whose mentorship has shaped me into the scientist I am today and whose friendship made waking up at 3:30am to isolate Kupffer cells bearable. I wish you the best of luck in starting your new laboratory. I'd also like to thank Martina Pasillas for her tireless support of my research and willingness to sacrifice her evenings to get one more sample off of the sorter. Bethany Fixsen, my MSTP colleague in the lab, has been a trusted friend whose thoughtful advice has been invaluable. Thanks also goes to Cassi Bruni Isidoro Cobo, Thomas Prohaska, Christian Nickl, Claudia Han, Marten Hoeksema, Zeyang Shen, Hannah Mummey, Verena Link and Jenhan Tao for their important contributions to my work. A special thanks to Nathaneal Spann, Addison Lana, and Johannes Schlahetzki for their scientific contributions both in and out of the lineup at Torrey Pines.

I would also like to acknowledge the outstanding mentors in the San Diego community who have supported my training as a physician scientist. I'd like to thank Professor Joseph Witztum and Professor Aaron Carlin for their career mentorship and insight at the many decision points that arise over the course of M.D./Ph.D. training; they are exemplary physician scientists.

Finally, I would like to recognize my friends and family for their support throughout my training. Thank you to my mother, Tammy, and father, Brad, for their unconditional love and support. Thank you to my brother, North, for your friendship and for imbuing my life with adventure and literature. Thank you to my partner, Emily, for bringing joy to each and every day of my life.

My graduate research was made possible in part by funding from the following grants: T32DK007202 and F30DK124980.

Chapter 1, except for material describing the effects of natural genetic variation, is a reprint of the material as it appears in: Bennett H, Troutman TD, Sakai M, Glass CK. Epigenetic Regulation of Kupffer Cell Function in Health and Disease. Front Immunol 11, 609618 (2021). The dissertation author was one of the primary investigators and authors of this paper.

Chapter 2, in full, is a reprint of material being prepared for submission as: Bennett H, Troutman TD, Seidman JS, Nickl C, Mummey H, Shen Z, Spann NJ, Link VM, Guzman C, Prohaska T, Zhou E, Pasillas M, Bruni CB, Vu B, Hosseini M, Glass CK. Predicting Transcriptional Mechanisms in Kupffer Cells Using Natural Genetic Variation. The dissertation author was one of the primary investigators and authors of this paper.

VITA

Education

2021 Ph.D., Biomedical Sciences	University of California San Diego
2014 B.S., Bioengineering	University of Washington

Publications

Bennett H, Troutman TD, Sakai M, Glass CK. Epigenetic Regulation of Kupffer Cell Function in Health and Disease. *Front Immunol* 11, 609618 (2021). doi:10.3389/fimmu.2020.609618.

Troutman TD, Bennett H, Sakai M, Seidman JS, Heinz S, Glass CK. Purification of mouse hepatic non-parenchymal cells or nuclei for use in ChIP-seq and other next-generation sequencing approaches. *Star Protocols* 2, 100363 (2021). doi:10.1016/j.xpro.2021.100363.

Han, CZ, Li RZ, Hansen E, Bennett H, poirion O, Buchanan J, Challacombe JF, Fixsen BR, Trescott S, Schlachetzki JCM, Preissl S, Wang A, O'Connor C, Warden AS, Shriram S, Kim R, Nguyen CT, Schafer D, Ramirez G, Anavim SA, Johnson A, Sajti E, Gupta M, Levy ML, Ben-Haim S, Gonda DD, Laurent L, Glass CK, Coufal NG. Gene regulatory networks underlying human microglia maturation. *bioRxiv.* (2021). doi:10.1101/2021.06.02.446636.

Seidman, JS, Troutman TD, Sakai M, Gola A, Spann NJ, Bennett H, Bruni CM, Ouyang Z, Li RZ, Sun X, Vu BT, Pasillas MP, Ego KM, Gosselin D, Link VM, Chong LW, Evans RM, Thompson BM, McDonald JG, Hosseini M, Witztum JL, Germain RN, Glass CK. Niche-Specific Reprogramming of Epigenetic Landscapes Drives Myeloid Cell Diversity in Nonalcoholic Steatohepatitis. *Immunity* 52, 1056-1074. (2020). doi:10.1016/j.immuni.2020.04.001.

Sakai M, Troutman TD, Seidman JS, Ouyang Z, Spann NJ, Abe Y, Ego KM, Bruni CM, Deng Z, Schlachetzki JCM, Nott A, Bennett H, Chang J, Vu BT, Pasillas MP, Link VM, Texari L, Heinz S, Thompson BM, McDonald JG, Geissman F, Glass CK. Liver-Derived Signals Sequentially Reprogram Myeloid Enhancers to Initiate and Maintain Kupffer Cell Identity. *Immunity* 51, 655-670. (2019). doi:10.1016/j.immuni.2019.09.002

Goldstein AM, Xiao Y, Sampson J, Zhu B, Rotunno M, Bennett H, Wen Y, Jones K, Vogt A, Burdette L, Luo W, Zhu B, Yeager M, Hicks B, Han J, De Vivo I, Koutros S, Andreotti G, Beane-Freeman L, Purdue M, Freedman ND, Chanock SJ, Tucker MA, Yang X. Rare germline variants in known melanoma susceptibility genes in familial melanoma. *Human Molecular Genetics* 26, 4486-4895. (2017). doi:10.1093/hmg/ddx368

Yang X, Killian J, Hammond S, Burke L, Bennett H, Wang Y, Davis S, Strong L, Neglia J, Stovall M, Weathers R, Robinson, L, Mabuchi K, Inskip P and Meltzer P. Characterization of Genomic Alterations in Radiation-Associated Breast Cancer among Childhood Cancer Survivors, Using Comparative Genomic Hybridization (CGH) Arrays. *PLoS ONE* 10, e0116078. (2015). doi:10.1371/journal.pone.0116078

Yang XR, Rotunno M, Xiao Y, Ingvar C, Helgadottir H, Pastorino L, van Doorn R, Bennett H, Graham C, Sampson J, Malasky M, Vogt A, Zhu B, Bianchi-Scarra G, Bruno W, Queirolo P, Fornarini G, Hansson J, Tuominen R, Genoa Pancreatic Cancer Study Group, Burdett L, Hicks B, Hutchinson A, Jones K, Yeager M, Chanock SJ, Landi MT, Hoiom V, Olsson H, Gruis N, Ghiorzo P, Tucker M, Goldstein AM. Multiple rare variants in high risk pancreatic cancer related genes may increase risk for pancreatic cancer in a subset of patients with and without CDKN1A mutations. *Human Genetics* 135, 1241-1249. (2016). doi: 10.1007/s00439-016-1715-1.

Shi J, Hua X, Zhu B, Ravichandran S, Wang M, Nguyen C, Brodie S, Palleschi A, Alloisio M, Pariscenti G, Jones K, Zhou W, Bouk AJ, Boland J, Hicks B, Risch A, Bennett H, Luke B, Song L, Duan J, Liu P, Kohno T, Chen Q, Meerzaman D, Marconett C, Laird-Offringa I, Mills I, Gail M, Pesatory AC, Consonni D, Bertazzi PA, Chanock S, Landi MT. Somatic Genomics and Clinical Features of Lung Adenocarcinoma: A Retrospective Study. *PLoS Medicine* 13, e1002162. (2016). doi:10.1371/journal.pmed.1002162.

Ramanathan R, Park J, Hughes S, Lykins W, Bennett H, Hladik F and Woodrow K. Effect of Mucosal Cytokine Administration on Selective Expansion of Vaginal Dendritic Cells to Support Nanoparticle Transport. Am J Reprod Immunol 74, 333-344. (2015). doi:10.1111/aji.12409.

Conference Presentations:

ASBMB Deuel Conference on Lipids, First Author Poster (2020)
UCSD Research Symposium, First Author Poster (2019)
Mary Gates Research Symposium, Oral Presentation (2014)
Biomedical Engineering Society National Conference, First Author Poster (2013)
Mary Gates Research Symposium, First Author Poster (2013)

Awards:

University of Washington College of Engineering Dean's Medalist (2014)
NASA Space Grant Scholar (2013-2014)
Barry M. Goldwater Scholarship Honorable Mention (2013)
Art Levinson Scholar (2012-2014)
Amgen Scholar, University of California Los Angeles (2012)
Mary Gates Scholar (2011-2014)
Washington State Scholar (2010)

Research Experience:

Ph.D. Candidate (2017 - present)
Advisor: Professor Christopher K. Glass, M.D., Ph.D., Department of Cellular and Molecular Medicine, University of California San Diego

Post-Baccalaureate Researcher (2014 - 2015)
Supervisors: Lisa Mirabello and Xiaohong R. Yang, Division of Cancer Epidemiology and Genetics, National Cancer Institute

Undergraduate Researcher (2010 - 2014)
Supervisor: Professor Kim Woodrow, Department of Bioengineering, University of Washington

Volunteering Experience

UCSD MSTP Symposium Planning Committee (2018-2020)
UCSD Free Clinic Inventory Manager (2015 - 2018)
UCSD Downtown Free Clinic, Manager (2015 - 2017)
District of Columbia Project Sunshine Chapter, Volunteer (2014 - 2015)
Shady Grove Adventist Hospital, Emergency Department Volunteer (2014 - 2015)
UW Department of Bioengineering, Outreach Team Member (2011-2014)

Fields of Study

Major Field: Biomedical Sciences

Studies in Genetics and Immunology
Professor Christopher K. Glass

ABSTRACT OF THE DISSERTATION

Interrogating *in vivo* Mechanisms of Kupffer Cell Transcriptional Regulation Using Natural Genetic Variation

by

Hunter Bennett

Doctor of Philosophy in Biomedical Sciences

University of California San Diego, 2021

Professor Christopher K. Glass, Chair.

Tissue macrophages are essential for the maintenance of organ homeostasis, but the cellular mechanisms specifying their phenotype are poorly understood. Here, we leverage natural genetic variation between inbred mouse strains as a tool to perturb Kupffer cell transcriptional regulation. We show that natural genetic variation disrupts Kupffer cell gene expression through *cis*-mediated disruption of transcription factor binding motifs and via *trans*-acting differences in the activity of gene regulatory machinery. We further divide *trans*-acting genetic variation into non-cell autonomous variation driven by changes in the Kupffer cell environment, and cell autonomous variation driven by changes in intracellular pathway activity. We show that careful

evaluation of each mode of genetic variation can reveal signaling pathways specifying Kupffer cell identity *in vivo*. Collectively, this work demonstrates a novel approach for understanding how genetic diversity impacts tissue macrophage behavior.

Chapter 1: Introduction

Elie Metchnikoff discovered macrophages in 1882 when he observed that, following injury, certain specialized cells of the starfish larva would surround and phagocytose foreign material. Although named for their ability to engulf pathogens, it is now understood that macrophages engage in remarkably diverse functions throughout the body (Metschnikoff, 1883, 1891).

The Hierarchal Collaborative Model of Transcription Factor Binding

At homeostasis, tissue macrophages exist in equilibrium with the surrounding parenchyma. Niche specific signals within organs play major roles in specifying tissue macrophage phenotypes (Blériot et al., 2020). Transcriptomic and epigenomic surveys of tissue macrophages demonstrate that while tissue macrophages share expression of some core transcription factors (TFs), they also express distinct TFs capable of driving tissue-specific gene expression patterns (Lavin et al., 2014; Mass et al., 2016). TFs drive gene expression by binding to enhancers and promoters. While promoters are the essential start sites for initiation of transcription of mRNA, they frequently do not provide sufficient information necessary for developmental and physiologic regulation. This additional information is generally provided by enhancers, which are genetic sequences located upstream, downstream or within genes that act to modulate promoter activity. The mammalian genome is estimated to contain on the order of a million putative enhancer elements, with each cell type of the body typically exhibiting twenty to thirty thousand active enhancers (Meuleman et al., 2020). The enhancer repertoire of a particular cell is a major determinant of its gene expression profile. The selection and activation of enhancers by TFs can be explained by a collaborative-hierarchal model of TF binding (Fig. 1.1A) (Heinz et al., 2015). Enhancer selection is initially driven by collaborative interactions

between relatively simple combinations of lineage-determining TFs (LDTFs) that enable their binding to enhancers in regions of closed chromatin. Common macrophage LDTFs include the ETS domain TF PU.1, the CCAAT/enhancer binding proteins (C/EBPs), and activator protein 1 (AP1) (Fig. 1.1A) (Heinz et al., 2010). The genome wide binding pattern of a particular transcription factor can be determined using chromatin immunoprecipitation followed by next generation sequencing (ChIP-seq) (Heinz et al., 2010). The collaborative binding of LDTFs to closed regions of chromatin results in remodeling of the nucleosome landscape from a closed chromatin structure to an open chromatin structure. Open chromatin regions can be detected by DNase hypersensitivity or the assay for transposase accessible chromatin followed by sequencing (ATAC-seq) (Adams & Workman, 1995; Boyes & Felsenfeld, 1996; Meuleman et al., 2020; Pham et al., 2013). These open regions of chromatin bound by TFs are known as primed or poised enhancers that contribute to basal levels of gene transcription from their target promoters and/or provide access to hierarchical binding of signal-dependent TFs (SDTFs) (Fig. 1.1A). SDTFs are often widely expressed proteins responsible for responding to internal and external stimuli. In most cases, SDTFs alone cannot remodel chromatin to establish poised enhancers, but instead are recruited to the pre-existing poised enhancer landscapes established by LDTFs as well as promoters (Mercer et al., 2011; Yáñez-Cuna et al., 2012). SDTF binding to a poised enhancer recruits co-regulators and co-activators including histone acetyltransferases and histone methyltransferases, ultimately resulting in increased enhancer activity and target gene expression (Kaikkonen et al., 2013). An important consequence of the hierarchical dependence of SDTFs on the prior actions of LDTFs is that the resulting genome wide binding and function of the SDTFs is determined by each cell's specific enhancer landscape, resulting in cell-specific transcriptional outputs (Fig. 1.1A).

Kupffer cells (KCs), the tissue-resident macrophages of the liver, were first described in 1899 as hepatic cells that phagocytose India Ink (Kupffer, 1899). Today, KCs are understood to perform a diverse array of functions beyond phagocytosis. At homeostasis KCs scavenge iron, clear microbial products from the gut, and maintain a tolerogenic immune environment within the liver. KCs also sense the state of hepatic tissue. Their responses to changes in the environment play an important role in the pathogenesis of liver disease.

KCs line the sinusoidal endothelium of the liver and are one of the first cells in the body exposed to portal blood, which carries metabolic products, nutrients, and compounds derived from the gut microbiota. KCs preferentially induce tolerogenic immunity in the absence of inflammation and are important for clearing gut-derived microbial material from the systemic circulation (Carpentier et al., 2019; Helmy et al., 2006; Liu et al., 2019; D. Sun et al., 2019). KCs express surface receptors that mediate the sampling and uptake of portal blood contents, including complement receptors, toll-like receptors, and other pathogen recognition receptors (Fig. 1.2A). In addition to sensing pathogenic material, recent work suggests that these pathways are important for sensing damage to the hepatic parenchyma.

KCs express a variety of SDTFs that integrate the signals from their surface receptors. Similar to other myeloid lineage cells, many KC SDTFs are involved in innate immunity, including NFκB and the majority of the interferon response factor (IRF) transcription factors (Sakai et al., 2019; Seidman et al., 2020). The diversity of immune signaling pathways active in KCs suggests that KCs are capable of fine-tuned responses that integrate the particular pathogen and the status of the larger hepatic environment. Lipopolysaccharide, a pathogen associated molecular pattern of Gram-negative bacteria, binds to toll-like receptor 4 (TLR4), leading to a signaling cascade that results in the activation of NFκB, AP1, and IRF signaling, which induces

the expression of inflammatory genes including the inflammatory cytokines pro-IL1β and pro-Il18. In their propeptide state IL1β and IL18 require cleavage by the inflammasome for activation, secretion, and inflammation. While at homeostasis there is evidence for NFκB activity as the NFκB motif is enriched in the total set of KC-specific enhancers compared to blood monocytes (Bonnardel et al., 2019; Sakai et al., 2019; Seidman et al., 2020), there is little evidence of inflammasome activation in KCs. This suggests a role of the TLR4-NFκB pathway in sensing and responding to portal lipopolysaccharide (LPS), a TLR4 agonist derived from Gram-negative bacteria, in a manner that does not result in IL1β-driven inflammation. However, inflammasome activation is an essential pathway in the progression of NASH, as will be discussed later in this review.

Natural Genetic Variation Alters Binding of Macrophage LDTFs.

Natural genetic variation results in phenotypic diversity across the tree of life (Maistrenko et al., 2020; Mets & Brainard, 2018). Genome-wide association studies (GWAS) of human populations demonstrate that specific genetic loci are associated with complex traits and disease susceptibility. Similar work in mouse genetics has been used to map loci associated with atherosclerosis, serum HDL levels, and gut microbiota diversity (Hui et al., 2015; Org et al., 2015; Pamir et al., 2019). However, interpretation of the effects of genetic variation at a given locus has proven difficult because a) GWAS establish correlation between phenotype and genotype but do not establish a causal relationship between the risk variant and disease and b) over 80% of GWAS loci that are found in noncoding regions of the genome making the downstream effects of variants difficult to predict (Hindorff et al., 2009).

One model for interpretation of non-coding genetic variants follows from the hierarchal collaborative model described above. Since the regulatory landscape of a particular cell type is

determined by a small combination of LDTFs and SDTFs in the hierarchal collaborative model, non-coding variants that alter the binding of these factors can be used to predict functional changes in the cell (Heinz et al., 2013). In mice, natural genetic variation between inbred strains can be used as an *in vivo* mutagenesis screen to examine how changes in DNA sequence lead to differences in LDTF and SDTF binding. Heinz and Romanoski used this approach to validate the hierarchal collaborative model of TF binding by performing ChIP-seq for the macrophage LDTFs PU.1 and C/EBPa in BALB/cJ and C57BL/6J thioglycolate elicited macrophages. Alignment of LDTF peaks with strain specific genomes revealed that roughly 40% of strain specific binding of the macrophage LDTFs PU.1 and C/EBPa were associated with motif mutations (Heinz et al., 2013). Sites of strain specific TF binding sites were 5-fold enriched for strain specific mutations compared to strain similar TF peaks (Heinz et al., 2013). Importantly, disruption of either a PU.1 or CEBP motif by a strain specific variant was correlated with decreased binding of both LDTFs. ChIP-seq for the p65 subunit of the SDTF NFkB revealed that Motif mutations in LDTF binding sites also impacted the recruitment of the SDTFs, providing another example of how small changes in DNA sequence affect multiple layers of transcriptional regulation (Heinz et al., 2013). Loss of LDTF and SDTF binding was associated with loss of downstream enhancer activation as assessed by H3K27ac ChIP-seq, supporting a collaborative model of enhancer selection by a defined set of TFs (Heinz et al., 2013). Subsequent work has leveraged the functional impact of motif mutations to create collaborative networks of TFs using generalized linear models (Link et al., 2018) and machine learning (Fonseca et al., 2019).

Initial work studying the natural genetic variation of TF binding in macrophages raised another question - why do 60% of strain specific TF binding sites lack a motif mutation. Genetic theory holds that these sites could either be determined in *cis* by nearby or distant genetic

sequences on the same chromosome, or in *trans* by the action of a diffusible intracellular factor that acts on both chromosomes equally within the nucleus (Signor & Nuzhdin, 2018). To assess the effect of *trans* acting genetic variation on nascent transcription Link et al applied applied 5' whole-genome run-on analysis coupled to deep sequencing (GRO-seq) to C57BL/6J, SPRET/EiJ and the F1 progeny of a C57BL/6J and SPRET/EiJ intercross to assess the effect of *trans* acting genetic variation on nascent transcription (Link et al., 2018). In this model, *cis* regulatory genetic variation can be identified when the allelic bias of a genomic locus observed in the parental strains is maintained in their F1 hybrid offspring, as this suggests that the variation is driven by local interactions on the parental chromosome. Using this framework, Link et al estimated that approximately 70% of strain specific sites are determined in *cis* (Link et al., 2018). This approach also identified instances of interconnected *cis*-regulatory domains, in which epigenetic signals vary in concert with each other over large (>1 megabase) contiguous regions of the strain genomes, even at sites lacking genetic variation (Link et al., 2018). This suggests that in some cases, through chromatin looping, local genetic variation can propagate large distances and establish strain specific regions. How local or distal genetic variation alters strain specific binding of transcription factors remains an important area for further study.

Since disruption of LDTF binding often leads to decreased transcription of nearby genes (Heinz et al., 2013; Link et al., 2018), it follows that if the LDTF set and enhancer distribution of a given cell type is reasonably well characterized, this information alone can be used to prioritize variants likely to have a functional consequence in a cell type of interest. This framework has been successfully used in several studies to identify the functional consequences of GWAS variants in diseases such as Alzheimer's disease, type 1 diabetes, and pancreatic cancer (Chiou et al., 2021; Gosselin et al., 2017; Nott et al., 2019).

Since the approach was published in 2013, many groups have used natural genetic variation coupled with high throughput sequencing to perform *in vivo* mutagenesis screens disrupting gene regulatory architecture. Detailed study of disrupted enhancers and promoters can then be used to trace regulatory mechanisms in cell types of interest. This approach has been used to gain mechanistic insight into genetic regulation in a number of cells and tissues, including bone marrow-derived macrophages (Fonseca et al., 2019; Heinz et al., 2013; Link et al., 2018), microglia (Gosselin et al., 2014; Yang et al., 2021), CD4+ and CD8+ T cells (Fasolino et al., 2020; van der Veeken et al., 2019, 2020), fibroblasts (Vierbuchen et al., 2017), and white adipose tissue (Li et al., 2019; Soccio et al., 2015). In macrophages, natural genetic variation has been used to validate the hierarchal collaborative model of enhancer selection (Link et al., 2018), identify collaborative TFs interacting with specific AP-1 family TFs (Fonseca et al., 2019), and identify lineage determining transcription factors in microglia (Gosselin et al., 2014).

Homeostatic Transcriptional Regulation of KC function.

KC cells are myeloid lineage cells derived from fetal yolk sac macrophages that seed the liver during embryogenesis (Perdiguero et al., 2015). As myeloid lineage cells, KCs express high levels of the monocyte/macrophage LDTFs PU1 (encoded by *Spi1*), CEBPα, and activator protein 1 (AP1) family of transcription factors (Heinz et al., 2015). Motifs for each of these TFs are significantly enriched in KC-specific enchancers. Comparative analysis of the epigenomes of tissue macrophages have also identified the nuclear receptor LXRα (encoded by *Nr1h3*) and SpiC as KC LDTFs (Fig. 1.1A) (Lavin et al., 2014; Mass et al., 2017). According to the collaborative-hierarchal model of TF binding, these lineage determining factors bind in a collaborative manner to open closed regions of chromatin, thereby creating a KC-specific enhancer landscape (Heinz et al., 2015). These open regions of chromatin then provide a location

for SDTFs to bind and further regulate transcriptional activity. Here we will review the SDTFs that have been studied in KCs and the homeostatic functions that they control.

While NFκB is the most well studied inflammatory SDTF in KCs, many others are expressed at high levels, including the interferon regulatory factors (IRFs). In particular, *Irf3* has been shown to mediate KC necroptosis in response to both viral and bacterial infections. In mice infected with *Listeria monocytogenes, Irf3* mediated KC necroptosis leads to an early inflammatory response and late reparative response that ultimately results in the clearing of infection (Blériot et al., 2015; Di Paolo et al., 2013). Interestingly, this function of *Irf3* does not require any of its known transcriptional activators (Di Paolo et al., 2013).
Transcriptomic surveys of tissue-resident macrophages found relative enrichment for genes involved in lipid metabolism. Examples of lipid-metabolic genes include the TFs *Nr1h2, Nr1h3, Ppard, Pparg, Srebf1,* and *Srebf2*. Indeed, *Nr1h3* encoding the liver x receptor α (LXRα) is the highest expressed TF in KCs (Fig. 1.1B). The LXRs are type I nuclear receptors that control cellular cholesterol export and bind to DNA as a heterodimeric complex with the retinoid x receptor α (Willy et al., 1995). In macrophages, LXR is activated by cholesterol derivatives and cholesterol synthesis intermediates, which then induce corepressor-coactivator exchange leading to transcription of LXRα target genes, including *Abca1* and *Abcg1* (Fig. 1.2A) (Laffitte et al., 2001; Venkateswaran et al., 2000). LXRα and LXRβ have both distinct and overlapping functions in macrophages. For example, both LXRα and LXRβ activate expression of *Abca1*, but *Cd5l* induction requires LXRα while *Apoc-I* induction requires LXRβ (Mak et al., 2002; Ramón-Vázquez et al., 2019). Oxysterols such as 24-Hydroxysterol, 27-Hydroxysterol, and 24-25 epoxycholseterol were the first endogenous LXR ligands discovered and were long thought to be the dominant LXR ligands in the liver. This theory has been challenged by recent lipidomic

analysis of LXR ligands in the liver at homeostasis and during NASH, which show that desmosterol is the predominant LXR ligand in the murine liver (Sakai et al., 2019; Seidman et al., 2020; Yang et al., 2006). Desmosterol, which is converted into cholesterol by Dhcr24 in the last step of the Bloch cholesterol synthesis pathway, was first described as a non-oxysterol LXR ligand by Helen Hobbs in 2006 (Yang et al., 2006). Desmosterol was also shown to control LXR activity in macrophage foam cells *in vivo*, suggesting that it could act as an LXR agonist across many tissue macrophage populations (Spann et al., 2012). Once LXR is bound by sterol ligands, it activates LXR target genes that facilitate export of cellular to high-density lipoprotein, which then delivers cholesterol to the liver in a process known as reverse cholesterol transport.

KC specific deletion of LXRα does not result in decreased expression of the canonical macrophage specific LXR target genes that are linked to cholesterol homeostasis. Instead, LXRα functions predominantly as a KC LDTF by guiding expression of genes specific to the KC niche. Genetic ablation LXRα specifically in KCs was associated with decreased expression of KC specific genes such as *Cd5l, Kcna2, and Il18b* (Sakai et al., 2019), suggesting a key role in pioneering regulatory regions for controlling expression of linked genes. In line with this, in the absence of LXR, KCs were found less fit for establishment in the KC niche (Bonnardel et al., 2019). Similarly, splenic marginal zoned and metallophilic macrophages also depend on LXR for proper existence in the tissue (A-Gonzalez et al., 2013). In addition to controlling lineage survival of some tissue macrophage populations, LXRα ablation in KCs also resulted in large scale changes in open chromatin as defined by ATAC-seq, indicating a direct role as a LDTF in enhancer selection. LXR signaling has also been shown to decrease inflammatory activity of macrophages in response to LPS (Ito et al., 2015; Tall & Yvan-Charvet, 2015). Whether this pathway is active in KCs has not been determined.

In addition to the LXRs, *Srebf1* and *Srebf2,* which encode sterol response binding protein 1 and 2 (SREBP1 and SREBP2), are expressed by KCs and have key roles in lipid metabolism (Fig. 1.1B). *Srebf1* expression is induced by LXR activation, leading to increased levels of SREBP1 protein (Repa et al., 2000). In settings of low cellular cholesterol, SREBPs are translocated from the ER to the Golgi in a SCAP-dependent manner, where they are proteolytically processed to generate active forms that translocate to the nucleus. Srebp1 primarily induces fatty acid synthesis whereas SREBP2 primarily induces cholesterol synthesis (Brown & Goldstein, 1997). The SREBPs are also linked to macrophage inflammatory pathways: following LPS activation, SREBP1 is required for synthesis of monounsaturated fatty acids that mediate inflammation resolution (Oishi et al., 2017) while SREBP2 is required for the resolution of inflammation mediated by tumor necrosis factor (TNF) (Kusnadi et al., 2019). Production of anti-inflammatory lipids is important for macrophages to return to homeostasis following tissue injury. Prolonged inflammatory activation following liver damage could lead to chronic hepatic inflammation and permanent tissue damage such as fibrosis. Genetic studies will be essential in evaluating the functional role of the SREBP pathway in KCs in both homeostasis and disease.

The peroxisome proliferator-activated receptors (PPARs) bind DNA in heterodimers with retinoid X receptors and are activated by fatty acids and fatty acid metabolites. In the context of atherosclerosis, PPARγ regulates transcriptional responses of macrophages invading atherosclerotic plaques. PPARγ does this in part by controlling expression of *Cd36* and *Msr1* (encoding SR-A), key scavenger receptors involved in lipid updtake (Bouhlel et al., 2007; Ricote et al., 1998). Activation of PPARγ also induces expression of LXRα, resulting in increased expression of target genes such as *Abca1* and cholesterol efflux (Chawla et al., 2001). Beyond

lipid metabolism, PPAR activation promotes an anti-inflammatory state in macrophages by blocking inflammation-induced expression of *Il1b*, *Il6*, and *Nos2*) (Bouhlel et al., 2007; Ricote et al., 1998). Consistent with this, synthetic ligands of PPARγ have been shown to reduce atherosclerosis in mouse models (Ricote et al., 1998). Myeloid deletion of PPARδ, but not PPARγ, led to decreased expression of alternative activation markers in KCs, suggesting that PPARδ signaling exerts more transcriptional control in homeostatic KCs than PPARγ (Fig. 1.1B) (Odegaard et al., 2007, 2008). Specific roles addressing PPARδ or PPARγ in KCs during disease are currently unknown.

KCs also participate in iron recycling by scavenging senescent red blood cells, heme, and hemoglobin. Iron from ingested heme is shuttled to hepatocytes for recycling via ferroportin (encoded by *Slc40a1*) (Nairz et al., 2017). This activity is in part controlled through elevated expression of *Bach1*, *Nfe2l2* (encoding NRF2), and *Spic*, the three key factors that control macrophage iron homeostasis (Fig. 1.1A) (Scott et al., 2016; Scott & Guilliams, 2018). Accumulation of heme in the KC in settings of extravascular hemolysis leads to degradation of BACH1, which promotes activation of NRF2 and increased transcription of *Spic*, resulting in the induction of genes required for heme degradation (Nairz et al., 2017). Notably, SPIC is also required for the development of iron-scavenging red pulp macrophages in the spleen. Interestingly, the iron recycling capacity of KCs may not be sufficient in cases of extreme hemolysis. In such cases, KCs that are overloaded with heme have been shown to undergo ferroptosis, leading to the recruitment of monocytes from the bone marrow. Upon entry into the

liver, bone marrow monocytes rapidly increase the transcription of SPIC, which then activates the iron recycling gene program (Theurl et al., 2016).

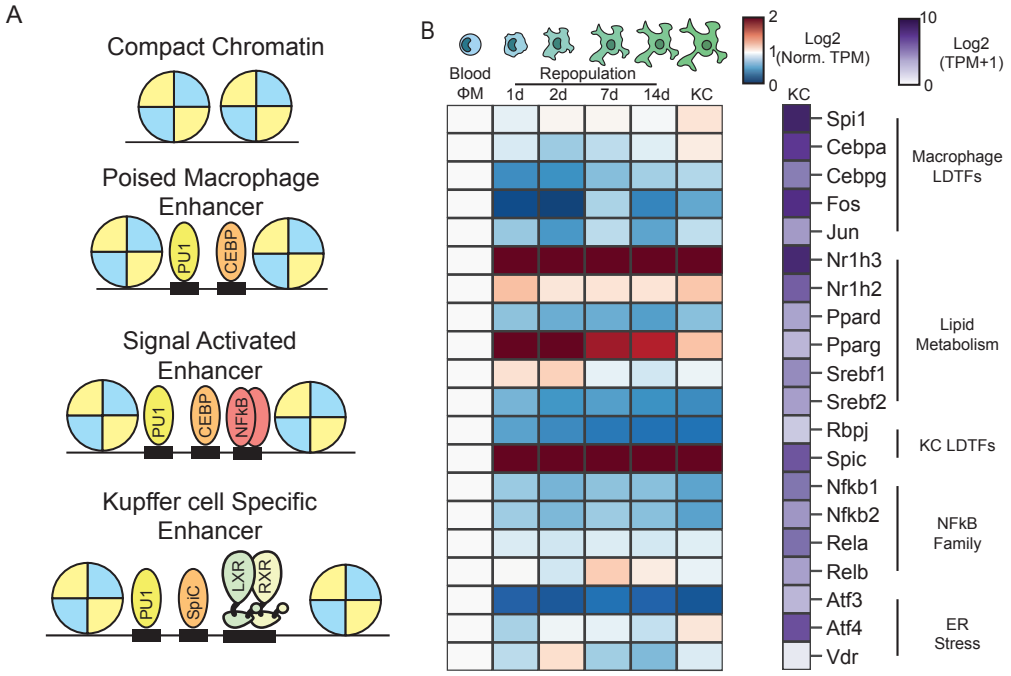

Figure 1.1: The Kupffer cell epigenome. In the collaborative-hierarchal model of TF binding, closed chromatin is remodeled by lineage determining transcription factors, which bind to DNA collaboratively to create poised enhancers(A). Signal dependent transcription factors are then recruited to poised enhancers upon activation of cellular signaling pathways. Kupffer cell LDTFs include LXRα and SPIC. Circulating monocytes recruited to the liver following KC depletion rapidly assume a TF profile similar to resident KCs (B). TFs associated with lipid metabolism are particularly enriched during monocyte to Kupffer cell differentiation. Data for Fig. 1.1B taken from Sakai et al. The blue-red expression heatmap in Fig. 1.1B shows expression (in TPM) normalized such that expression in blood monocytes is equal to 1 (Sakai et al., 2019).

Signals in the sinusoidal niche guide the expression of KC TFs.

Recent studies show that KCs extend cellular processes into the perisinusoidal space, where they make contact with hepatocytes and hepatic stellate cells in addition to their contacts with the sinusoidal endothelium (Bonnardel et al., 2019). This close cellular contact suggests integrated cell-cell communication between KCs and the surrounding cells of the liver parenchyma (Fig. 1.2A). Recently, two papers identified liver-derived signals that instruct KC

identity by leveraging KC depletion/repopulation in the mouse as a model system (Bonnardel et al., 2019; Sakai et al., 2019). Treatment of mice expressing the diphtheria toxin receptor (DTR) specifically in KCs with diphtheria toxin (DT) resulted in rapid and nearly complete ablation of the KC population (Scott et al., 2016). Loss of KCs induced the transient expression of chemokines and adhesion molecules in hepatic stellate cells and liver sinusoidal endothelial cells (LSECs), resulting in rapid colonization of the empty sinusoidal niche by circulating monocytes (Fig. 1.2A) (Bonnardel et al., 2019). Within hours of their recruitment to the liver, these blood monocytes began differentiating to KC-like liver macrophages. A week after KC depletion, the transcriptional profiles of the recruited macrophages were nearly indistinguishable from embryonic KCs (Fig. 1.1B) (Bonnardel et al., 2019; Sakai et al., 2019; Scott et al., 2016). This KC-DTR depletion model provided a powerful system for identifying molecules and pathways required for KC differentiation.

In two recent papers, Sakai et al. and Bonnardel et al. used the KC-DTR model to discover three signals in the hepatic sinusoid, Notch ligand DLL4, TGFβ/BMP family ligands, and endogenous LXR ligands that sequentially drive KC differentiation (Bonnardel et al., 2019; Sakai et al., 2019). Bonnardel et al. utilized deep transcriptional profiling of hepatic non-parenchymal cells coupled with the bioinformatic algorithm NicheNet to identify putative signals that induce KC differentiation following DT mediated KC depletion (Bonnardel et al., 2019). NicheNet predicts ligand-receptor interactions using transcriptomic data and known gene regulatory networks (Browaeys et al., 2020). NicheNet predicted that hepatic stellate cell derived *Csf1* and bone morphogenic proteins (BMPs) including BMP4, BMP5, BMP9, BMP10, and GDF6 could influence blood monocytes within the hepatic niche (Fig. 1.2A) (Bonnardel et al., 2019). LSECs were also shown to express ligands that could bind receptors expressed during KC

differentiation, including BMPs (BMP2, BMP, INHBB) as well as the Notch pathway ligands DLL1 and DLL4 (Fig. 1.2A) (Bonnardel et al., 2019). In parallel, Sakai et al. studied the transcriptional and epigenetic landscape of blood monocytes as they differentiated into KCs. H3K27Ac ChIP-seq identified large changes in the enhancer landscape of recruited liver macrophages 24h after KC depletion. The majority of activated enhancers were associated with pre-existing open chromatin regions as determined by ATAC-seq, including enhancers upstream of highly expressed KC transcription factors such as LXRα, SPIC, and MAFb, whose transcription is rapidly induced upon recruitment of monocytes into the hepatic parenchyma (Fig. 1.2B) (Sakai et al., 2019). As discussed above, ligands for the LXRα and SPIC pathways are abundant in the hepatic sinusoid, including desmosterol, hydroxysterols, and heme (Chen et al., 2007; Janowski et al., 1996; Muse et al., 2018; Yang et al., 2006). Motif enrichment analysis of enhancers activated in recruited liver macrophages at 24h revealed enrichment for the motif of the Notch pathway TF RBPJ (Sakai et al., 2019). This finding supports Bonnardel's identification of the Notch ligands DLL1 and DLL4 as essential for KC differentiation (Fig. 1.2B). Sakai et al. then demonstrated that the TFs LXRα and SMAD4 were essential for maintenance of homeostatic KC identity (Sakai et al., 2019). Notably, SMAD4 signaling is downstream of the BMP signals identified as essential for KC differentiation by Bonnardel et al. Collectively, these results suggest a model where DLL1 and DLL4 on LSECs induce rapid activation of a poised enhancer landscape in monocytes, leading to the rapid increase in expression of KC LDTFs such as LXRα and SPIC. Once translated into protein, collaborative interactions between LXRα, SPIC, and existing macrophage LDTFs such as PU.1 and CEBP establish the KC specific cistrome (Fig. 1.2B).

The Notch-RBPJ pathway is essential for the differentiation of specific tissue macrophages, including tumor-associated macrophages (Franklin et al., 2014) and mammary gland stromal macrophages (Chakrabarti et al., 2018). In the mammary glands, stem cells express the ligand DLL1 to activate macrophage Notch signaling and induce Wnt family ligand expression (Chakrabarti et al., 2018). Interestingly, the consequences of Notch activation differ in each of these examples and the mechanisms by which Notch activation induces cell specific responses is a promising area for future study. The diverse consequences of Notch activation in macrophages might be caused by other tissue-specific signals acting in concert with Notch signaling. Support for this idea comes from *in vitro* studies showing that stimulation of bone marrow progenitor cells with TGF-β in addition to DLL4 induces more KC-specific genes than either DLL4 or TGFβ alone (Sakai et al., 2019). In addition to different ligand co-expression patterns, diversity in tissue macrophage responses to Notch activation could depend on the particular Notch ligand expressed in a given niche. The Notch ligands DLL1 and DLL4 activate distinct targets by pulsatile or sustained Notch activation dynamics (Nandagopal et al., 2018). Whether these differences in Notch dynamics could result in the establishment of different macrophage transcriptional responses is an interesting area for further study.

SPIC is a transcription factor known to be expressed in iron-recycling macrophages. As discussed above, heme is the most well-known activator of SPIC expression in macrophages, and SPIC is highly expressed in KCs (Fig. 1.1B) (Haldar et al., 2014). Interestingly, Notch signaling also induced SPIC expression in KCs (Bonnardel et al., 2019; Sakai et al., 2019). Furthermore, *Spic* expression is upregulated in SMAD4 knockout KCs, even as other KC TFs such as *Nr1h3* are downregulated (Sakai et al., 2019). BMP2 and BMP6 secreted by LSECs are involved in

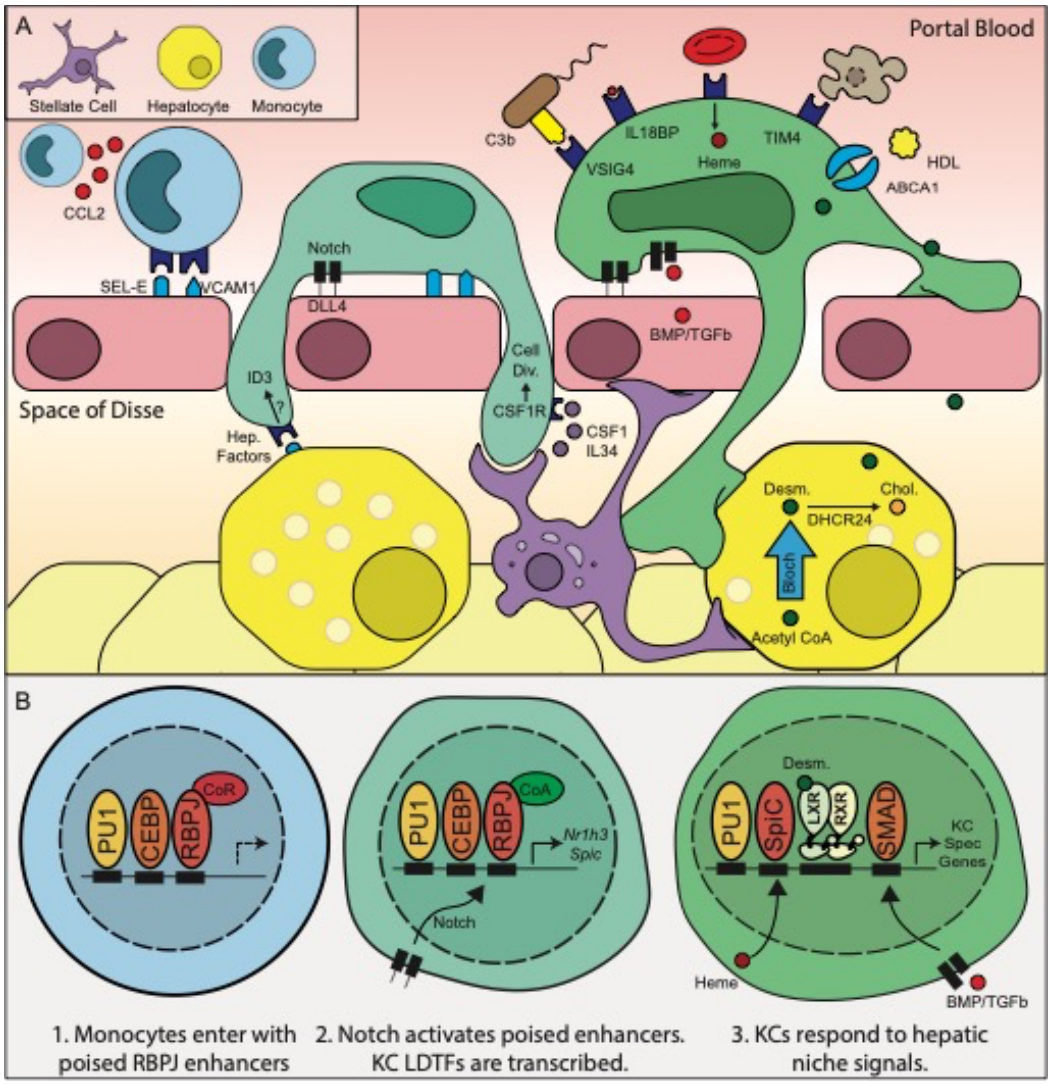

Figure 1.2: Hepatic niche signals induce monocyte to Kupffer cell differentiation. Following depletion of KCs by diptheria toxin, hepatic stellate cells and liver sinusoidal endothelial cells secrete chemokines and adhesion molecules, recruiting circulating monocytes to the hepatic sinusoid (**A**). Notch signaling subsequently activates expression of KC LDTFs (**B**), which in turn establish the Kupffer cell cistrome.

iron-regulated hepcidin expression by hepatocytes (Parrow & Fleming, 2017). BMPs might also regulate iron metabolism in KCs though *Spic* suppression via SMAD signaling in KCs.

These studies provide an example of how transcriptomic and epigenetic-led hypothesis generation can be used to predict key molecular pathways coordinating monocyte to tissue

resident macrophage differentiation. Using molecules which mimic liver environment signals, it is possible to partially induce KC-specific genes in mouse bone marrow-derived macrophages (Bonnardel et al., 2019; Sakai et al., 2019). This technology will provide improved in vitro systems for modeling pathological features of KCs in metabolic and inflammatory liver diseases. However, the transcriptome of bone marrow-derived macrophages treated with DLL4, TGF-b, and the synthetic LXR agonist DMHCA still does not recapitulate the transcriptome of *ex vivo* KCs or repopulating liver macrophages. This disparity indicates the limitations of the *in vitro* study of tissue macrophages (Sakai et al., 2019). There are likely to be many contributing factors to the remaining differences, including a requirement for additional liver-derived factors and inhibitory effects of the in vitro environment. For example, the enrichment of NFκB motifs in KC-specific enhancers may reflect exposure of KCs to gut-derived LPS present in portal blood (Sakai et al., 2019). The *in vitro* environment also lacks the three-dimensional structure of the hepatic environment as well as the hepatic cells that KCs are in close contact with *in vivo* (Bonnardel et al., 2019). Collectively, these studies provided significant new insights into the sequential mechanisms by which niche signals induce the selection and action of LDTFs during KC differentiation.

NAFLD and NASH alter regulation of the KC epigenome.

NAFLD is a growing threat to public health in Westernized societies. In the United States alone, liver-related deaths amongst individuals with NAFLD are predicted to grow exponentially over the next ten years, reaching 206,300 deaths by 2030 (Estes et al., 2018). The development and progression of NAFLD is associated with sequential changes in the hepatic environment. Simple NAFLD is diagnosed by the presence of hepatic steatosis without clinically significant consumption of alcohol (Kleiner et al., 2005). A subset of NAFLD patients subsequently develop

non-alcoholic steatohepatitis (NASH) which is associated with histologically observable hepatocyte dysfunction and immune infiltration (Kleiner et al., 2005). Roughly 20% of patients with NASH will go on to develop hepatic fibrosis, in which areas of the hepatic parenchyma are replaced with collagen scars (Sanyal et al., 2019). Hepatic fibrosis is a feature of severe NAFLD and a strong clinical predictor of liver related mortality (Angulo et al., 2015).

KCs express a suite of TFs that respond to the metabolic and inflammatory signals found in both NAFLD and NASH. Lipid metabolic TFs such as the LXRs, SREBPs, and PPARs respond to changes in nutrient levels while inflammatory TFs such as NFκB respond to tissue damage (Fig. 1.3C). However, early studies of KCs were limited due to the difficulty of resolving different myeloid cell populations in the liver during NAFLD. Recent advances in immunology and single-cell sequencing have provided deep insight into the transcriptional and epigenomic profile of KCs and other hepatic macrophages during the progression of NAFLD. Early in NASH, KCs produce cytokines such as TNFα and IL1β, which worsen hepatic steatosis by inhibiting hepatic PPARα activity (Stienstra et al., 2010) and act as paracrine signals by increasing KC and hepatic stellate cell expression of CCL2, which recruits inflammatory monocytes to the liver (Lanthier et al., 2010; Tosello-Trampont et al., 2012). Interestingly, a recent single cell study of hepatic macrophages in NASH suggests that KCs do not upregulate inflammatory gene expression early in NASH (Remmerie et al., 2020). It is possible that apoptotic KCs are the source of TNF during NASH progression, as KC apoptosis in the KC-DT model system induces TNF dependent upregulation of CCL2 in stellate cells (Bonnardel et al., 2019). KCs also contribute to metabolic disease, as depletion of KCs after 3 days, 2 weeks, and 3 weeks of high fat diet improves glucose tolerance and insulin resistance (Huang et al., 2010; Neyrinck et al., 2009). During later stages of NASH, the myeloid population of the liver

increases in size and complexity to include KCs, Ly6C^{hi} and Ly6C^{lo} macrophages (Fig. 1.3A). While at homeostasis embryonic KCs are self-renewing and constitute the majority of hepatic macrophages (Huang et al., 2010), but in late-stage NASH embryonic KCs coexist with bone marrow derived KCs that arise from Ly6C^{hi} hepatic macrophages recruited from the systemic circulation (Devisscher et al., 2017). Upon entry into the liver, Ly6C^{hi} monocytes differentiate into F4/80^{+} macrophages. Eventually, a subset of F4/80^{+} BM-MΦ differentiate into BM-KCs expressing the KC marker gene CLEC4F. CLEC4F^{+} BM-KCs are transcriptionally similar to embryonic derived KCs; however, a small subset of genes remains differentially expressed (Sakai et al., 2019). Importantly, embryonic derived KCs can be differentiated from BM-KCs by expression of the surface marker *Timd4* (TIM4^{+}) (Scott et al., 2016). Whether BM-KCs and embryonic derived KCs function differently in NASH is unclear. One recent study showed that replacement of embryonic derived KCs with BM-KCs prior to initiation of the methionine-choline deficient NASH model diet resulted in impaired hepatic triglyceride storage and increased hepatocyte damage as measured by ALT (Tran et al., 2020). In contrast, a second study found no changes in inflammatory cytokines or NASH histology in livers populated by BM-KCs compared to livers populated by embryonic KCs (Seidman et al., 2020).

During NASH KCs recruit BM-MΦ at least in part by TLR4- and TNF-mediated upregulation of CCL2. Both genetic and pharmacologic approaches to blocking CCR2 mediated infiltration of bone marrow derived macrophages decrease fibrosis, inflammation, and metabolic disease during NASH (Heymann & Tacke, 2016; Mossanen et al., 2016). Cenicriviroc, a CCR2/CCR5 antagonist, is in phase III clinical trials for the treatment of fibrosis in NASH (Lefebvre et al., 2016). Collectively, hepatic macrophages (BM-MΦ, BM-KCs, KCs) augment metabolic disease during NASH; hepatic steatosis, insulin resistance, and oral glucose tolerance

improve in mice with fibrotic NASH following depletion of hepatic macrophages (Krenkel & Tacke, 2017; Miura et al., 2012; Reid et al., 2016; Tosello-Trampont et al., 2012).

Hepatic macrophages can also be found in areas of hepatic fibrosis. These Scar associated macrophages (SAMacs) can be distinguished from other macrophage populations by their high expression of TREM2, CD9, and SPP1, as well as their close physical association with areas of hepatic fibrosis in both mice and humans (Fig. 1.3A) (Ramachandran et al., 2019; Remmerie et al., 2020; Xiong et al., 2019). The SAMac phenotype is evolutionarily conserved between mice and humans, as SAMacs have been observed in multiple different mouse models of hepatic fibrosis. SAMacs are transcriptionally similar to KCs and BM-KCs (Krenkel et al., 2019; Ramachandran et al., 2019; Xiong et al., 2019). Ontologically SAMacs have been shown to arise from embryonic derived KCs and BM-KCs in mice, whereas in humans *in silico* pseudotemporal analysis of human SAMacs suggests that SAMacs derive mainly from recruited BM-MΦ (Krenkel et al., 2019; Ramachandran et al., 2019; Seidman et al., 2020; Xiong et al., 2019). While it is possible that these results reflect a species-specific difference in KC biology, in our view it is more likely that SAMacs can arise from either embryonic KCs or bone marrow derived KCs. Therefore, the differences in results in mice and humans could instead reflect a much higher proportion of bone marrow derived KCs in the human liver compared to the mouse.

The SAMac phenotype appears to be linked to disease burden. In human NAFLD patients, TREM2 mRNA levels correlated with markers of liver damage and fibrosis (Xiong et al., 2019). However, the functional role of SAMacs during NASH progression is not understood. Current evidence suggests that the functions of SAMacs in NASH are complex. scRNA-seq data from fibrotic human livers shows that SAMacs express the profibrotic ligands TGFβ, IL1β, and PDGFβ, suggesting that SAMacs could promote collagen deposition by stellate cells (Fig. 1.3A)

(Ramachandran et al., 2019). However, SAMacs also express high amounts of TREM2, which has been associated with protective macrophage functions in Alzheimer's disease and obesity (Jaitin et al., 2019; Keren-Shaul et al., 2017). Future studies will be needed to fully assess the functions of SAMacs in the fibrotic liver.

The development of NASH is associated with increased diversity in the hepatic myeloid compartment. NASH is also associated with changes in the behavior of KCs themselves. However, knowledge gained from studying homeostatic KCs cannot always be extended to KCs in diseased tissue. KCs from healthy livers can behave quite differently than KCs from NASH livers (Heymann et al., 2015; Leroux et al., 2012). One notable study showed that KCs from healthy livers preferentially promoted expansion of $Foxp3^{+}$ $CD25^{+}$ T cells when presented with ovalbumin coated antigenic particles, suggesting that KCs act as tolerogenic antigen presenting cells. However, KCs from mice fed the methionine choline deficient NASH diet displayed decreased surface PDL1 and increased surface levels of the activating marker CD80. Following this result, KCs lost their ability to induce $Foxp3^{+}$ $CD25^{+}$ T cells expansion during NASH (Heymann et al., 2015). The hierarchal collaborative model holds that differences in a cell's response to the same stimulus can be explained by changes in the enhancer landscape and LDTFs of that cell. Using these studies as a guide, we can begin to study the epigenetic circuits that guide macrophage behavior during NASH and delineate both adaptive and maladaptive gene expression programs. Here we review the current understanding of the transcriptional control of

hepatic macrophages during NASH and how these pathways may be targeted by future therapeutic strategies.

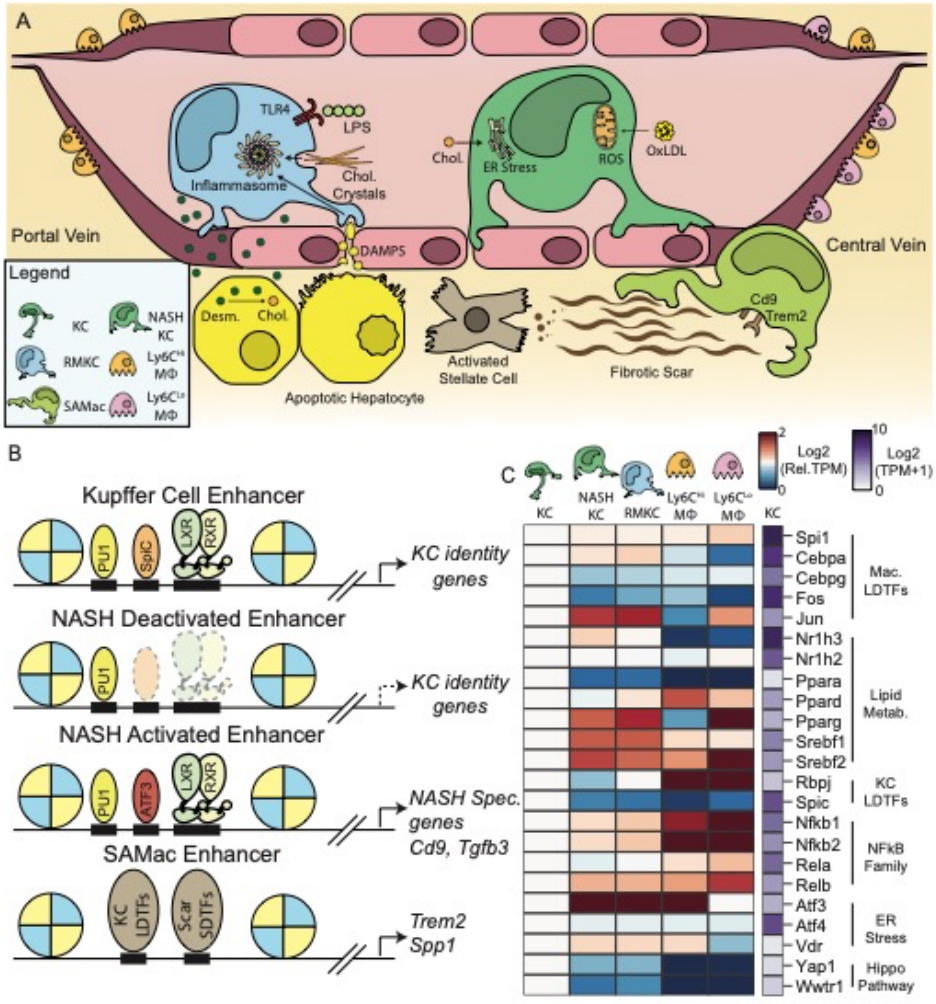

Figure 1.3: The NASH environment induces changes in the Kupffer cell niche. NAFLD and NASH alter the Kupffer cell microenvironment. Within the sinusoid, NASH increases the amount of LPS, oxidized LDL, and cholesterol circulating in portal blood(**A**). In Kupffer cells NASH is associated with a loss of LXR at Kupffer cell specific enhancers and the recruitment of LXR to de novo NASH enhancers in collaboration with ATF3(**B**). The blue-red expression heatmap shows expression (in TPM) normalized such that expression in homeostatic Kupffer cells is equal to 1 (**C**). Data from Fig. 1.3C adapted from Seidman et al. (Seidman et al., 2020).

NASH induced reprogramming of LXR

LXRs function in cholesterol metabolism was first described in 1998, when it was shown that mice lacking LXRα develop NASH when fed a 2% cholesterol diet due to impaired

hepatocyte cholesterol excretion (Peet et al., 1998). Following this pioneering work, LXRs have been shown to control important functions in stellate cells, LSECs, and KCs during NASH. It is well established that LXR activation inhibits inflammatory signaling in macrophages both *in vivo* and *ex vivo.* This function of LXR extends to KCs, as activation of LXR signaling led to decreased TNF production by KCs in a mouse model of endotoxemia (Wang et al., 2009). Conversely, loss of LXR signaling in KCs is associated with increased inflammation in response to LPS. Mice lacking one or both LXRs were fed a NASH model diet and subsequently injected with LPS. Macrophages from mice lacking LXRα or both LXRα and LXRβ produced more inflammatory cytokines following LPS injection than control mice (Endo-Umeda et al., 2018). This could be due to loss of LXR mediated trans-repression of inflammatory signaling, as LXR activation in *ex vivo* KCs was shown to inhibit inflammatory activation in a neuron-derived orphan nuclear receptor-1 dependent manner (He et al., 2015). Increased inflammatory activation of KCs lacking LXR could also be due to changes in endoplasmic reticulum cholesterol levels or direct competition with the inflammatory TF IRF3 for binding with transcriptional co-activators (Ito et al., 2015; Miao et al., 2016). These studies convincingly demonstrate the involvement of LXR signaling in modulating KC inflammatory signaling.

In a recently published paper, Seidman et al. demonstrate that KC LXR signaling is fundamentally altered during NASH pathogenesis. RNA-seq revealed that KCs from NASH livers expressed lower amounts? of KC specific genes such as *Timd4*, *Pcolce2*, and *Arg2*. *Timd4* and *Arg2* were also decreased in KCs lacking LXRα knockout, suggesting that loss of LXR activity at their enhancers results in deactivation in the NASH environment (Seidman et al., 2020). Genome wide analysis of LXR binding in KCs revealed that the NASH environment significantly alters the localization of LXR in KCs and that of the sites with reduced LXR

binding during NASH, 39% were linked KC specific gene Fig. 1.3B) (Seidman et al., 2020). Similar analysis of KC specific enhancers demonstrated that LXR binding was required to maintain the homeostatic KC enhancer landscape during NASH (Seidman et al., 2020). Taken together, this result suggests a loss of LXR LDTF function in KCs during NASH. The loss of KC specific genes could have important functional consequences in NASH (Fig. 1.3B). Tim-4 (encoded by *Timd4*) is a phosphatidylserine receptor involved in the clearance of apoptotic cells (Morioka et al., 2019). *Il18bp* is another KC specific gene with decreased expression during NASH. Il18bp blocks Il18 signaling by binding Il18 with higher affinity than Il18 receptors (Dinarello et al., 2013). Il18 is required for metabolic homeostasis in the liver, as genetic deletion of Il18 leads to development of NASH in chow-fed mice (Yamanishi et al., 2016). Loss of *Il18bp* expression by KCs during NASH could therefore adaptively promote proper metabolism, however this hypothesis has not been explicitly tested. In contrast to the decrease in LXR LDTF function, LXR ChIP-seq also showed that LXR retained many of its canonical targets (*Abca1*, *Abcg1*, *Mylip*) in KCs during NASH (Seidman et al., 2020). How the loss of KC specific gene expression affects the development of NASH has not been studied but remains a promising area for future research.

Globally, NASH was associated with loss of LXR binding at over 1000 genomic loci. In loci that lost LXR binding during NASH the SPIC motif was highly enriched, suggesting that loss of the SPIC-LXR collaborative pair leads to enhancer deactivation and histone deacetylation at NASH deactivated loci (Fig. 1.3B). KC expression of SPIC steadily decreased as mice developed NAFLD and then NASH (Fig. 1.3C). KC expression of SPIC target genes such as *Hmox1* was also decreased during NASH, suggesting that this loss of SPIC also led to less transcriptional activity at its target enhancers (Fig. 1.3B). Based on these observations, it is

tempting to speculate that NASH KCs have a lower capacity for erythrophagocytosis and iron. The striking loss of SPIC transcription that occurs in KCs during NASH progression could be explained by a loss of an activating homeostatic signal or gain of a repressive NASH-associated signal. The interplay of NASH and iron homeostasis in KCs could be a promising area for future research.

The most enriched motif in NASH-specific LXR binding sites was the AP1 motif (Seidman et al., 2020). The AP1 motif is bound by many transcription factors, including c-FOS, c-JUN, and the activating transcription factor (ATF) family of TFs. Amongst these TFs, ATF3 is highly induced in KCs during NASH. Subsequent ChIP-sequencing of ATF3 bound genomic loci found that the NASH environment roughly tripled the number of loci bound by Atf3 in KCs (Seidman et al., 2020), with a substantial fraction of new ATF3 binding sites occurring and new LXRα binding sites. These findings support the hypothesis that activation of ATF3 promotes relocalization of LXR during NASH to genomic locations that contain combinations of ATF3 and LXR binding motifs (Fig. 1.3B). Of particular interest, genes with NASH induced enhancer that are occupied by increased levels of ATF3 and LXRα include *Trem2* and *Cd9*, which are markers of the SAMac phenotype. ATF3 is canonically induced by endoplasmic reticulum (ER) stress along with *Atf4* and *Xbp1,* and activates a gene expression program necessary for the restoration of cellular homeostasis (Hernandez et al., 2020; Rong et al., 2013). ER stress can be induced by the accumulation of cholesterol in the ER, which has a low tolerance for the changes in membrane fluidity associated with increased levels of cholesterol. Recently cholesterol has begun to be appreciated as an important mediator of NASH pathogenesis: cholesterol was shown to be correlated with hepatic fibrosis in mice fed high fat diets with different concentrations of cholesterol (McGettigan et al., 2019), and cholesterol has a direct fibrogenic role in mouse

hepatocytes (Wang et al., 2020). The connection between ER stress and epigenetic reprogramming of KCs remains an interesting area for future study.

Inflammasome Activation and NFκB signaling

NASH is associated with increases in gut permeability and increased translocation of gut-derived microbial products from the intestinal lumen to the portal blood (Fig. 1.3A) (Carpino et al., 2019; Mouries et al., 2019; Schnabl, 2013). Patients with NASH had higher serum levels of lipopolysaccharide compared to healthy controls. NASH patients also had a higher concentration of TLR4+ macrophages in their liver (Carpino et al., 2019). Ligand mediated activation of TLR4 leads to activation of a number of TFs, including NFκB , AP1, IRF3 and others. Collectively, these signal dependent TFs promote a large transcriptional response in LPS stimulated macrophages (Kawai & Akira, 2010). This response includes increased expression of the proinflammatory cytokines *Il1b*, *Il6*, and *Tnf* as well as components of the inflammasome. Inflammasome activation lies downstream of multiple important NASH pathways. Cholesterol crystals have been shown to activate the inflammasome in macrophages within atherosclerotic plaques (Duewell et al., 2010). Furthermore, cholesterol crystals have been shown to accumulate in KCs and hepatic macrophages in murine models of NASH (Fig. 1.3A) (Ioannou et al., 2017). Similar to pathogen associated molecular patterns, damage associated molecular patterns from dying hepatocytes such as mitochondrial DNA and ATP and reactive oxygen species produced by metabolic dysfunction are also thought to activate the inflammasome during NASH (Fig. 1.3A). Finally, activation of TLR4 by LPS alone has been shown to lead to inflammasome activation via IRAK-1 activation (Fernandes-Alnemri et al., 2013; K.-M. Lin et al., 2014). This pathway is essential for the progression of NASH, as deletion of the NLRP3 inflammasome resulted in decreased inflammation and fibrosis in mice (Mridha et al., 2017). Targeted inhibition

of hepatic NLRP3 is a promising approach in the treatment of NASH. NFκB is an upstream activator of inflammasome transcription, therefore therapeutic approaches that block NFκB activation could also prove beneficial in NASH. However, this approach is limited by non-transcriptional mechanisms of inflammasome activation, many of which occur during NASH.

Histone modifications.

TFs are one class of many DNA binding proteins within the nucleus. Histones are structural proteins that bind DNA into a unit known as the nucleosome. The core nucleosome consists of an octamer of four histones, H2A, H2B, H3, and H4, encircled by roughly 147 bp of DNA (Bannister & Kouzarides, 2011; Zhou et al., 2011). TFs act in concert with histone modifying enzymes that covalently alter histone proteins at specific amino acid residues (Zhou et al., 2011). Histone modifications subsequently impact chromatin structure and the binding of effector molecules, resulting in activation or repression of enhancers and promoters. Here we will briefly review key concepts in histone modifications, but interested readers are encouraged to consult a number of excellent reviews in this area, including a review of the relevance of histone modification to innate immunity (Bannister & Kouzarides, 2011; Dai et al., 2020; Smale et al., 2014). Two of the most common modifications are histone acetylation and histone methylation. The most well studied of these modifications occur at lysine residues in the N-terminal histone tail. Histone acetylation is determined by histone acetyltransferases (HATs) and histone deacetylases (HDACs) while histone methylation is determined by histone lysine methyltransferases (HKMTs) and histone demethylases (Bannister & Kouzarides, 2011). Genome wide studies of histone modifications show that particular histone modifications are enriched in certain regions of the genome (Zhou et al., 2011). Histone acetylation eliminates the positive charge of lysine residues and results in the relaxation of chromatin locally, allowing

increased access to DNA by TFs and other modifying enzymes (Bannister & Kouzarides, 2011). The bromodomain region of bromodomain and extraterminal (BET) proteins such as BRD2 and BRD4 binds specifically to ε-aminoacetyl groups present on acetylated histones. BRD2 recruits E2F proteins, HATs and HDACs that induce both additional chromatin remodeling and active transcription (Belkina & Denis, 2012). Notably, the BET BRD4 is important for macrophage inflammatory signaling in response to LPS (Filippakopoulos & Knapp, 2014). Inhibition of BRD4 with the synthetic inhibitor JQI was shown to suppress NFκB mediated activation of *Il1b* and *Il6 in vitro* (Nicodeme et al., 2010). Due to the downstream activity of BETs, acetylation of lysine 27 on histone 3 (H3K27Ac) is predominantly associated with active regions of chromatin, particularly active enhancers and promoters (Zhou et al., 2011). The function of histone methylation depends on the particular lysine that is methylated and whether the loci is mono-, di-, or tri-methylated. This is due in part to the high specificity of effector proteins for particular histone modifications. H3K4 mono- and di-methylation are associated with active enhancers while H3K4 di- and tri-methylation are associated with active promoters. In contrast, H3K9 di- and tri-methylation are associated with inactive promoters (Zhou et al., 2011).

Aberrant gene expression is a feature of diseases, including NASH. Studying the H3K27Ac landscape of cells therefore allows the inference of active transcriptional pathways. KC have a distinct H3K27Ac landscape compared to blood monocytes (Sakai et al., 2019). The KC H3K27Ac landscape is also sensitive to environmental perturbations. When KCs isolated from murine livers with NASH were compared to KCs isolated from homeostatic murine livers, over 6000 enhancers were found to have significant differences in H3K27Ac. Activated enhancers (defined by increased H3K27Ac) were enriched for the AP1, NFAT, RUNX, and EGR motifs, while repressed enhancers (defined by decreased H3K27Ac) were enriched for the MITF,

MAF, IRF, and LXR motifs (Seidman et al., 2020). The H3K27Ac data from the two studies cited here provide a map of putative active enhancers in murine KCs. However, no comparable map exists for human KCs.

Given that chromatin modifications lie upstream of changes in gene expression, the chromatin remodeling enzymes discussed above are compelling targets for correcting dysregulated gene expression. However, given the broad functions of many histone effector proteins, it is difficult to predict the exact consequences of the inhibition or activation of a given histone modifier (Szyf, 2009). HDAC inhibitors (HDACis) have had some success in the treatment of cancer and show promise for the treatment of type 2 diabetes, a disease closely linked to NAFLD (Szyf, 2009). However, current HDACis are limited by their low target specificity, leading to off target effects. Targeted HDACis, such as MGCD0103, which is selective for HDAC1, are being developed (Szyf, 2009). The use of targeted HDACis or other epigenetic drugs requires a deep understanding of the cell specific functions of a given histone modifier.

Certain histone modifiers have been shown to have functional roles in KCs during liver disease. Histone deacetylace 11 (HDAC11) is induced in KCs from mice exposed to a model of alcoholic liver disease and is associated with decreased IL10 expression (Bala et al., 2017). Furthermore, knockout of HDAC11 resulted in increased IL10 expression and decreased TNF secretion by RAW 264.7 macrophages, suggesting a role for HDAC11 in promoting inflammation (Bala et al., 2017). HDAC11 is the only class IV HDAC, suggesting that targeted inhibition of HDAC11 could be feasible. However, further work is required to establish whether this pro-inflammatory function of HDAC11 in KCs is due to acetyltransferase activity or a separate function of the protein.

Histone methylation is an epigenetic mark associated with both activation and repression. In KCs histone H3 lysine 4 trimethylation of the TNF promoter was required for full induction of TNF expression by LPS (Ara et al., 2008). Inhibition of KC methyltransferase activity of KCs with the methyl group donor S-adenosylmethionine or its metabolite methyladenosine blocked LPS mediated TNF expression and secretion and iNOS expression by murine KCs by inhibiting promoter H3K4 trimethylation (Ara et al., 2008). The transcription factor and HKMT EZH2 acts as a methyltransferase to promote H3K27 trimethylation (H3K27Me3) at promoters, which ultimately results in gene repression. Induction of acute liver failure in mice using LPS/d-galactosamine led to increased expression of KC *TNF* and decreased H3K27Me3 and EZH2 occupancy at the TNF promoter in KCs (T. Zhou et al., 2018). These studies establish a functional role for histone methylation in KCs at the TNF promoter. Extending these findings to the whole genome level studies using ChIP-seq would yield deeper insight into the function of each of these histone marks and the TFs that guide their deposition across the genome.

DNA methylation

DNA methylation is a covalent epigenetic mark found on cytosine nucleotides, predominately within regions of the genome enriched for cytosine-guanine dinucleotide repeats. When deposited at promoters, DNA methylation is predominately associated with transcriptional repression. DNA methylation can be transmitted to offspring. In mice, maternal high-fat diet is associated with changes in methylation at metabolic genes in offspring (Wankhade et al., 2017). DNA methylation at certain genomic loci can also be used as a proxy for aging, also known as an ‘epigenetic clock’. Epigenetic clocks are constructed by performing a supervised machine learning regression linking chronological age with epigenetic marks such as DNA-methylation (Horvath & Raj, 2018). While the exact mechanisms underlying the clock are unknown, the

correlation of groups of methylation loci with chronological age is well established across a variety of tissues. In humans, NASH is associated with accelerated aging as measured by the Horvath clock in peripheral blood monocytes (Loomba et al., 2018). DNA methylation patterns vary by cell type and thus more detailed work is required to unravel its cell specific functions during NASH (Deaton et al., 2011). DNA methylation patterns have also been shown to be heritable, and a deep understanding of the function of DNA methylation during NASH could shed light on non-coding contributions to NASH heritability through actions in KCs and other hepatic cell types.

Long noncoding RNA signaling.

Non-transcriptional mechanisms of gene regulation are highly relevant in metabolic disease. In particular, the role of RNA-mediated gene regulation by micro-RNAs (miRNAs) and long noncoding RNAs (lncRNAs) is increasingly recognized as important to understanding the progression of liver disease. LncRNAs are non-coding, transcribed RNA molecules greater than 200bp in length. LncRNAs engage in a diversity of cellular functions, including activating or repressing genes via the recruitment of transcriptional co-activators or co-repressors, acting as scaffolds for the formation of large biological complexes, and acting as decoys for RNA and DNA binding proteins (Wang & Chang, 2011). Similar to TFs, lncRNAs act in a cell specific manner by modulating gene expression at the level of enhancer and promoter activity. In the hepatic environment lncRNAs have an established role in the progression of hepatocellular carcinoma (HCC). The lncRNA downregulated in liver cancer stem cells (lnc-DILC) controls proliferation of liver cancer stem cells and is downregulated in aggressive subtypes of HCC (Wang et al., 2016). Lnc-DILC acts as a transcriptional repressor by binding to the IL6 promoter and blocking its transcription downstream of NFκB activation. Loss of autocrine IL6 signaling

led to decreased expansion of liver cancer stem cells both *in vitro* and *in vivo* (Wang et al., 2016). In contrast, increased expression of lncRNA-ROR is associated with HCC. lncRNA-ROR acts as a molecular decoy for miR-145, preventing miRNA mediated repression of the transcription factor ZEB2 (Li et al., 2017). Increased expression of ZEB2 downstream of lncRNA-ROR promoted epithelial to mesenchymal transformation and metastasis of HCC (Li et al., 2017). The lncRNA-ROR signaling pathway is of interest in myeloid cells, as ZEB2 is a LDTF for KCs and other tissue macrophages. Another well studied lncRNA is MeXis, which amplifies LXR mediated activation of the gene *Abca1* in bone marrow macrophages and in macrophages within the aortic plaque (Sallam et al., 2018). While LXR and Abca1 are highly expressed in KCs, this pathway has not been confirmed to be active in KCs *in vivo*.

A number of lncRNAs have been also associated with NASH in human studies, but in contrast to lncRNAs in HCC, the cell specific mechanisms by which these lncRNAs act remain largely unknown (Atanasovska et al., 2017; Leti et al., 2017; Sun et al., 2015). Lnc18q22.2 was recently shown to be upregulated in whole liver tissue from patients with NASH compared to those with NAFLD. *In vitro* knockdown of lnc18q22.2 in hepatocyte cell lines resulted in slower cell growth and increased apoptosis in response to cisplatin or hydrogen peroxide challenge, suggesting that lnc18q22.2 is required for hepatocyte growth and viability (Atanasovska et al., 2017). RNA-seq studies of lnc18q22.2 knockdown suggest that it could have a role in regulating the response of hepatocytes to oxidative stress (Atanasovska et al., 2017). However, much remains to be learned regarding the function of lnc18q22.2 and other NASH associated lncRNAs. Pertinent areas for further study include deeper study of the molecular mechanisms of NASH lncRNAs, the identification of transcriptional pathways upstream of lncRNA expression in NASH and investigation of the cell type specific function for NASH lncRNAs, particularly

those that act by modulating chromatin activity and gene expression. Notably, the lncRNA MeXis has well described functions in macrophages (Sallam et al., 2018). MeXis amplifies LXR mediated activation of the gene *Abca1* in bone marrow macrophages and in macrophages within the aortic plaque (Sallam et al., 2018). While LXR and Abca1 are highly expressed in KCs, pathway has not been confirmed to be active in KCs *in vivo*.

MicroRNA signaling.

miRNAs are short noncoding RNAs that act in concert with the RNA-induced silencing complex (RISC) to repress translation of target messenger RNAs (mRNAs). There are a number of reviews on the functions of miRNAs in inflammatory cells, including macrophages in the setting of liver disease (Lin et al., 2020; McDaniel et al., 2014; O'Connell et al., 2012; Szabo & Satishchandran, 2015). Here we will briefly review important miRNAs known to function in myeloid cells during NASH.

miR-155 was one of the initial miRNAs to be directly implicated in inflammation. In macrophages, miRNA-155 is a target of NFκB and acts to repress inflammatory signaling by repressing translation of PU.1, SOCS1, and SHIP1 in RAW 264.7 macrophages (O'Connell et al., 2009). When fed a NASH model diet, mice lacking global miRNA-155 have less histological steatosis and inflammation, as well as lower liver triglycerides and ALT (Csak et al., 2015). KCs extracted from mice in a model of alcoholic liver disease expressed more miR-155 than control KCs. In contrast, treatment of miR-155 deficient murine KCs with LPS *in vitro* led to increased expression of the anti-inflammatory cytokine IL10 and decreased expression of TNF. The *in vitro* function of miR-155 in KCs was attributed in part to interaction of miR-155 with the IRAK-M mRNA, suggesting that miR155 might have a different function in KCs than in other NASH relevant cell types (Bala et al., 2017). *IRAK3,* encoding IRAK-M, is specifically

expressed in monocytes and macrophages and is induced by TLR4 signaling (Kobayashi et al., 2002). The IRAK-M protein negatively regulates TLR4 signaling by inhibiting IRAK and IRAK2 activation by TLR4 (Kobayashi et al., 2002). Cellular responses to TLR4 activation can therefore be toggled by adjusting the amount of IRAK-M protein available in the cytosol (Kobayashi et al., 2002). Loss of IRAK-M repression by miR-155 should therefore lead to increased NFκB activity in the nucleus of KCs stimulated with LPS, making the observation that loss of mIR-155 leads to increased IL-10 expression a surprising result (Bala et al., 2017). A possible explanation for this observation is the presence of NFκB responsive enhancer regions near IL-10 in KCs. Careful study of dynamic enhancer regulation from *ex vivo* KCs could yield deeper insight into the role this signaling network plays in the KC LPS response.

miRNAs can also act intercellularly. Hepatocytes derived from high-fat high-cholesterol diet treated rats secreted exosomes laden with miR-192-5p (Bala et al., 2017). Treatment of macrophages with miR-192-5p *in vitro* induced inflammation as assessed by upregulation of *IL6* and *TNF*. miR-192-5p was shown to bind and inhibit the translation of Rictor, which has previously described roles in macrophage inflammatory pathways (Bala et al., 2017). This mechanism is not specific to miR-192-5p, as hepatocytes treated with ethanol produced exosomes with miR-122, which sensitized macrophages to LPS mediated activation *in vitro* (Momen-Heravi et al., 2015). Collectively, this work suggests that miRNAs are important modulators of KC inflammatory signaling. Notable KC TFs such as PU.1, STAT1, and LXR are indeed targets of miRNA regulation, which suggests the possibility that miRNAs can also tune KC transcription. However, further work with KC specific knockouts will be necessary to understand the specific function of miRNAs in KCs during NASH.

Transcription factors as therapeutic targets

Cholesterol / ER stress modulators

Cholesterol accumulation in hepatic macrophages is emerging as a key feature of NASH (Ioannou, 2016; Leroux et al., 2012; McGettigan et al., 2019). KCs have increased concentrations of cholesterol and other lipids during NASH and cholesterol crystals have been shown to directly activate the NLRP3 inflammasome (Ioannou et al., 2017). Cholesterol accumulation also induces ER stress and augments inflammatory TLR4 signaling in macrophages (Fig. 1.3A) (Ito et al., 2015; Tall & Yvan-Charvet, 2015). Furthermore, prolonged ER stress has been shown to induce inflammation on macrophages (Hotamisligil, 2010). Clinically, patients treated with cholesterol lowering drugs such as statins tend to have improved liver histology compared to matched, untreated patients, although the effect is slight (Ioannou, 2016; Park et al., 2011; Takeshita et al., 2014). Cell specific therapies that directly reduce KC ER stress or lower KC cholesterol levels may dampen NASH associated inflammation and slow or reverse disease progression.

Activation of LXRs promotes cholesterol export from macrophages to high density lipoprotein via Abca1 (Venkateswaran et al., 2000), and this transcriptional circuit remains active despite significant reprogramming of LXR in KCs during NASH (Seidman et al., 2020). Treatment of $Ldlr^{-/-}$ mice with the LXR agonist 27-hydroxycholesterol decreased hepatic infiltration of macrophages, T cells, and neutrophils when mice were fed a high-fat, high-cholesterol diet (Bieghs et al., 2013). Treatment with 27-hydroxycholesterol during NASH was also associated with decreased appearance of foamy macrophages and cholesterol aggregates in the liver, suggesting that 27-hydroxycholesterol promotes cholesterol export in KCs during NASH (Bieghs et al., 2013). Subsequently, the same group also showed that raising the levels of 27-hydroxycholesterol in myeloid lineage cells alone also improved hepatic inflammation

independently of increased serum levels of 27-hydroxycholesterol (Hendrikx et al., 2015). Historically, the development of LXR agonist drugs has been limited by their induction of steatohepatitis via activation of SREBP transcription (Repa, Turley, et al., 2000). However, recently a class of LXR agonists termed "desmosterol-mimetics" raises the potential of circumventing this side effect by simultaneously blocking SREBP processing through inhibition of their association from INSIGs in the endoplasmic reticulum (Muse et al., 2018; Yu et al., 2016). Furthermore, one of these compounds, DMHCA, specifically activated LXR in macrophages but not hepatocytes (Muse et al., 2018). The observation that DMHCA does not activate LXR signaling in hepatocytes is promising, as LXR activation in hepatocytes is associated with adverse side effects of LXR agonists, most notably hypertriglyceridemia and hepatosteatosis (Joseph et al., 2002; Repa et al., 2000). The combination of cholesterol-lowering and anti-inflammatory actions make desmosterol-mimetic LXR agonists a promising therapy in the treatment of NASH.

Macrophage ER stress can also be alleviated by activation of the vitamin D receptor (VDR) (Riek et al., 2012). VDR is expressed by hepatic macrophages and activation interferes with TLR4 signaling, making it an appealing candidate for the treatment of NASH (Fig. 1.3C) (Zhang et al., 2012). Treatment of mice with a VDR agonist and tunicamycin, an ER stress inducer, resulted in less hepatic inflammation than mice treated with tunicamycin alone. Subsequent experiments determined that VDR exerted its effect by decreasing inflammatory activation of KCs (Ying Zhou et al., 2019). Recently, Dong et al. showed that the VDR activation decreases hepatic inflammation in a diet-induced model of NASH (Dong et al., 2020). Mice treated with the VDR agonist calcipotriol showed decreased hepatic inflammation, decreased steatosis, and improved insulin resistance compared to vehicle treated controls.

Furthermore, hepatic macrophages were shown to be the primary target of calcipotriol, as depletion of hepatic macrophages with clodronate liposomes abrogated the effect of the treatment (Dong et al., 2020).

Hippo pathway modulation

The Hippo pathway has an established role in promoting hepatocellular carcinoma. Recently, members of the Hippo pathway have also been shown to be activated in the development of human and murine NASH (Xiaobo Wang et al., 2016). In NASH, Hippo-mediated activation of the transcriptional coactivator yes-associated protein (YAP) was essential for hepatic stellate cell activation and production of collagen. Blocking YAP with verteporfin or siRNAs led to decreased HSC activation *in vitro*. In hepatocytes the YAP paralogue TAZ was found to promote both features of inflammation and fibrosis development (Xiaobo Wang et al., 2016, 2020). Intriguingly, the Hippo pathway was recently found to be active in KCs during NASH. Song et al. found that YAP promotes inflammatory signaling downstream of TLR4 in KCs (Fig. 1.3C) (Song et al., 2019). Treatment of KCs with LPS led to increased transcription of YAP in a TLR4 and AP1 dependent manner (Song et al., 2019). YAP was then found to bind to the promoters of *Cxcl1 (*also known as monocyte-chemoattractant protein 1*)*, *Il6*, and *Tnf*, facilitating their transcription following LPS stimulation. Deletion of YAP in myeloid cells decreased hepatic inflammatory infiltration, AST, and ALT in a mouse model of NASH. These results suggest that targeting the Hippo pathway could ameliorate NASH through cell specific actions in multiple hepatic cell types.

PPARγ agonists

The metabolic and anti-inflammatory functions of PPARγ have made it an appealing target for the treatment of NASH. In humans, administration of thiazolidinedione class PPARγ

ligand pioglitazone improved steatosis and hepatic inflammation, but was also found to promote weight gain, which has limited its clinical use thus far (Sanyal et al., 2010). The PPARγ ligand rosiglitazone was also found to have a beneficial effect on NASH while also promoting weight gain (Ratziu et al., 2010). A meta-analysis of thiazolidinediones in NASH echoed these findings, showing that as a class they slightly improve histological evidence of disease but also cause significant weight gain (Mahady et al., 2011). Research in animal models suggests that this effect is at least in part due to the effect of PPARγ ligands on myeloid lineage cells, including KCs. Luo et al. found that treatment of RAW macrophages with the PPARγ agonist GW1929 decreased expression of the inflammatory genes *iNos2, Tnf, and Il6* in response to palmitic acid treatment. The anti-inflammatory effect of PPARγ agonism was correlated with decreased activity of the NFκB signaling pathway *in vitro* (Luo et al., 2017). Treatment of mice with rosiglitazone during the final 4 weeks of a 16-week course of high-fat diet led to decreased macrophage infiltration in the liver as measured by F4/80 histological staining. KCs from mice treated with rosiglitazone also expressed lower levels of *Tnf*, *Il6*, and *IL1b* compared to mice treated with vehicle (Luo et al., 2017). Further research will be needed to determine whether the effect of rosiglitazone is due to improved lipid homeostasis in the liver, decreased inflammation in KCs, or a combination of each of these effects. As mentioned above, PPARγ agonism also increases expression of LXRα, so it is possible that some of the anti-inflammatory effect of rosiglitazone is induced by activation of LXR target genes in KCs.

Acknowledgements:

Chapter 1, except for material describing the effects of natural genetic variation, is a reprint of the material as it appears in: Bennett H, Troutman TD, Sakai M, Glass CK. Epigenetic Regulation of Kupffer Cell Function in Health and Disease. *Front Immunol* **11**, 609618 (2021). The dissertation author was one of the primary investigators and authors of this paper.

Chapter 2: Predicting Transcriptional Mechanisms in Kupffer Cells Using Natural Genetic Variation.

Abstract:

Noncoding genetic variation is thought to drive substantial phenotypic variation within species. Tissue-resident macrophages exhibit diverse phenotypes based on tissue environment, but the degree to which these phenotypes vary across genetically diverse individuals is poorly understood. Here, we evaluated the phenotypic diversity of Kupffer cells from three inbred strains with genetic distances between 2.5-5 million single nucleotide polymorphisms and small insertions and deletions, a distance similar to that observed between an average human individual and the human reference genome. Over 10% of core Kupffer cell identity genes varied in at least one pairwise comparison of inbred strains. Transcriptomic and epigenetic profiling chimeric and F1 hybrid mouse Kupffer cells was utilized to estimate the relative effect of *cis* and trans *genetic* variation in Kupffer cells and was able to quantify the effects of cell autonomous and non-cell *trans* effects on Kupffer cell transcriptional output. By applying a bioinformatic model of cellular signaling networks, we show that transcriptional variation of the Kupffer cells can be used to infer biological pathways that control transcription within the Kupffer cell niche. These studies quantify the degree to which natural genetic variation affects the phenotype of tissue macrophage and establish a framework for leveraging the effects of natural genetic variation to identify signaling pathways that act to control cellular identity *in vivo.*

Introduction:

Tissue macrophages populate all mammalian organs and enact specific functional programs that maintain homeostasis within their tissue of residence (Lavin et al., 2014). Recently discovered examples of this behavior include metabolism of dysfunctional cardiomyocyte derived mitochondria by cardiac macrophages (Nicolás-Ávila et al., 2020) and the formation of cell-cell junctions by microglia in response to neuronal activity (Cserép et al., 2019). Studies of macrophage tissue specific functions have found that the tissue environment, or niche, is capable of instructing macrophage function (Lavin et al., 2014; Mass et al., 2016).

The transcriptional identity of Kupffer cells, the resident macrophages of the liver, is specified by interactions with the three other cell types of the liver: hepatocytes, liver sinusoidal endothelial cells, and hepatic stellate cells (Bonnardel et al., 2019; Sakai et al., 2019). Clearance of the Kupffer cell niche results in recruitment of blood monocytes into the hepatic sinusoids. Within the sinusoids LSEC derived NOTCH ligands DLL1 and DDL4 activate a poised enhancer landscape to induce transcription of Kupffer cell specific transcription factors, including the Kupffer cell lineage determining transcription factors SPIC and LXRa (Bonnardel et al., 2019; Sakai et al., 2019). Subsequently, LSEC and stellate cell derived bone morphogenic protein (BMP) signaling activates SMAD signaling, and hepatocyte derived desmosterol activates LXRa, resulting in a monocyte derived Kupffer cell with a similar transcriptional profile to an embryonic derived resident Kupffer cell (Bonnardel et al., 2019; Sakai et al., 2019). Genetic disruption of this transcriptional network or experimental blockade of niche signals leads to loss of tissue fitness, Kupffer cell apoptosis, and replacement of dying Kupffer cells by circulating monocytes (Bonnardel et al., 2019; Sakai et al., 2019). This raises the intriguing possibility that natural genetic variation could alter Kupffer cell function. This concept is supported by the

recent finding that BALB/cJ Kupffer cells phagocytosed less apoptotic hepatocytes compared to Kupffer cells in genetically distinct FVB mice (An et al., 2020). We hypothesized that natural genetic variation could alter Kupffer cell transcriptional regulation via two mechanisms: 1. Alteration of the environmental levels of Kupffer cell niche signals and 2. Disruption of Kupffer cell gene regulatory networks via alteration of TF binding motifs, a process that has been shown to occur in bone marrow derived macrophages (BMDMs) and T cells (Fasolino et al., 2020; Heinz et al., 2013; Link et al., 2018; van der Veeken et al., 2019, 2020). However, current studies of Kupffer cell transcription have been performed in the inbred C57BL/6J mouse strain and are unable to test these hypotheses.

Here we use the genetic diversity between three inbred strains of mice, C57BL/6J, BALB/cJ, and A/J to assess the stability of the Kupffer cell transcriptional and epigenetic program. While the core Kupffer cell transcriptional program is stable across diverse inbred strains, many strain dependent genes were found to be cis-regulated. Interestingly, a larger fraction of Kupffer cell specific genes were non-cell autonomous than predicted from comparison with prior in vitro studies. We also provide evidence that differential activity of leptin and lipopolysaccharide signaling pathways act to establish strain specific Kupffer cell gene expression programs *in vivo*.

Methods:

Experimental models and subject details

Mice

A/J, BALB/cJ, C57Bl/6J, and CB6F1/J mice used in this study were sourced directly from Jackson laboratories. Immunodeficient NOD-*scid* IL2Rg^{null} mice were obtained from the UC San Diego Moore's Cancer Center. For leptin treatment mice were injected with mouse recombinant

leptin (rmLeptin, R&D Systems, Stock No.498-OB) at a concentration of 1 mg/kg body weight intraperitoneally 6 hours prior to Kupffer cell isolation. Leptin was reconstituted at 1 mg/mL in 20 mM Tris-EDTA pH 8.0. Prior to injections Leptin was diluted to 0.33 mg/mL in PBS. For LPS treatment mice were injected with 0.1 mg/kg body weight LPS (Sigma Aldrich LPS E. Coli O111:B4, LPS25) intraperitoneally 2 hours prior to Kupffer cell isolation

Mixed bone marrow chimera

NOD-scid IL2Rgnull mice were conditioned with the myeloablative agent busulfan at 25 mg/kg for 2 consecutive days, as previously described (Peake et al., 2015). On the third day, mice were engrafted with 200-400 thousand erythrocyte lysed bone marrow cells at a 1:1 ratio from BALB/cJ and C57BL/6J donors. Engraftment was monitored at 4 weeks and 8 weeks in the peripheral blood by flow cytometry using antibodies targeted to strain specific haplotypes.

NASH-Model Diets

Mice were fed for up to 30 weeks with a NASH-model diet (Research Diets, D09100301 or D17010103) composed of 40 kcal% from fat, 20 kcal% from fructose, and 2% cholesterol by mass.

Method details

Hepatocyte purification and RNA isolation

Primary hepatocytes were isolated from C57BL/6J, A/J, and BALB/cJ mice as described previously (Sakai et al., 2012, 2019). Briefly, livers were perfused through the inferior vena cava with HBSS with Ca^{2+} or Mg^{2+} (GIBCO) supplemented with 10 mM HEPES (GIBCO for 3 minutes at 5 mL/min. to clear blood from the hepatic circulation. Next, livers were perfused for 18 minutes with the same base solution, this time supplemented with 0.32 mg/mL collagenase

type I (Worthington) and protease inhibitor cocktail complete - EDTA free (Roche). Hepatocytes were subsequently isolated using a Percoll (Sigma) density gradient centrifugation method. Purified hepatocytes were dissolved in Trizol (ThermoFisher 15596026) and hepatocyte RNA was extracted using the Direct-zol RNA Microprep isolation kit (Zymo Research, R2062).

Cell sorting a flow cytometry

Non-parenchymal cells from digested livers were prepared as previously described (Troutman et al., 2021). The resulting non-parenchymal cells were labeled with fluorescent antibodies and desired cell populations were purified using a Beckman Coulter Mo-Flo Astrios EQ configured with spatially separated 355 nm, 405 nm, 488 nm, 561 nm, and 642 nm lasers. Kupffer cells were defined as 355:FSCLow, SSCLow, CD146Neg, CD45Pos, F4/80High, CD11bIntermediate, Live, Singlets. Liver sinusoidal endothelial cells were defined at 355: FSCLow, SSCLow, CD45Neg, CD146Pos, Live, Singlets. Hepatic stellate cells were defined as 355: FSCHigh, SSCIntermediate, Live, Singlets.

Next generation sequencing libraries

ATAC-seq

Transposase reactions and sequencing libraries were generated as described previously (Buenrostro et al., 2013) using 25,000 to 50,000 FACS purified Kupffer cells. For each biological replicate, tagmented DNA was purified using Zymo ChIP Clean & Concentrate columns and PCR amplified for 14 cycles using barcoding primers. Libraries were size selected by gel excision to 175-225 bp (Link et al., 2018) and purified as previously outlined (Texari et al., 2021).

ChIP-seq

Chromatin immunoprecipitation and sequencing libraries were generated as outlined in a recent publication (Texari et al., 2021) with modifications to lysis, immunoprecipitation buffer, and washing buffer (Eichenfield et al., 2016; Seidman et al., 2020). In brief, FACS purified cells were fixed with 1% paraformaldehyde for 10 min at room temperature. Next, 2.625M glycine was added to 125mM to quench fixation and cells were collected by centrifugation with the addition of 0.01% Tween-20 at 1,200 X G for 10 min at 4C. Cells were washed once with 0.01% Tween-20 in PBS and collected by centrifugation at 1,200 XG for 10 min at 4C. Cell pellets were then snap frozen and stored at -80C. For ChIP reactions, cell pellets were thawed on ice and lysed in 80 ml LB3 (10mMTris/HCl pH 7.5, 100mMNaCl, 1mMEDTA, 0.5mM EGTA, 0.1% deoxycholate, 0.5% sarkosyl, 1 3 protease inhibitor cocktail, and 1 mM sodium butyrate). Lysate was sonicated using a Covaris for 12 cycles with the following setting: time, 60 s; duty, 5.0; PIP, 140; cycles, 200; amplitude, 0.0; velocity, 0.0; dwell, 0.0. Samples were collected and sufficient 10% Triton X-100 was added to produce 1% final concentration. One percent of the sonicated lysate was saved as a ChIP input. For each chromatin immunoprecipitation, aliquots of ~500,000 cells were added to 20 ml Dynabeads Protein A with 2 mg anti-H3K27ac (Active Motif) and incubated with slow rotation at 4C overnight. The following day, beads were collected using a magnet and washed three times each with wash buffer I (20 mM Tris/HCl pH 7.5, 150 mM NaCl, 1% Triton X-100, 0.1% SDS, 2 mM EDTA, and 1 3 protease inhibitor cocktail) and wash buffer III (10 mM Tris/HCl pH 7.5, 250 mM LiCl, 1% Triton X-100, 0.7% Deoxycholate, 1 mM EDTA, and 1 3 protease inhibitor cocktail). Beads were then washed twice with ice cold 10 mM Tris/HCl pH 7.5, 1 mM EDTA, 0.2% Tween-20. Sequencing libraries were prepared for ChIP

products while bound to the Dynabeads Protein A initially suspended in 25 ml 10 mM Tris/HCl pH 8.0 and 0.05% Tween-20.

RNA-seq

Poly-A RNA-seq libraries were generated as previously described (Gosselin et al., 2017; Heinz et al., 2013; Oishi et al., 2017) using 50,00 to 100,000 FACS purified cells stored in lysis/Oligo d(T) Magnetic Beads binding buffer and stored at -80˚ C, or 500 ng of purified RNA using the Zymo Research Direct-zol RNA microprep kit. mRNAs were enriched by incubation with Oligo d(T) Magnetic Beads (NEB, S1419S) and then fragmented/eluted by incubation at 94˚C for 9 min. Poly A enriched mRNA was fragmented in 2x Superscript III first-strand buffer with 10 mM DTT (Invitrogen), by incubation at 94C for 9 min, then immediately chilled on ice before the next step. The 10 µL of fragmented mRNA, 0.5 µL of Random primer (Invitrogen), 0.5 µL of Oligo dT primer (Invitrogen), 0.5 µL of SUPERase-In (Ambion), 1 µL of dNTPs (10 mM) and 1 µL of DTT (10 mM) were heated at 50C for three minutes. At the end of incubation, 5.8 µL of water, 1 µL of DTT (100 mM), 0.1 µL Actinomycin D (2 mg/mL), 0.2 µL of 1%Tween-20 (Sigma) and 0.2 µL of Superscript III (Invitrogen) were added and incubated in a PCR machine using the following conditions: 25C for 10 min, 50C for 50 min, and a 4C hold. The product was then purified with RNAClean XP beads according to manufacturer's instruction and eluted with 10 µL nuclease-free water. The RNA/cDNA double-stranded hybrid was then added to 1.5 µL of Blue Buffer (Enzymatics), 1.1 µL of dUTP mix (10mMdATP, dCTP, dGTP and 20 mMdUTP), 0.2 µL of RNase H (5 U/mL), 1.05 µL of water, 1 µL of DNA polymerase I (Enzymatics) and 0.15 µL of 1% Tween-20. The mixture was incubated at 16C for 1 h. The resulting dUTP-marked dsDNA was purified using 28 µL of Sera-Mag Speedbeads (Thermo Fisher Scientific),

diluted with 20% PEG8000, 2.5M NaCl to final of 13% PEG, eluted with 40 µL EB buffer (10 mM Tris-Cl, pH 8.5) and frozen at -80C. The purified dsDNA (40 µL) underwent end repair by blunting, A-tailing and adaptor ligation as previously described (Heinz et al., 2010) using barcoded adapters (NextFlex, Bioo Scientific). Libraries were PCR-amplified for 9-14 cycles, size selected by gel extraction, quantified using a Qubit dsDNA HS Assay Kit (Thermo Fisher Scientific) and sequenced on a Hi-seq 4000, NextSeq 500, or a NovaSeq 6000 (Illumina) according to the manufacturer's instructions.

Quantification and statistical analysis

Sequencing data analysis

FASTQ files from sequencing experiments were mapped to strain specific genome assemblies for A/J, BALB/cJ, C57BL/6J (Keane et al., 2011) as described previously (Link et al., 2018). RNA-seq files were mapped using STAR with default parameters (Dobin et al., 2013). ChIP-seq and ATAC-seq files were mapped using Bowtie2 with default parameters (Langmead & Salzberg, 2012). SAM files generated by STAR and Bowtie2 were shifted from the strain of interest to the mm10 reference genome using MMARGE (Link, et al., 2018b). Tag directories were generated from shifted SAM files using the HOMER (version 4.10, http://homer.ucsd.edu/homer/) command "makeTagDirectory" (Heinz et al., 2010).

ATAC-seq and ChIP-seq analysis

ATAC-seq and H3K27Ac ChIP-seq were used to generate genome wide maps of accessible and active chromatin. ATAC-seq peaks were called using the HOMER command with the following parameters: -style factor -L 0 -C 0 -fdr 0.9 -minDist 200 -size 200 (Heinz et al., 2010). Irreproducible discovery rate (IDR) (Q. Li et al., 2011) was used to test for reproducibility of

ATAC-seq peaks; only ATAC-seq peaks with an IDR < 0.05 were used for subsequent analysis. For sample groups with > 2 ATAC-seq libraries, peak sets from all pairwise IDR combinations were merged into a final set of peaks for further analysis. For differential peak analysis ATAC-seq tags were annotated over the merged set of ATAC-seq peaks using the HOMER command "annotatePeaks.pl" with the following parameters: -size 200 -raw. Visualization of ATAC-seq peaks was performed using normalized peak counts generated using "annotatePeaks.pl" with the following parameters -size 200 -norm 1e7. Differential H3K27ac ChIP-seq analysis was performed by annotating merged ATAC-seq peaks with ChIP-seq tag directories using the HOMER command "annotatePeaks.pl" parameters -size 1000 -raw (Heinz et al., 2010) and visualization of ATAC-seq peaks was performed using normalized peak counts generated using "annotatePeaks.pl" with the following parameters -size 1000 -norm 1e7 (Heinz et al., 2010). Differential ATAC and H3K27ac sites were called using the HOMER command "getDiffExpression.pl" with the following parameter: -peaks (Heinz et al., 2010).

RNA-seq analysis

Gene expression data was quantified using the HOMER command analyzeRepeats. Raw count data was aggregated using the following parameters: rna mm10 -condenseGenes -count exons -noadj. TPM count data was aggregated using the following parameters: rna mm10 -count exons -tpm (Heinz et al., 2010). TPM values were matched to the isoforms with the highest raw count values. Only genes with an average expression level > 8 TPM were considered for differential gene analysis. Differentially expressed genes were identified using DESeq2 with betaPrior set to TRUE (Love et al., 2014). Spider plots were generated using gene ontology enrichment analysis performed by the HOMER command "findGO.pl" (Heinz et al., 2010). All other gene ontology enrichment analyses were performed using Metascape (Zhou et al., 2019).

Motif Enrichment

Motif enrichment for experiments was performed using the MMARGE command denovo_motifs with the strain of interest set as the foreground and background strain and the -len parameter set to 8,10,12,14,16. (Link, et al., 2018b). MMARGE denovo_motifs utilizes the HOMER command findMotifsGenome.pl (Heinz et al., 2010) to perform motif enrichment while also incorporating the strain specific sequence at a given genomic locus. Background sequences were either drawn from random GC matched sequences from the strain of interest or from background peaks as identified in each analysis.

NicheNet analysis

NicheNet is a computational model that ranks ligands expressed by one or more cell types by their ability to induce target gene expression in a cell of interest (Browaeys et al., 2020). To assess putative strain specific ligand activity we first filtered the NicheNet ligand-target matrix to only consider ligands in which:

1. The ligand was expressed by a cell of the hepatic niche within that strain at > 10 TPM .
2. The receptor was expressed by Kupffer cells from that strain at > 10 TPM.

We also included selected metabolic ligands for which expression data were not available. Target genes were selected to be any gene that had significantly higher expression in a pairwise comparison of that strain ("union" gene set, adjusted p value < 0.05, log fold change > 2, TPM > 10 expression in Kupffer cells). As a background we considered all genes that were expressed at TPM > 10 in Kupffer cells. The NicheNet ligand activity score was then computed as the Pearson correlation coefficient between the ligand-target score and the binary vector indicating whether a target gene was differentially expressed. For heatmaps two top scoring ligands from each strain were aggregated and displayed with ligand z-scores. Ligand receptor interaction

scores were displayed for ligand-receptor pairs with a receptor expressed by Kupffer cells in at least one strain. For the circos plot analysis ligand-target interaction scores were displayed as arrow thicknesses linking a ligand to its target gene.

Deep learning

We implemented a neural network model for predicting accessible and active enhancers in C57BL6/J Kupffer cells using the DeepSea model architecture (Zhou & Troyanskaya, 2015) in Keras v2.3.1. Accessible enhancers were defined as IDR replicated ATAC-seq peaks with > 16 normalized ATAC-seq tags. Active enhancers were defined as IDR replicated ATAC-seq peaks with > 32 normalized H3K27Ac ChIP-seq tags. We trained two models: accessible enhancers vs. random background (auROC = 0.950) and active enhancers vs. random background (auROC = 0.902). Models were trained on 300 bp enhancer sequences, spanning ± 150bp around the peak center. Sequences from chromosome 8 and chromosome 9 were held out of model training and used as validation and testing sets, respectively. As described previously, a binary cross-entropy was used as the loss function and random background was generated using nearby GC matched sequences drawn from mm10. The fully trained models were then used to generate nucleotide 'importance scores' at base pair resolution using DeepLIFT (Shrikumar et al., 2017) for both the forward and reverse complement sequence at each peak. These scores were collapsed into a single score per bp by taking the maximum score at a given base pair.

Statistical Analysis

Genome wide signals for RNA-seq, ATAC-seq, and ChIP-seq were evaluated for differential levels using DESeq2 (Love et al., 2014). The raw p-values from DESeq2 for a given peak or gene were corrected for multiple testing using the Benjamini-Hochberg procedure. The significance of differences in promoter H3K27Ac ChIP-seq and ATAC-seq levels for particular

gene sets was evaluated using a two-sided student's t-test. To evaluate overlap between gene sets induced by LPS or leptin treatment and strain specific gene sets, we used the Fisher's exact test with the total number of genes in the contingency table set to genes with an average expression > 8 TPM in any of the sub-groups being compared. Divergence of the relative overlap of F1 and NSG strain specific genes and F0 strain specific genes was tested using the two-sided χ^2 test.

Data Visualization

Data were visualized using the UCSC genome browser (Kent et al., 2002) and custom R and Python scripts.

Results:

Genetic variation in mice alters the transcriptional programs of hepatic cells

Three in-bred mouse strains, A/J, BALB/cJ, and C57BL/6J, were selected as a genetically diverse cohort for study. These strains were selected based on publicly available genome assemblies and documented trait diversity using common models of liver disease (An et al., 2020; Farrell et al., 2014; Hui et al., 2015). A/J mice are the most genetically distant strain from the C57BL/6J reference strain, and have 1,175,330 private SNPs and 178,775 private InDels, while BALB/cJ mice have 851,619 private SNPs and 156,033 private InDels. A/J and BALB/cJ are the most closely related of the three strains with 2.0 million pairwise SNPs, whereas 4.2 million and 3.9 million SNPs separate A/J or BALB/cJ from the C57BL/6J reference strain (Supplementary Fig. 1A). Of note, the total genetic diversity between the strains is similar to the divergence between a typical human genome and the human reference genome (Auton et al., 2015); however, this is only a fraction of the diversity existing between C57BL/6J mice and wild-derived mouse strains such as CAST/EiJ and SPRET/EiJ (Keane et al., 2011)

Genetic variation contributes to trait diversity; the underlying transcriptional changes are mediated by both *cis*- and *trans*-regulatory effects. Significant progress has been made in the study of *cis* regulatory genetic variants, as well as estimation of the relative contribution of *cis* and *trans* genetic variation in cells *in vitro* and whole tissues (Bryois et al., 2014; Goncalves et al., 2012; Link et al., 2018). However, *in vivo* models studying natural genetic variation in a specific cell type are complicated by the effect of natural genetic variation in the tissue environment as a whole—these non-cell autonomous trans effects can alter the cellular niche and affect transcriptional output of the cell type being studied. These trans-effects can lead to qualitative state changes in transcriptional programs independent of cell-autonomous *cis* and *trans* genetic variation.

To understand the contribution of genetic variation to hepatic niche alterations, hepatocytes, Kupffer cells, liver sinusoidal endothelial cells, and hepatic stellate cells were purified from three mouse strains for transcriptomic comparisons (Fig. 2.1A, Supplemental Figure 2.1B). The transcriptomic data clustered predominantly by cell type and displayed cell specific gene expression patterns (Fig. 2.1B, Supplemental Figure 2.1C). We noticed contamination of stellate cells with LSEC and Kupffer cells and decided to filter these cells from subsequent analysis. We then performed pairwise comparisons of the strains to identify strain dependent transcripts. A total 4,526 genes were identified as differentially strain dependent across the cells of the hepatic niche (false discovery rate [FDR] of 0.05, 2-fold cutoff) (Fig. 1C, Supplemental Figure 2.1D). We then asked whether the effect of natural genetic variation on transcription was the same across cell types. We found that the three cell types studied displayed similar amounts of strain-dependent transcriptional diversity (Fig. 1C). Transcriptional diversity

tended to increase with the genetic distance of the strains being compared, in line with previous studies (Fig. 1D) (Link et al., 2018).

Due to the observed strain dependent variation in cellular transcription, we assessed whether the core Kupffer cell transcriptional program was differentially expressed using an orthogonal dataset. We quantified the overlap between an established list of Kupffer cell identity genes that were generated by comparison of Kupffer cells to other tissue macrophage (Lavin et al., 2014). Of the 303 Kupffer cell identity genes identified in this dataset, 33 were found to vary in at least one pairwise comparison of strains (Fig. 2.1E). By comparison, Kupffer cell specific deletion of the LDTF LXRa only altered expression of 25 out of 303 Kupffer cell identity genes using similar cutoffs (Sakai et al., 2019). Kupffer cell identity genes that were differentially regulated between strains included genes involved in core macrophage functions including efferocytosis, recruitment of effector cells, and response to reactive oxygen species (Fig. 2.1F). *Ccl24* (eotaxin-2), which is highly expressed by BALB/cJ Kupffer cells and involved in recruitment of eosinophils (Lee et al., 2020). BALB/cJ Kupffer cells also express a relatively low amount of *Trpm2,* a gene involved in the processing of reactive oxygen species and essential in the mucosal immune response to H. pylori in mice (Beceiro et al., 2017). A/J mice are depleted for expression of *Nr4a1* a transcription factor that promotes efferocytosis and is required for proper differentiation of Ly6C^{low} monocytes (Fig. 2.1F) (Hanna et al., 2012; Thomas et al., 2016). Deletion of Nr4a1 in hematopoietic stem cells led to increased inflammatory polarization of macrophages within the atherosclerotic plaque (Hanna et al., 2011). This reveals an unexpected level of variation in the core Kupffer cell transcriptional machinery across inbred strains of mice.

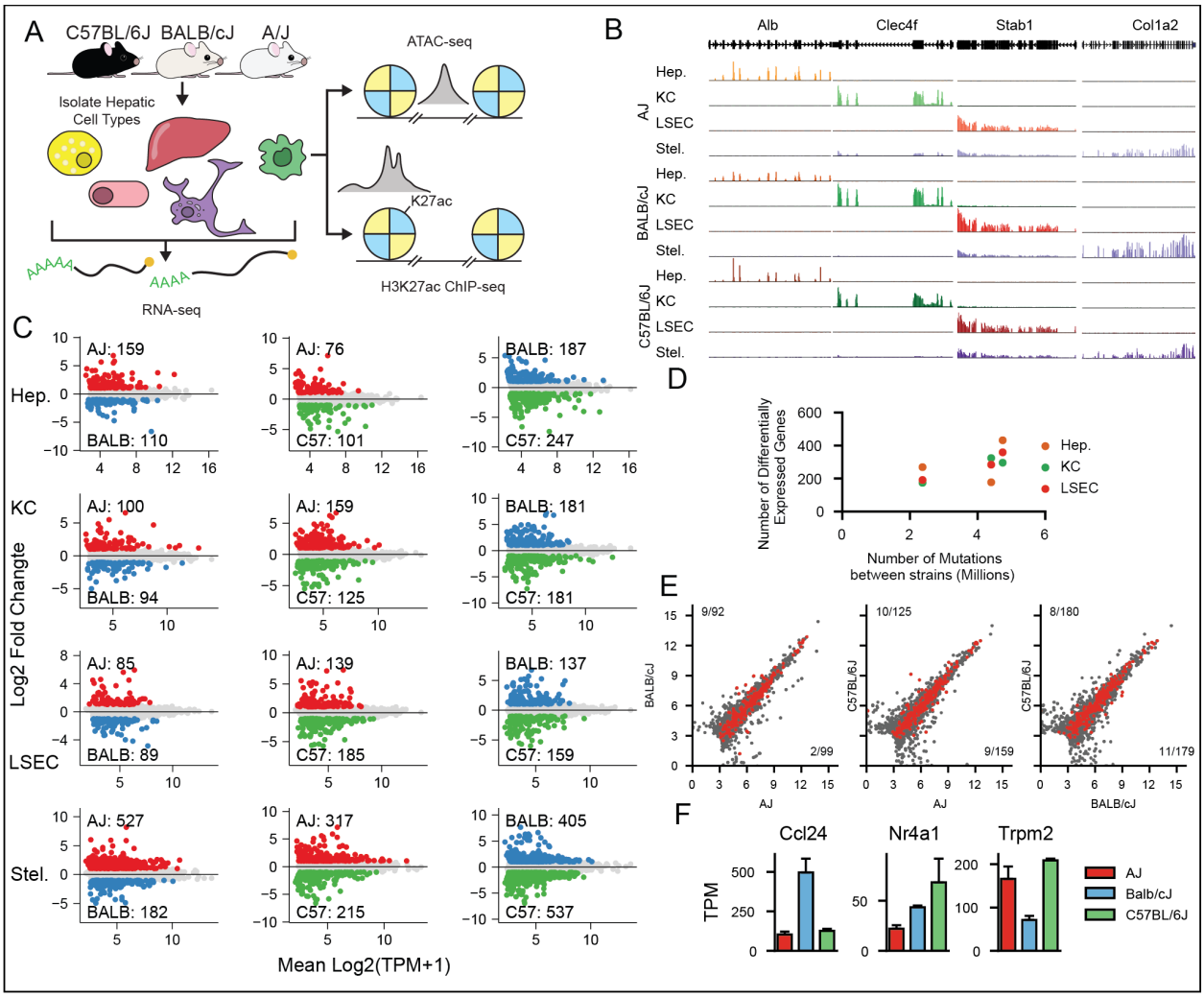

Figure 2.1: Transcriptional diversity of the hepatic niche. (A) Study design: four hepatic cell types were sorted from three inbred strains of mice. RNA-seq was performed on all cells while ATAC-seq and ChIP-seq were performed on Kupffer cells. (B) Genome browser tracks of cell-type specific genes. (C) DE genes in each pairwise comparison of strains for each cell type. (D) Relationship between mutational distance between strains and number of differentially expressed genes as determined by DESeq2. (E) Number of Kupffer cell identity genes differentially expressed in each pairwise comparison of strains. Fraction of Kupffer cell identity genes out of total differential expressed genes is shown in the corners of each scatter plot. (F) Expression of Kupffer cell identity genes varies across inbred strains. N=2 mice per group for Kupffer cell experiments and n=3-4 mice per group for all other cell types. Kupffer cells, LSECs and stellate cells were sorted from the same mice for RNA-sequencing data.

Kupffer cells from inbred strains have divergent epigenomes

We hypothesized that strain diversity of the Kupffer cell transcriptome is in part driven by strain differences in the Kupffer cell epigenome. We evaluated this hypothesis by performing

assay for transposase-accessible chromatin using sequencing (ATAC-seq) and chromatin immunoprecipitation followed by next generation sequencing (ChIP-seq) for histone 3 lysine 27 acetylation (H3K27ac) in homeostatic Kupffer cells from A/J, BALB/cJ, and C57BL/6J mice. IDR analysis identified a set of 86,302 ATAC peaks present in at least one strain. We then performed differential peak analysis for the three possible pairwise combinations of strains and identified peaks that were strain specific by selecting peaks that demonstrated increased tag counts (FDR of 0.05, 2-fold cutoff) across both comparisons. Examples of strain specific epigenetic loci are shown in Fig. 2.2A. A total of 9,282 ATAC peaks were differentially accessible in at least one comparison and 5,465 ATAC peaks were differentially acetylated (Supplemental Fig. 2.2A). We found between 594 and 1551 strain specific ATAC peaks, indicating substantial variation of the open chromatin landscape of Kupffer cells across the strains (Fig. 2.2B). Overall H3K27Ac signal was strongly correlated with ATAC signals; Spearman Rho values for intra-strain correlations of ATAC-seq and H3K27Ac ChIP-seq signal were between 0.575 and 0.586 (Supplemental Figure 2.2B). Next, we asked whether differentially acetylated regions were also differentially accessible and vice versa. We found that roughly 20-30% of differentially accessible regions were also differentially acetylated and that over 50% of differentially acetylated regions were differentially accessible (Supplemental Fig. 2.2D-E). This observation is consistent with the hierarchal collaborative model of enhancer activation, which holds that that activity of pioneering transcription factors is often required to open strain specific regions of the genome but requires the collaborative binding of other transcription factors to generate strain specific active enhancers.

Increased H3K27Ac signal at promoters is correlated with active gene expression (Nott et al., 2019). We investigated whether ATAC and H3K27Ac signal at the promoter of strain

specific genes would be highest in the corresponding strain. We found that levels of both marks at strain specific genes were significantly higher in the corresponding strain in comparison with the two other strains (Fig. 2.2C). Collectively this data suggests that strain specific levels of gene expression are due to upstream changes in the gene regulatory landscape.

Altered enhancer transcription factor binding due to motif mutations can alter transcriptional output at target promoters (Heinz et al., 2013; Hoeksema et al., 2021; Link et al., 2018; Shen et al., 2020). This phenomenon can be leveraged to identify transcription factors associated with an epigenetic mark of interest such as histone acetylation or transcription factor binding. We applied the tool MAGGIE to detect motifs whose disruption was associated with the loss or gain of ATAC-seq or H3K27Ac ChIP-seq signal. We found that MAGGIE predominantly detected transcription factors known to be important for Kupffer cell function, including PU.1, ETS factors, AP-1 family members, and IRF family members (Supplemental Fig. 2.2C).

Next, we sought to assess whether differences in the enhancer landscape were attributable to differential activity of transcription factors or local genetic variation. We assessed the potential of local genetic variation to drive strain specific opening/activation of enhancers by annotating strain specific regions with mutations using MMARGE. In support of prior work, we found that loci with strain specific ATAC and H3K27Ac signal were also associated with a 46-55% rate of mutation compared to 15-18% strain similar genomic loci (Fig. 2.2D) (Heinz et al., 2013; Link et al., 2018). Notably, this finding suggests that the remaining 50% of strain specific epigenetic loci are established by distal *cis* regulatory variation or *trans* effects.

Trans mediated changes in gene expression are driven by a diffusible factor existing within the nucleus. Conceptually, *trans* changes result either from alterations in the function of transcriptional regulators (“regulatory trans”) or from changes in the activity of upstream

signaling pathways ("sensory trans") (Tirosh et al., 2009). Regardless of mechanism, transcriptional regulators often act as this diffusible factor, and differences in transcription factor concentration or activity generate downstream *trans* effects (Bryois et al., 2014; Emerson & Li, 2010; Goncalves et al., 2012). Following this model, differential *trans* signaling pathway activity between the strains should be detectable by motif enrichment analysis of strain specific enhancers. We performed *de novo* motif enrichment analysis of strain specific open chromatin regions using both ATAC-seq and H3K27Ac ChIP-seq signal. We found that each strain was enriched for a distinct set of *de novo* motifs (Fig. 2.2E and 2.2F), suggesting that differential activity of these transcription factors could be partially responsible for establishing strain specific patterns of gene expression. Notably, the motifs for IRFs were found in nearly 10% of A/J-specific accessible regions (Fig 2.2E), and motifs for the MITF family of TFs were found in 25.67% of BALB/cJ-specific activated regions (Fig 2.2F). The high level of enrichment of these motifs at strain specific loci suggests they function to establish the regulatory landscape of A/J and BALB/cJ Kupffer cells, respectively.

We further explored the possibility that differential activity of TFs could explain strain specific loci by comparing motif enrichment scores for known transcription factor motifs in HOMER 4.10 across all strain specific peaks to enrichment scores at all accessible or active genomic loci. When calculating enrichment of motifs in a particular strain, we utilized a MMARGE wrapper function to extract strain-specific sequences from mm10 based peak coordinates. We found that the motif enrichment scores were highly correlated when all peaks were considered ($R > 0.99$ for accessible and active peaks), but markedly less so when only strain specific peaks were considered (Fig. 2.2G). These data suggest *trans* acting differences in

transcription factor activity are responsible for a subset of differences in gene expression observed in genetically diverse Kupffer cells.

Figure 2.2: Epigenetic diversity of Kupffer cells. (A) Browser tracks of strain specific loci. (B) Heatmaps of strain specific ATAC-seq peaks and associated ATAC-seq (right) and H3K27Ac ChIP-seq (left) tag density. Each column is 3kb wide. (C) Strain specific genes are associated with increased promoter ATAC-seq and H3K27Ac levels. P values calculated by students t-test. * indicates $p < 0.001$. (D) Mutational burden at strain similar and strain differential loci (fold change cutoff indicated in table, adjusted p value < 0.05). (E-F) Strain specific *de novo* motif enrichment in ATAC-seq (E) and H3K27Ac ChIP-seq (F) data, for each motif, we provide the percent of peaks within the set that contain the motif, and a p-value indicating the significance of motif enrichment within the set. (G) Correlation of known motif enrichment scores at all poised or active loci or at strain specific ATAC and H3K27Ac loci. ATAC-seq peaks were calculated using 4 biological replicates. H3K27Ac ChIP-seq data was generated using 3 biological replicates pooled from 6 mice.

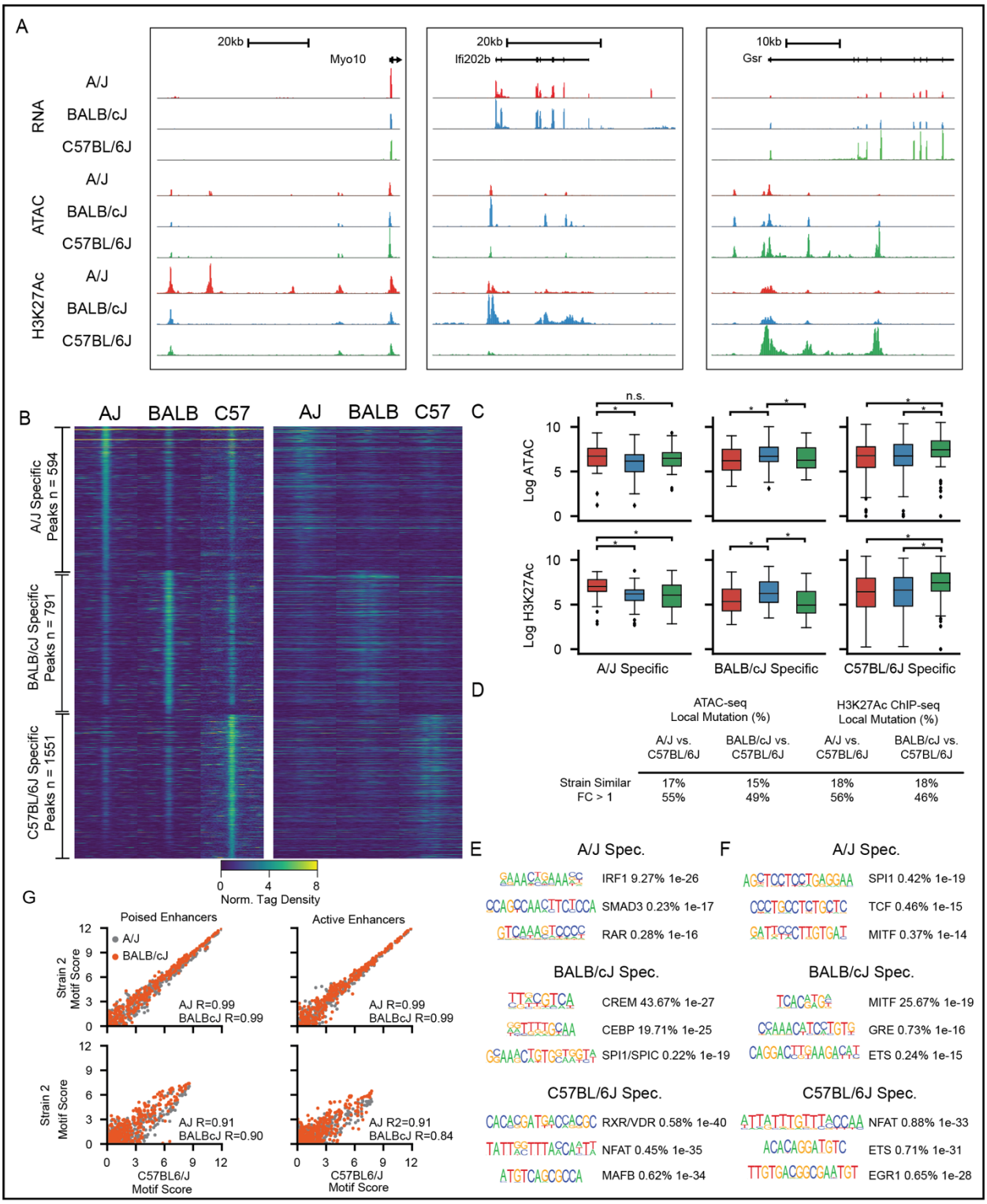
A
20kb
Myo10
20kb
Ifi202b
10kb
Gsr
RNA
ATAC
H3K27Ac
A/J
BALB/cJ
C57BL/6J
B
AJ BALB C57 AJ BALB C57
A/J Specific Peaks n = 594
BALB/cJ Specific Peaks n = 791
C57BL/6J Specific Peaks n = 1551
Norm. Tag Density
C
n.s.
Log ATAC
Log H3K27Ac
A/J Specific
BALB/cJ Specific
C57BL/6J Specific
D
ATAC-seq Local Mutation (%)
H3K27Ac ChIP-seq Local Mutation (%)
A/J vs. C57BL/6J
BALB/cJ vs. C57BL/6J
A/J vs. C57BL/6J
BALB/cJ vs. C57BL/6J
Strain Similar 17% 15% 18% 18%
FC > 1 55% 49% 56% 46%
E
A/J Spec.
IRF1 9.27% 1e-26
SMAD3 0.23% 1e-17
RAR 0.28% 1e-16
BALB/cJ Spec.
CREM 43.67% 1e-27
CEBP 19.71% 1e-25
SPI1/SPIC 0.22% 1e-19
C57BL/6J Spec.
RXR/VDR 0.58% 1e-40
NFAT 0.45% 1e-35
MAFB 0.62% 1e-34
F
A/J Spec.
SPI1 0.42% 1e-19
TCF 0.46% 1e-15
MITF 0.37% 1e-14
BALB/cJ Spec.
MITF 25.67% 1e-19
GRE 0.73% 1e-16
ETS 0.24% 1e-15
C57BL/6J Spec.
NFAT 0.88% 1e-33
ETS 0.71% 1e-31
EGR1 0.65% 1e-28
G
Poised Enhancers
Active Enhancers
A/J
BALB/cJ
Strain 2 Motif Score
AJ R=0.99
BALBcJ R=0.99
AJ R=0.91
BALBcJ R=0.90
AJ R2=0.91
BALBcJ R=0.84
C57BL6/J Motif Score

Non-cell autonomous genetic variation drives a majority of *trans* mediated gene expression differences in Kupffer cells

Kupffer cells reside in contact with liver sinusoidal endothelial cells, hepatocytes and stellate cells; given their residence in lumen of hepatic sinusoids, they are also exposed to putative ligands in the portal circulation. We suspected that differences in extracellular signaling ligands in the Kupffer cell niche were driving a substantial amount of the observed transcriptional variation between the strains. We also considered an alternative model in which cell-intrinsic differences in signaling pathway sensitivity or activity could explain *trans* differences in gene expression. We refer to these two models as cell-autonomous *trans* effects and non-cell autonomous *trans* effects. To discern the impact of cell autonomous and non-cell autonomous *trans* genetic variation we used a combination of model systems. First, we transplanted bone marrow from C57BL/6J mice or BALB/cJ mice into NOD-Scid-gamma recipient mice whose bone marrow had been ablated by busulfan treatment (Fig. 2.3A) (Peake et al., 2015). Busulfan treatment also depletes resident hepatic macrophages allowing bone-marrow derived monocytes from the donor strain to repopulate the liver of the NSG recipient mice. Kupffer cells from NSG chimeric mice exist within a matched hepatic niche but retain a strain specific intracellular environment (Supplemental Fig. 2.3A). The second model used mice from the first-generation intercross of C57BL/6J male mice and BALB/cJ female mice (CB6F1/J mice). In CB6F1/J mice the autosomal BALB/cJ and C57BL/6J genomes exist within a matched extracellular and intracellular environment, thereby exposing each genome to the same set of cell autonomous and non-cell autonomous *trans* effects of genetic variation (Fig. 2.3A).

We then performed RNA-sequencing on Kupffer cells from CB6F1/J mice and NSG chimeric mice. In order to discern allelic bias from CB6F1/J RNA-seq data we mapped the raw

sequence to each parental genome and compared the levels of perfectly mapped reads spanning mutations between the parental strains, as described previously (Heinz et al., 2013; Link et al., 2018). NSG and F1 Kupffer cells displayed similar levels of strain bias using identical statistical thresholds (Fig. 2.3B). This was surprising as we were only able to compare a total of 4407 genes in the F1 due to the relatively small amount of genetic diversity between the mRNA sequences of the two strains, whereas in NSG mice we considered all transcripts that met a minimum level of gene expression. We then compared the strain bias of NSG and F1 Kupffer cell transcripts to the strain bias observed in parental (F0) Kupffer cells. We found that 150/361 genes that were differential between BALB/cJ and C57BL/6J F0 Kupffer cells were also differential between BALB/cJ and C57BL/6J Kupffer cells isolated from NSG chimeras, while 83/361 transcripts showed allelic bias in RNA isolated from F1 Kupffer cells (Fig. 2.3B). Direct comparison of differential gene sets from each pairwise comparison shows that F0 and NSG mice share more differential genes than F0 and F1 mice (150/244 overlap in NSG versus 83/244 in F1, P=1.7e-9) (Fig. 2.3C). These observations support a model in which both cell-autonomous and non-cell autonomous (environmental) effects drive strain specific expression in Kupffer cells.

Cell-autonomous changes in gene expression can be mediated in *cis* or by *trans* changes in the activity of signaling pathways independent of extracellular ligand levels. In order to more accurately quantify the relative contribution of *cis*, cell autonomous *trans*, and cell-non autonomous *trans* variation, we compared the fold change C57Bl/6J and BALB/cJ specific genes between F0 and NSG or F0 and F1 Kupffer cells (Fig. 2.3D). We defined *cis* regulated genes to be genes that displayed significant (Fold Change > 2, adjusted p value < 0.05) strain specific bias in the same direction, *trans* genes as genes that displayed strain specific bias in the F0 but not the

NSG or F1, and *mixed* genes as those that displayed strain specific bias in the NSG or F1 but not the F0. We found that evidence that 172 genes were regulated in *trans* in the NSG hybrid, while only 124 genes were regulated in *trans* in the F1 hybrid Kupffer cells (Fig. 2.3D). We then filtered the set of *trans* genes that lacked mutations from both comparisons to only consider genes in which we were able to detect allelic bias in the F1 (Fig. 2.3E). We then asked whether a given transcript was determined to be *trans* in the NSG, F1, or both. We found that of the transcripts in which we were able to establish allelic bias in the F1, the majority (79/125) were detected to be *trans* in both the NSG and F1 mice and are likely to be driven by environmental *trans* effects in the F0 parental strain that are lost in both the NSG and F1 models. Many of the remaining transcripts (38/125) were found to be *trans* in the F1 mouse but not the NSG mouse, suggesting that they are caused by cell-autonomous differences upstream of transcription factor binding. A small proportion (8/125) genes were found to be *trans* regulated in the NSG mouse but not the F1. Examples of each type of *trans* gene are shown in Fig. 2.3F. Based on these data, we estimate that roughly 2/3 of *trans* mediated genetic variation in Kupffer cells is driven by cell non-autonomous differences in environmental signals, while 1/3 of *trans* mediated genetic variation is due to cell-autonomous differences in signaling or transcriptional activity.

Figure 2.3: Regulation of gene expression by cell autonomous and non-autonomous trans effects. (A) Graphic depicting model systems used to resolve cell autonomous and non-autonomous *trans* effects of genetic variation. (B) Scatter plots demonstrating genetic diversity in NSG chimeras and F1 hybrids and the overlap of strain specific genes in this system with strain specific genes in the F0 mice. (C) Overlap of differential gene sets from each pairwise comparison. (D) Log-log plots illustrating the identification of *cis*, *trans*, and *mixed* gene sets. (E) Separation of *trans* regulated genes into genes that are trans in one or both model systems. (F) Bar plots showing expression of *trans* regulated genes that are shared by NSG and F1 or NSG/F1 specific, fold change between strains is noted above the bar plot for each comparison.

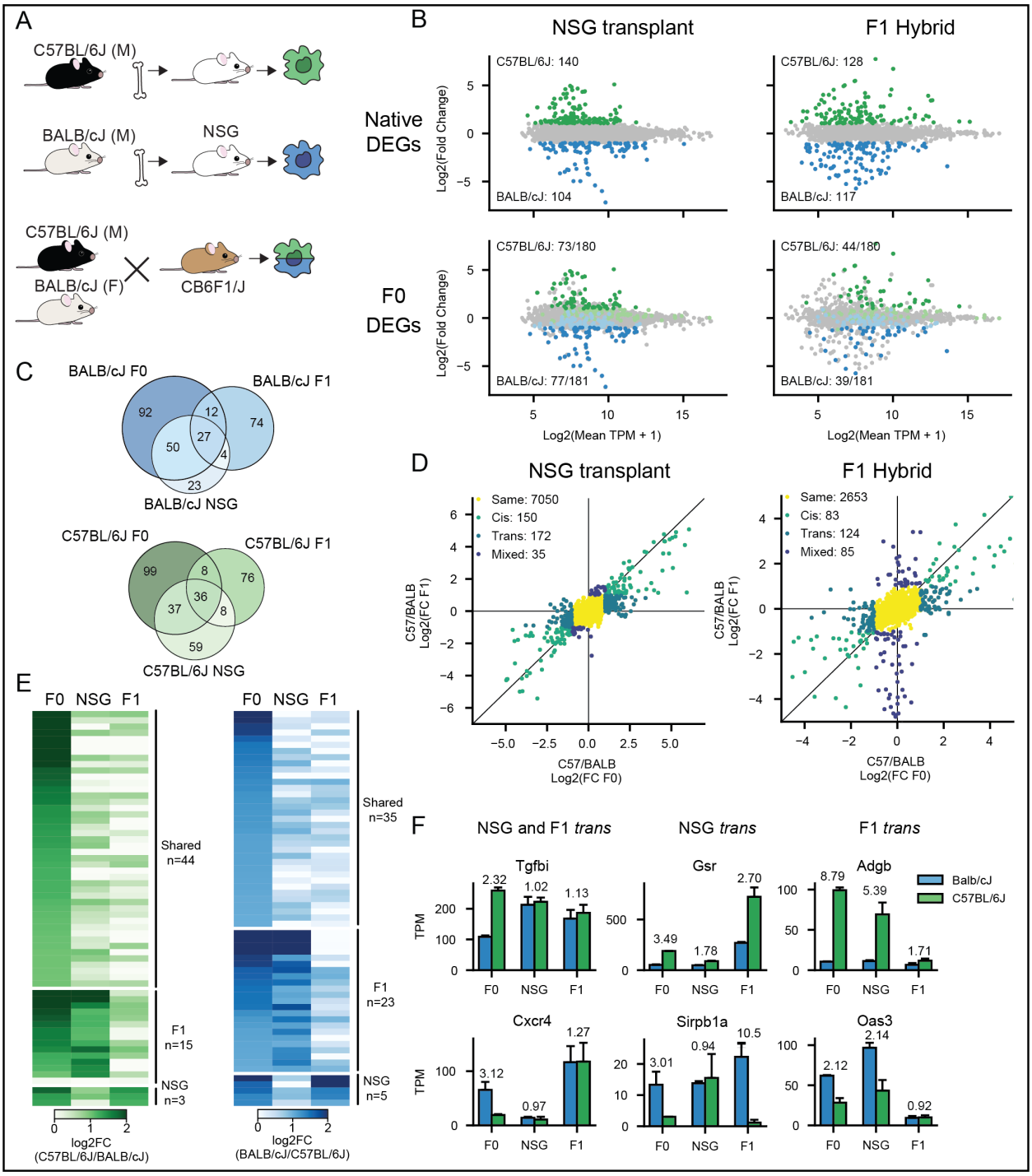
A
C57BL/6J (M)
BALB/cJ (M)
NSG
C57BL/6J (M)
BALB/cJ (F)
CB6F1/J
B
NSG transplant
F1 Hybrid
Native DEGs
F0 DEGs
C57BL/6J: 140
BALB/cJ: 104
C57BL/6J: 128
BALB/cJ: 117
C57BL/6J: 73/180
BALB/cJ: 77/181
C57BL/6J: 44/180
BALB/cJ: 39/181
Log2(Fold Change)
Log2(Mean TPM + 1)
C
BALB/cJ F0
BALB/cJ F1
BALB/cJ NSG
C57BL/6J F0
C57BL/6J F1
C57BL/6J NSG
D
NSG transplant
F1 Hybrid
Same: 7050
Cis: 150
Trans: 172
Mixed: 35
Same: 2653
Cis: 83
Trans: 124
Mixed: 85
C57/BALB Log2(FC F1)
C57/BALB Log2(FC F0)
E
F0 NSG F1
Shared n=44
F1 n=15
NSG n=3
Shared n=35
F1 n=23
NSG n=5
log2FC (C57BL/6J/BALB/cJ)
log2FC (BALB/cJ/C57BL/6J)
F
NSG and F1 trans
NSG trans
F1 trans
Tgfbi
Gsr
Adgb
Cxcr4
Sirpb1a
Oas3
Balb/cJ
C57BL/6J
TPM

F1 hybrid transcriptomics reveal differential lipopolysaccharide - toll like receptor 4 signaling pathway activity in Kupffer cells

Our studies of the NSG and F1 models suggest that a substantial fraction of strain-differential genes observed in F0 Kupffer cells were driven by differences in the Kupffer cell niche between the F0 strains. We reasoned that differences in environmental signaling should result in the activation of distinct transcriptional modules within the strains. Therefore, bioinformatic analysis of *trans* gene sets could identify signaling pathways that are differentially active in F0 mice but lost when Kupffer cells are transplanted into a matched environment.

We identified *trans* regulated genes as those differentially expressed (fold change > 2, adjusted p value < 0.05) between C57BL/6J and BALB/cJ that also show significant differences in allelic expression in CB6F1/J mice. By these criteria 124 genes are *trans* regulated, where 61 have greater expression in C57BL/6J mice and 63 have greater expression in BALB/cJ mice. Gene ontology analysis revealed that C57BL/6J *trans* regulated genes are enriched for genes involved in antigen presentation and response to lipopolysaccharide, including *Aoah, Lbp*, and *Tnfaip3*, whereas BALB/cJ *trans* regulated genes were enriched for cell removal and chemokine signaling programs, including *Cxcr4* and *Pf4* (Fig 2.4A, B). Kupffer cells are exposed to portal lipopolysaccharide and other microbial endotoxins derived from the gut microbiota (Carpino et al., 2019). Differences in C57BL/6J *trans* gene expression could be due to upstream differences in toll-like receptor signaling. Known motif enrichment analysis of C57BL/6J *trans* gene promoters revealed enrichment for motifs bound by NFκB, as well as a motif for the PU1:IRF8 heterodimer (Fig 2.4C). In total, 22.95% of C57BL/6J *trans* promoters displayed a functional NFκB-p65 motif, including the C57BL/6J *trans* gene *Tnfaip3* (Fig. 2.4D). Collectively, these

data suggest that a subset of *trans* differences in C57BL/6J and BALB/cJ gene expression is due to differences in NFκB activity at target promoters.

Next, we asked whether differential recruitment of inflammatory transcription factors such as NFκB or the IRF family could be detected when comparing BALB/cJ and C57BL/6J Kupffer cell epigenetic data. When comparing ATAC-seq and H3K27Ac ChIP-seq levels at IDR-validated ATAC-seq peaks, we observed 6,527 genetic loci at which BALB/cJ and C57BL/6J Kupffer cells differed in ATAC-seq signal intensity and 4,871 sites at which they differed in H3K27Ac signal intensity (Fig. 2.4E, F). Known motif enrichment of strain specific sites revealed that C57BL/6J specific regions of both open and active chromatin were enriched for sequences containing the ISRE motif and that C57BL/6J-specific regions of open chromatin were enriched for sequences containing the NFκB motif (Fig. 2.4G). In comparison BALB/cJ-specific regions of open and active chromatin were enriched for AP-1 factor, RUNX, and MITF family member motifs (Fig. 2.4G).

Based on these results, we predicted that treating BALB/cJ mice with lipopolysaccharide would increase expression of C57BL6/J *trans* genes in BALB/cJ Kupffer cells. We tested this hypothesis by isolating Kupffer cells from BALB/cJ mice treated with 0.1 mg/kg intraperitoneal LPS for 2 hours (Fig. 2.4H). RNA-seq on LPS-treated BALB/cJ Kupffer cells demonstrated that 1,452 transcripts were induced by LPS treatment (Fig. 2.4I). We found significant overlap between LPS-induced genes and C57BL/6J *trans*-specific genes but not between LPS-repressed genes and C57BL/6J *trans*-specific genes (26/61 transcripts, P=3.0e-7, 0/61 of LPS-repressed genes in C57BL/6J *trans*-specific gene sets, P=1.0) (Fig. 2.4J, K). This finding provides additional evidence that differential activity of inflammatory pathways contributes to strain specific differences in Kupffer cell gene expression.

Figure 2.4: Trans genetic diversity between the strains is putatively regulated by differential NF-kB signaling. (A) Metascape pathway enrichment for C57BL/6J and BALB/cJ *trans* genes. (B) Fold change comparisons of select C57BL/6J and BALB/cJ *trans* genes. (C) *de novo* motif enrichment at promoters of C57BL/6J *trans* genes. (D) Browser shot of H2-Q7 locus, a *trans* expressed gene whose promoter contains an NFkB motif. (E-F) Epigenetic differences between C57BL6/J and BALB/cJ. Differential genes calculated using DESeq2 for ATAC (E) and H3K27Ac (F) data. (G) Motif enrichment scores for known HOMER motifs at BALB/cJ and C57BL/6J specific ATAC-seq and H3K27Ac ChIP-seq peaks. (H) Graphic illustrating the approach used for the LPS study. (I) Kupffer differential gene expression induced by LPS treatment of BALB/cJ mice. (J) Convergence of the BALB/cJ and C57BL/6J Kupffer cell transcriptomes following treatment of BALB/cJ mice with LPS.

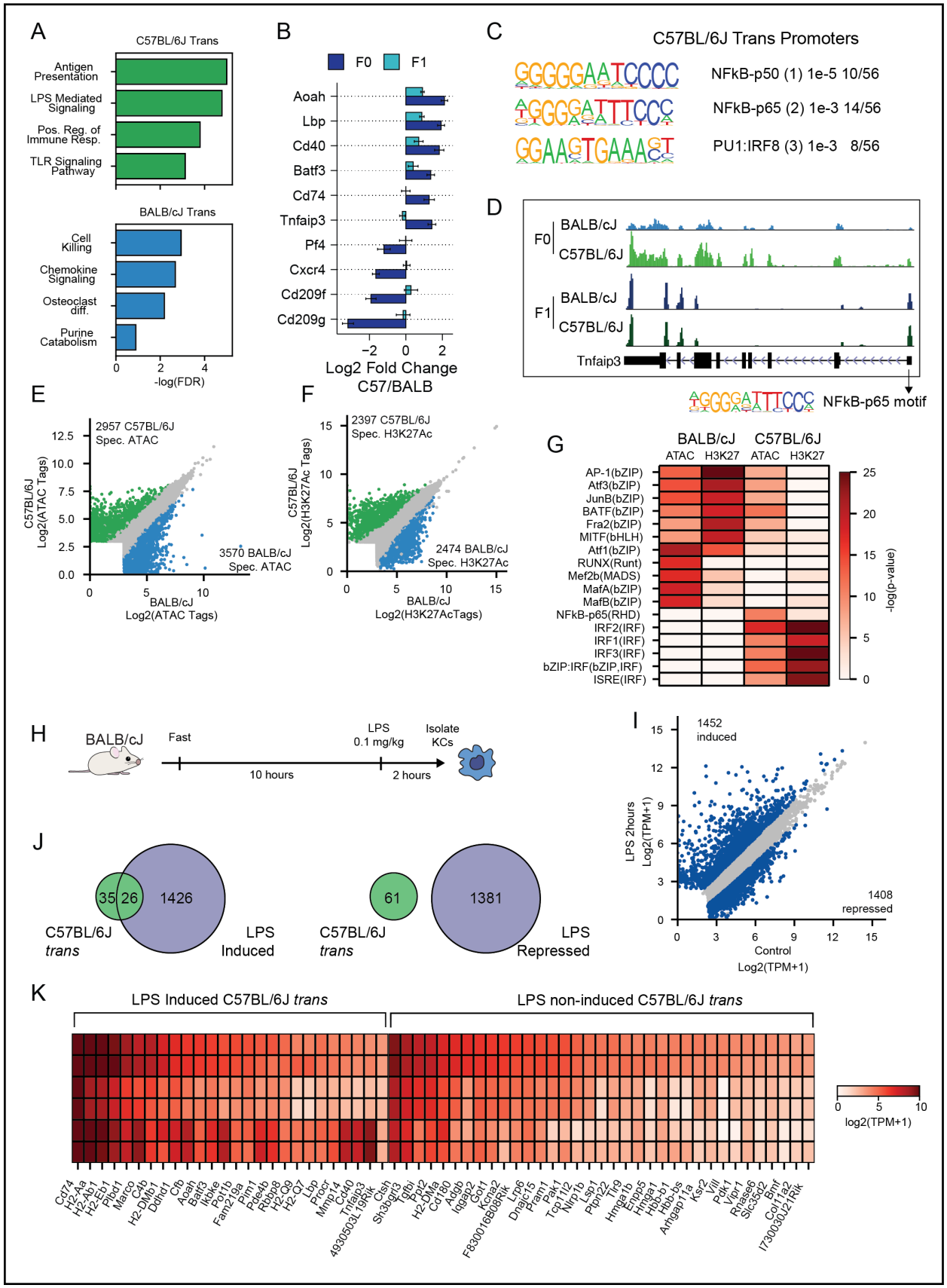
A
C57BL/6J Trans
Antigen Presentation
LPS Mediated Signaling
Pos. Reg. of Immune Resp.
TLR Signaling Pathway
BALB/cJ Trans
Cell Killing
Chemokine Signaling
Osteoclast diff.
Purine Catabolism
-log(FDR)
B
F0
F1
Aoah
Lbp
Cd40
Batf3
Cd74
Tnfaip3
Pf4
Cxcr4
Cd209f
Cd209g
Log2 Fold Change C57/BALB
C
C57BL/6J Trans Promoters
NFkB-p50 (1) 1e-5 10/56
NFkB-p65 (2) 1e-3 14/56
PU1:IRF8 (3) 1e-3 8/56
D
F0
BALB/cJ
C57BL/6J
F1
BALB/cJ
C57BL/6J
Tnfaip3
NFkB-p65 motif
E
2957 C57BL/6J Spec. ATAC
3570 BALB/cJ Spec. ATAC
C57BL/6J Log2(ATAC Tags)
BALB/cJ Log2(ATAC Tags)
F
2397 C57BL/6J Spec. H3K27Ac
2474 BALB/cJ Spec. H3K27Ac
C57BL/6J Log2(H3K27Ac Tags)
BALB/cJ Log2(H3K27AcTags)
G
BALB/cJ
C57BL/6J
ATAC
H3K27
AP-1(bZIP)
Atf3(bZIP)
JunB(bZIP)
BATF(bZIP)
Fra2(bZIP)
MITF(bHLH)
Atf1(bZIP)
RUNX(Runt)
Mef2b(MADS)
MafA(bZIP)
MafB(bZIP)
NFkB-p65(RHD)
IRF2(IRF)
IRF1(IRF)
IRF3(IRF)
bZIP:IRF(bZIP,IRF)
ISRE(IRF)
-log(p-value)
H
BALB/cJ
Fast
10 hours
LPS 0.1 mg/kg
2 hours
Isolate KCs
I
1452 induced
1408 repressed
LPS 2hours Log2(TPM+1)
Control Log2(TPM+1)
J
35
26
1426
C57BL/6J trans
LPS Induced
61
1381
C57BL/6J trans
LPS Repressed
K
LPS Induced C57BL/6J trans
LPS non-induced C57BL/6J trans
log2(TPM+1)
Cd74 H2-Aa H2-Ab1 H2-Eb1 Plbd1 Marco C4b H2-DMb1 Ddhd1 Cfb Aoah Batf3 Ikbke Pcdh1b Fam219a Pim1 Pdeab Rbpj8 H2-Q9 H2-Q7 Lbp Procr Mmp14 Cd40 Tnfaip3 4930503L19Rik Ctsh Sh3bgrl3 Tgfbi Pdl2 H2-DMa Cd180 Adgb Itgap2 Gol1 Kcna2 F830016B08Rik Lrp6 Dnajc15 Pram1 Pak1 Top1l2 Nlrp1b Lsp1 Ptpn22 Tir9 Hmga1b Enpp5 Hmga1 Hbb-b1 Hbb-bs Arhgap11a Ksr2 Vill Pdk1 Vipr1 Rnase6 Slc35d2 Bmf Col1a2 I730030J21Rik

Leptin, amyloid precursor protein, and apolipoprotein E are putative trans acting factors driving Kupffer cell transcriptional variation

Our observations in the F1 mouse suggest that strain specific hepatic environment controls a substantial amount of Kupffer cell gene expression differences. According to this model, strain specific differences could be driven by genetic diversity in expression levels of signaling ligands in the hepatic niche or by expression levels of cognate receptors in Kupffer cells. We next sought to identify signals driving strain specific transcriptional profiles using NicheNet, a bioinformatic model of cell signaling that connects ligands to downstream target genes (Browaeys et al., 2020). Of the curated NicheNet ligands, 88 had strain specific expression in at least one cell of the hepatic niche, while 37 NicheNet curated receptors displayed strain specific expression in Kupffer cells (Fig. 2.5A).

We used NicheNet to predict hepatic niche ligands that could contribute to strain specific gene expression. As Kupffer cells are also exposed to portal blood, we also included a selection of hormones that could alter Kupffer cell gene transcription. The top 2 ligands from each strain specific analysis and their expression levels in the hepatic niche are shown in Fig. 2.5B. Potential hepatocyte derived ligands included *ApoE*, a secreted apolipoprotein that binds the low-density lipoprotein receptor, which was predicted to induce BALB/cJ specific Kupffer cell gene expression (Fig. 2.5B). *ApoE* expression levels are significantly higher in BALB/cJ hepatocytes compared to both A/J and C57BL/6J hepatocytes, suggesting that differential levels of hepatic APOE production could lead to changes in Kupffer cell transcription (Fig. 2.5B, lower panel). LSEC-derived ligands included *Bmp2*, a member of the bone morphogenic (BMP) ligand family. BMPs are known to influence Kupffer cell expression via SMAD signaling (Bonnardel et al., 2019; Sakai et al., 2019). *Adam17* and *App* were identified as putative ligands that were

expressed at similar levels in LSECs and hepatic stellate cells. *App*, or amyloid precursor protein, was predicted to drive the C57BL/6J gene expression profile, including a selection of C57 specific inflammatory genes including *Ccl5* an*d Tnfaip3*. *Lep*, encoding the adipokine Leptin, was the top scoring ligand for prediction of BALB/cJ-upregulated Kupffer cell genes (Fig. 2.5B, upper panel). We then used the NicheNet model to link these ligands to target receptors expressed on Kupffer cells and assessed the expression of target receptors across the strains (Fig. 2.5C, upper panel). Strain specific expression of *Lepr*, the transcript encoding the leptin receptor, correlated with the NicheNet ligand activity score for leptin in each strain, with BALB/cJ expressing the most leptin receptor, followed by C57BL/6J, and A/J expressing the least (Fig. 2.5C, lower panel). Finally, we used a circos plot to link top scoring NicheNet ligands to their target genes (Fig. 2.5D). This visualization emphasizes the role of leptin in driving BALB/cJ upregulated genes and APP in driving C57BL/6J specific gene expression (Fig. 2.5D).

Next, we probed the NicheNet model to extract a putative list of TFs downstream of the top identified ligands and plotted the expression and motif enrichment values for the associated TF motifs across the inbred strains (Supplementary Fig. 2.4A). Activation of the leptin receptor by leptin leads to activation of the Janus kinase-signal transducer and activator of transcription (JAK-STAT) signaling pathway in macrophages (Maeda et al., 2009). Stimulation of macrophages with leptin has been shown to induce chemokine expression (Kiguchi et al., 2009), as well as expression of the anti-inflammatory gene suppressor of cytokine signaling 3 (*Socs3*). While we did not observe any differences in STAT motif enrichment or SOCS3 expression between the strains, we did observe enrichment for IRF motifs in A/J specific enhancer sequences (Fig. 2.2A), suggesting that the relative absence of leptin signaling in this strain could result in the increased activation of IRF family TFs due to decreased inhibition in A/J mice.

Collectively, these results suggest that a relative absence of leptin receptor signaling in A/J mice could contribute to strain specific differences in gene expression, particularly in comparison to BALB/cJ mice.

We tested this hypothesis by isolating Kupffer cells from A/J mice treated with 1 mg/kg leptin for 6 hours (Fig. 2.5E). We performed RNA-seq and ATAC-seq to assess the effect of leptin on the A/J transcriptome and epigenome. We found that at this timepoint and dose leptin was associated with a modest effect on gene expression (Supplemental Fig. 2.4B). However, there was significant overlap between genes expressed significantly higher in BALB/cJ Kupffer cells compared to A/J Kupffer cells and genes induced by treatment of A/J Kupffer cells with leptin. (10/37 leptin induced, $P< 1e-6$). By comparison the overlap between leptin repressed genes and those expressed highly by BALB/cJ Kupffer cells was not significant (1/27 leptin repressed, $P=0.69$) (Fig. 2.5F). Similarly, 4/27 genes were leptin-repressed were also repressed in A/J Kupffer cells relative to BALB/cJ Kupffer cells ($P< 0.01$) (Fig. 2.5E). Treatment of A/J mice with leptin altered the open chromatin landscape of Kupffer cells (Supplemental Fig. 2.4D). Motif enrichment analysis of enhancers with decreased accessibility following leptin treatment were for IRF3 and NFκB motifs in repressed enhancers, suggesting that leptin treatment could suppress the activity of these transcription factors in Kupffer cells (Supplemental Fig. 2.4E). Motif analysis also detected enrichment for the ZEB2 motif (Supplemental Fig. 2.4E). ZEB2 is essential for specification of Kupffer cell identity (Scott et al., 2018), raising the possibility that leptin signaling is involved in Kupffer cell differentiation. In full, these results demonstrate that the transcriptional diversity of inbred strains of mice can be leveraged to identify putative ligand-receptor interactions that determine strain specific programs of gene expression.

Figure 2.5: NicheNet analysis identifies leptin as trans acting Kupffer cell ligand in inbred strains. (A) Expression diversity of NicheNet annotated receptors in Kupffer cells and NicheNet annotated ligands in other hepatic cell types. (B) Scoring of top 2 ligand per strain in NicheNet (upper panel). Expression of ligands identified by NicheNet in cells of the hepatic niche (lower panel). (C) Ligand-receptor affinity scores in the NicheNet model (upper panel). Expression of the cognate receptors of top scoring NicheNet ligands (lower panel). (D) Circos plot demonstrating regulatory gene targets of top scoring NicheNet ligands. (E) Design of leptin treatment experiment. (F, G) Convergence of A/J transcriptome towards BALB/cJ following treatment with intraperitoneal leptin.

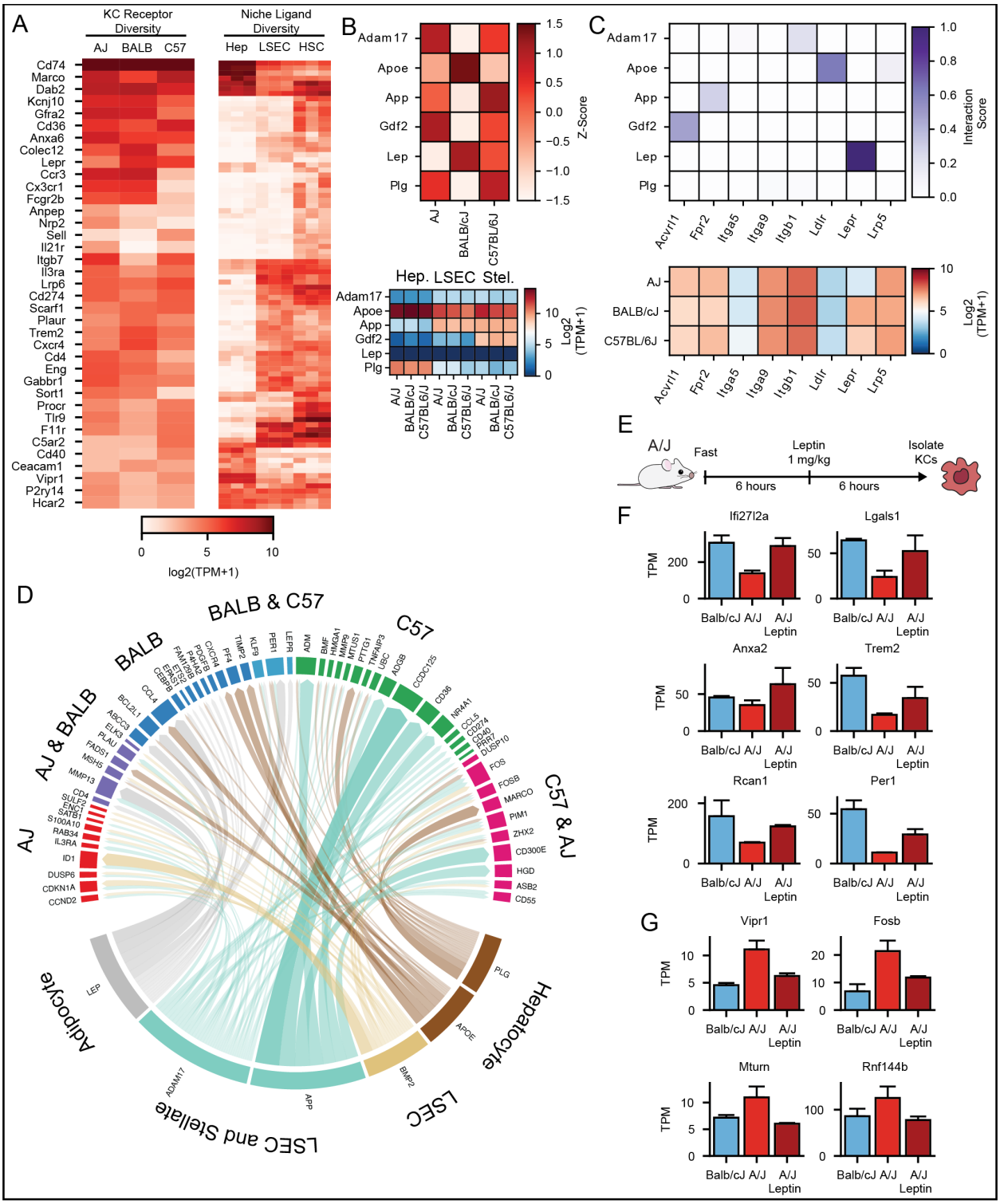
A
KC Receptor Diversity
AJ BALB C57
Niche Ligand Diversity
Hep LSEC HSC
Cd74
Marco
Dab2
Kcnj10
Gfra2
Cd36
Anxa6
Colec12
Lepr
Ccr3
Cx3cr1
Fcgr2b
Anpep
Nrp2
Sell
Il21r
Itgb7
Il3ra
Lrp6
Cd274
Scarf1
Plaur
Trem2
Cxcr4
Cd4
Eng
Gabbr1
Sort1
Procr
Tlr9
F11r
C5ar2
Cd40
Ceacam1
Vipr1
P2ry14
Hcar2
0 5 10
log2(TPM+1)
B
Adam17
Apoe
App
Gdf2
Lep
Plg
AJ
BALB/cJ
C57BL/6J
1.5 1.0 0.5 0.0 −0.5 −1.0 −1.5
Z-Score
Hep. LSEC Stel.
A/J BALB/cJ C57BL6/J A/J BALB/cJ C57BL6/J A/J BALB/cJ C57BL6/J
10 5 0
Log2 (TPM+1)
C
1.0 0.8 0.6 0.4 0.2 0.0
Interaction Score
Acvrl1 Fpr2 Itga5 Itga9 Itgb1 Ldlr Lepr Lrp5
AJ
BALB/cJ
C57BL/6J
10 5 0
Log2 (TPM+1)
D
BALB & C57
BALB
C57
AJ & BALB
C57 & AJ
AJ
Adipocyte
Hepatocyte
LSEC
LSEC and Stellate
E
A/J
Fast
Leptin 1 mg/kg
Isolate KCs
6 hours
6 hours
F
Ifi27l2a
Lgals1
Anxa2
Trem2
Rcan1
Per1
TPM
Balb/cJ A/J
A/J Leptin
G
Vipr1
Fosb
Mturn
Rnf144b
TPM
Balb/cJ A/J
A/J Leptin

Combination of parental chromosomes within a shared cellular environment generates new instances of allelic bias.

In our study of the F1 hybrid and NSG models we found a set of genes that displayed no allelic bias in F0 strains but large fold changes between the C57BL/6J and BALB/cJ alleles in the F1 or NSG mice. Strikingly, many *mixed* genes in the F1 mice had > 2-fold differences in allelic bias, whereas most NSG *mixed* genes had fold change < 2 (Fig. 2.6A). We hypothesized that mixed genes could be caused by the activation of novel transcription networks in F1 mice due to the *de novo* interactions of BALB/cJ and C57BL/6J in the same nucleus.

We investigated the gene regulatory mechanisms acting upstream of *mixed* genes by performing ATAC-seq and H3K27Ac ChIP-seq on Kupffer cells from CB6F1/J mice. We filtered ATAC-seq and ChIP-seq reads to consider only those that were perfectly mapped and spanned a mutation between the two strains. Prior to determining allelic bias, we compared the distribution of reads spanning mutations to the distribution of perfectly aligned reads. We found that mutation spanning reads were relatively depleted for low expression genes but showed an overall similar distribution shape as perfectly mapped reads (Supplemental Fig. 2.5A). We also noted substantially more diversity in mutation spanning reads compared to perfectly aligned reads, suggesting that we could detect allele-specific genomic loci (Supplemental Fig. 2.5B). We then compared mutation spanning ATAC-seq and ChIP-seq data aligned to either the C57BL/6J and BALB/cJ genome and found many instances of allelic bias in the F1 Kupffer cells (Supplemental Fig. 2.5C).

We found evidence of *trans*, *cis*, and *mixed* genetic regulation in both ATAC-seq and H3K27Ac ChIP-seq data (Fig. 2.6A-B). To aid in the interpretation of the role of motif mutations in *cis* regulatory loci, we trained two machine learning models to predict regions of open and

active chromatin, respectively. Our model was built using the DeepBind framework and showed good predictive power on our validation set of Kupffer cell peaks (AUC 0.950 for accessibility-trained model, 0.902 for activity-trained model) (Alipanahi et al., 2015; Hoeksema et al., 2021). We then used DeepLift to assign importance scores on a single nucleotide basis and identify nucleotides likely to alter chromatin activation or accessibility (Shrikumar et al., 2017; Zheng et al., 2020). We found many instances in which *cis*-regulated peaks were associated with high scoring mutations in putative TF motifs. An example is shown in Fig. 2.6C at the *Marco* locus, in which a single nucleotide polymorphism disrupts an LXR binding motif and is associated with loss of ATAC and H3K27Ac signal. We overlaid this region with LXR ChIP-seq data and found that the motif lies within an LXR binding peak (Seidman et al., 2020).

We were able to detect more total sites of differential regulation in H3K27Ac ChIP-seq data due to the increased number of mutations that could be detected in the 1000 bp window used to aggregate H3K27Ac ChIP-seq data. We observed a slightly increased fraction of *mixed* loci in each dataset (~1.1% of ATAC-seq peaks, ~1.7% of H3K27Ac ChIP-seq peaks), suggesting that activation of a pre-existing Kupffer cell enhancer landscape could be more important for driving *mixed* gene expression.

To determine whether the same set of transcription factors was responsible for establishing each *cis, trans, and mixed* genetic loci, we assessed enrichment of known HOMER motifs in context-specific peaks detected in ATAC-seq and ChIP-seq data and compared the known motif enrichment scores for each strain. We found that *cis* genetic loci were well-correlated in ATAC-seq data (spearman Rho 0.39), but markedly less so in H3K27Ac ChIP-seq data (spearman Rho -0.09) (Fig. 2.6D). By comparison, we found that *trans* were anti-correlated, indicating that most *trans* motifs were strain specific. This suggests that *trans* loci are

determined by distinct sets of transcription factors in C57BL/6J and BALB/cJ, further supporting our transcriptomic observations.

We then examined the top enriched known motifs in the *mixed* gene sets. C57BL/6J and BALB/cJ mixed ATAC-seq peaks were enriched primarily for macrophage LDTFs such as PU.1 and CEBP despite being compared to all other IDR peaks in F1 mice. This suggests that some *mixed* loci are opened by LDTFs only in the F1 strain. We hypothesize that this could be due to collaboration between LDTFs and SDTFs that were not detected in this analysis due the small number of total peaks. Interestingly, BALB/cJ H3K27Ac mixed peaks were enriched for the IRF2 motif, which was also enriched in C57BL/6J specific ATAC-seq and ChIP-seq peaks (Fig. 2.6E), while C57BL/6J H3K27Ac mixed peaks were enriched for a progesterone receptor motif that was found to be highly enriched in BALB/cJ specific peaks in F0 mice (Fig. 2.6E). This result supports a model in which the activity of certain transcription factor pathways is maintained cell autonomously in the F1, thereby exposing the genome of the additional parental strain to new *trans* acting factors, resulting in their activation and the opening or activation of new regions of chromatin in the additional parental strain. In this model the lack of chromatin modification in the 'donor' strain would be due to *cis* regulatory genetic variation.

Collectively, these data provide a quantitative estimation of the relative contributions of *trans* and *cis* acting genetic variation in murine Kupffer cells. Our data supports a model in which local genetic variation drives *cis* regulated genomic loci, while loss of activity in strain specific transcription factors from F0 mice leads to loss of allelic specificity in *trans* regulated loci in the F1. Finally, we identify and describe *mixed* regulation genomic loci that show allelic bias in the F1 strain but not in the F0 parental mice.

Figure 2.6: Epigenetic assessment of mixed genomic loci suggests model for their transcriptional regulation. (A-B) Log-log plots of ATAC-seq (A) and H3K27Ac ChIP-seq (B) data between CB6F1/J mice and their F0 parental strains. (C) Example of cis-regulated genetic locus. DeepLift score of each nucleotide within highlighted peak is shown in the bottom panel. The mutation in BALB/cJ disrupts a putative LXR motif. (D) Correlation of motif enrichment scores in *cis*, *mixed*, and *trans* peak sets. (E) Top scoring known motifs in *mixed* gene sets for both strains in ATAC-seq and H3K27Ac ChIP-seq data. Motif rank is shown in parentheses, percentage indicates percent of peaks in which the motif is found.

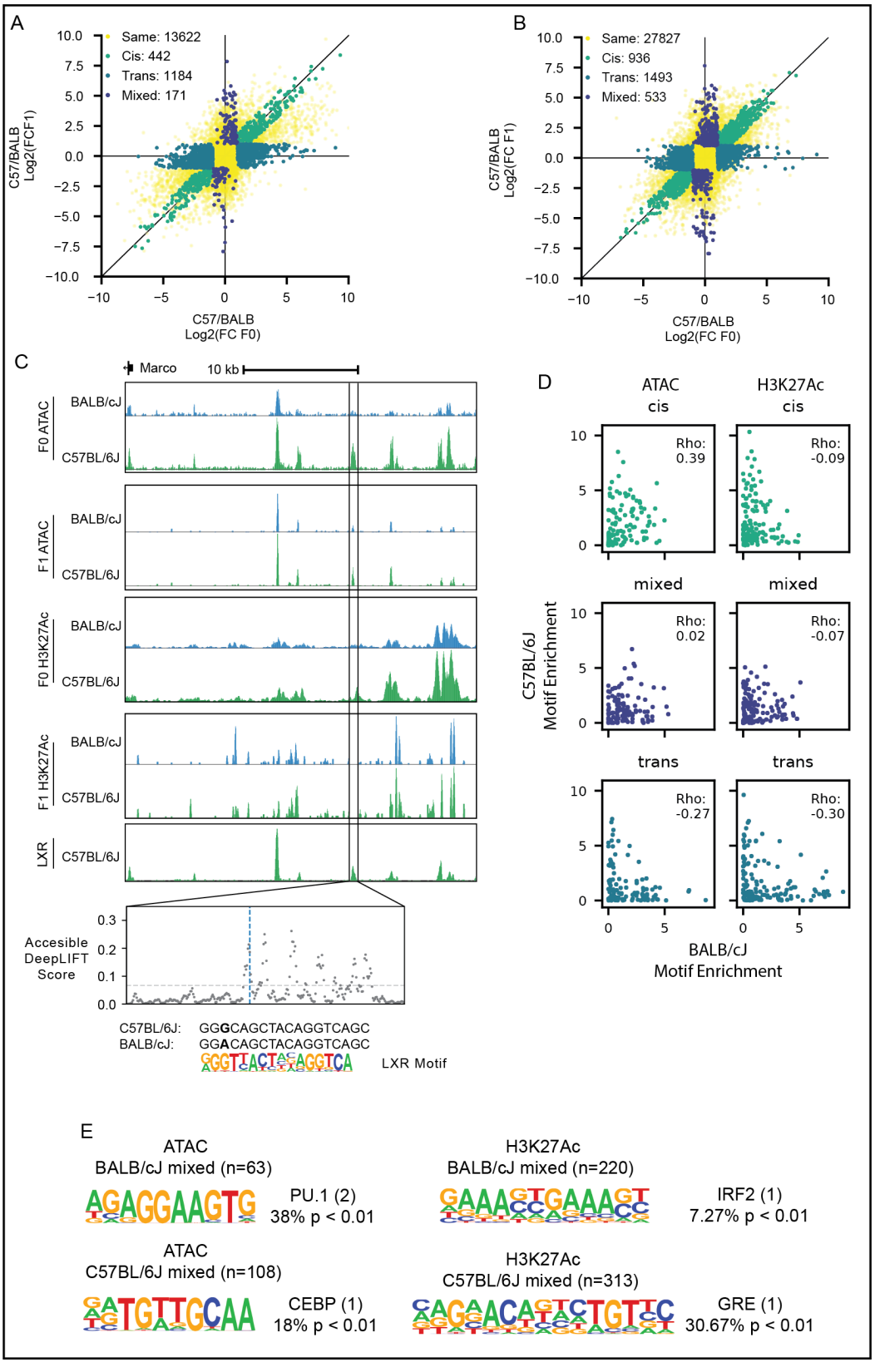
A
Same: 13622
Cis: 442
Trans: 1184
Mixed: 171
C57/BALB Log2(FCF1)
C57/BALB Log2(FC F0)
B
Same: 27827
Cis: 936
Trans: 1493
Mixed: 533
C57/BALB Log2(FC F1)
C57/BALB Log2(FC F0)
C
Marco
10 kb
F0 ATAC
F1 ATAC
F0 H3K27Ac
F1 H3K27Ac
LXR
BALB/cJ
C57BL/6J
Accesible DeepLIFT Score
C57BL/6J: GGGCAGCTACAGGTCAGC
BALB/cJ: GGACAGCTACAGGTCAGC
LXR Motif
D
ATAC
H3K27Ac
cis
mixed
trans
Rho: 0.39
Rho: -0.09
Rho: 0.02
Rho: -0.07
Rho: -0.27
Rho: -0.30
C57BL/6J Motif Enrichment
BALB/cJ Motif Enrichment
E
ATAC
BALB/cJ mixed (n=63)
PU.1 (2)
38% p < 0.01
H3K27Ac
BALB/cJ mixed (n=220)
IRF2 (1)
7.27% p < 0.01
ATAC
C57BL/6J mixed (n=108)
CEBP (1)
18% p < 0.01
H3K27Ac
C57BL/6J mixed (n=313)
GRE (1)
30.67% p < 0.01

Discussion:

These studies report systematic analysis of the cell autonomous and non-cell autonomous effects of natural genetic variation in *ex vivo* murine Kupffer cells. We find that roughly half of transcriptional variation within inbred strains of mice is due to *cis*-acting genetic variation and half is due to *trans*-acting differences in transcription factor activity. Using F1 hybrids and NSG chimeric mice, we show that approximately 2/3 of *trans* acting variation in Kupffer cells is driven by non-cell autonomous differences in the Kupffer cell niche, while the remaining 1/3 is due to cell autonomous differences such as ligand-receptor expression or sensitivity to intracellular signal transduction. We show that *trans* and *cis* regulated variation can be detected at both the mRNA transcript level and at epigenetic loci using allele specific analyses of F1 mice, and that this can be leveraged to infer transcription factor pathways controlling gene expression differences in the parental strains. We used this approach to identify the NFκB signaling pathway as a putative driver of differential gene expression in C57BL6/J mice compared to BALB/cJ mice and validated this prediction by treating mice with the TLR4 agonist LPS, which induced expression of nearly 50% of C57BL/6J biased *trans* genes in BALB/cJ mice.

Comparison of F1 and F0 mice also revealed genes that displayed large levels of allelic bias in F1 mice but not in F0 mice or NSG mice. We termed these to be *mixed* genes and set out to characterize them. Mixed genes did not cluster into functional modules or contain clear patterns of promoter motif enrichment, suggesting that in contrast to *trans* genes they were not driven by a small, distinct set of transcription factors. We therefore extended our studies to the active enhancer landscape as determined by H3K27Ac, and chromatin accessibility as determined by ATAC-seq. We found evidence for *mixed* genomic loci that demonstrated allelic

bias in the F1 but not the F0. Mixed H3K27Ac loci were enriched for transcription factor motifs that were associated with *trans* activation of chromatin of the opposite parental strain (IRF in BALB/cJ mixed loci and the PR nuclear receptor motif in C57BL/6J mixed loci). One possible mechanism for specification of *mixed* loci involved epistatic interactions between *cis* and *trans* variants. These interactions can either be enhancing (*cis* and *trans* genetic variants exert effects in the same direction) or compensating (*cis* and *trans* genetic variants exert effects in the opposite direction). Studies in several model organisms have provided evidence that compensating *cis*-*trans* pairs are preferentially selected over enhancing pairs, suggesting that it is a mechanism for stabilizing gene expression amidst the effects of natural genetic variation (Brawand et al., 2011; Goncalves et al., 2012; Signor & Nuzhdin, 2018). Compensating variation could plausibly explain *mixed* loci observed in the F1 model, as *cis* acting variants compensating for changes in *trans* transcription factor activity within the strains are exposed to a higher (or lower) functioning transcription factor from the other parental strain, resulting in an enhancing rather than compensating effect on gene expression. This is supported by the observation that *mixed* genes are more common and pronounced in the F1 model, in which transcription factors from both strains can operate within a shared nucleus, than in the NSG chimeric model, in which cells retain their distinct intracellular composition. However, it is also possible that the *mixed* genes are driven by changes in the extracellular environment that are dominantly inherited in the F1 mouse and subsequently sensed by F1 Kupffer cells. Transplantation of C57BL/6J or BALB/cJ bone marrow into CB6F1/J chimeric mice could provide deeper insight into whether cell-autonomous or non-autonomous *trans* effects are responsible for *mixed* genetic regulation by exposing C57BL/6J or BALB/cJ Kupffer cells to the CB6F1/J environment.

Under a model of compensating variation, motifs corresponding to transcription factors with differential activity should be enriched within *mixed* genetic loci because of enhancing epistatic interactions. The observation that IRF motifs are enriched both in C57BL/6J specific H3K27Ac peaks from parental Kupffer cells and BALB/cJ specific H3K27Ac *mixed* peaks from F1 Kupffer cells follows this pattern, suggesting that BALB/cJ could have a cell-autonomous defect in Kupffer cell IRF signaling. Such a defect would be consistent with the observation that BALB/cJ derived macrophages respond less intensely to lipopolysaccharide treatment than C57BL/6J derived macrophages (Watanabe et al., 2004).

We also show that tools generated for the analysis of transcription factor motif mutations can be used to identify transcription factors controlling Kupffer cell identity despite the interference of *trans* driven variation that is not correlated with motif mutations. We also used the DeepBIND and DeepLIFT machine learning network to identify nucleotides whose mutations are likely to alter chromatin activation or accessibility (Alipanahi et al., 2015; Shrikumar et al., 2017). Notably, we identified a genetic variant between C57BL/6J and BALB/cJ mice that disrupts an LXR binding element in an enhancer upstream of *Marco*, which is expressed at a significantly lower level in BALB/cJ mice than C57BL/6J mice. Whether this mutation alters LXR binding in BALB/cJ mice is an important question for future research.

Marco encodes the protein macrophage receptor with collagenous structure (MARCO), a scavenger receptor mediating phagocytosis. Prior work has shown that hepatic induction of *Marco* transcription in response to infection with *Listeria monocytogenes* is LXR dependent (Joseph et al., 2004). Here, we provide evidence that basal transcription of *Marco* is also LXR dependent. Interestingly, BALB/cJ Kupffer cells have been observed to be less phagocytic in comparison with FVB mice, resulting in increased susceptibility of BALB/cJ mice to

thioacetamide induced liver damage (An et al., 2020). Prior work has shown that LXR is a Kupffer cell LDTF essential for establishment of Kupffer cell identity, raising the intriguing possibility that LXR-mediated control of MARCO is required for the maintenance of a phagocytic Kupffer cell population, and that loss of MARCO could predispose mice to liver disease. Deeper study of the role of LXR in the control of MARCO expression during the development of murine NASH is a promising area for further research.

The utility of natural genetic variation as a genome-wide mutagenesis screen has proved to be valuable in the study of transcriptional regulation. Since its introduction nearly a decade ago, this approach has yielded insight into transcriptional regulation across many cell types, including macrophages, microglia, T-cells, and white adipose tissue (Fasolino et al., 2020; Heinz et al., 2013; Soccio et al., 2015; van der Veeken et al., 2020). Here we show that, when applied *ex vivo*, natural genetic variation can be used to discover *trans* acting drivers of genetic variation via natural perturbations of the cellular environment. We provide evidence that signaling ligands and receptor levels vary widely within the hepatic niche and show that bioinformatic tools can be used to infer differential activity in upstream signaling pathways. We used this framework to identify leptin as a putative *trans* acting factor driving expression differences between A/J and BALB/cJ mice. We provide some evidence that treatment of A/J mice with leptin results in convergence A/J and BALB/cJ Kupffer cell transcriptomes. However, it is unclear why treatment of A/J mice with leptin resulted in a large change in chromatin accessibility but a small change in gene expression. It is possible that the effect we are observing is due to indirect effects of leptin on other cells and tissues. It has been reported that intraperitoneal injection of leptin results in activation of STAT3 in target tissues within 30 minutes (Ozcan et al., 2009). Furthermore, injection of leptin was found to alter hepatic lipid composition within 2 hours. In this study, we

injected leptin 6 hours prior to isolating Kupffer cells, so it is plausible that rapid changes in other tissues could result in the delayed activation of Kupffer cells, which could then drive changes in the ATAC-seq profile of Kupffer cells without resulting in robust gene expression differences. More work will need to be done to assess the effect of acute leptin treatment in Kupffer cells, including the testing of different doses and different durations of treatment prior to Kupffer cell isolation.

Notably, leptin signaling was not identified in two recent papers describing the Kupffer cell niche; in part this could be due to the models used in these studies, which relied on repopulation of the Kupffer cell niche by bone marrow derived monocytes. The leptin receptor is not expressed by monocytes or monocyte-derived Kupffer cells, rendering them incapable of responding to leptin (Bonnardel et al., 2019; Sakai et al., 2019). Expression of the leptin receptor in myeloid derived cells is required for proper response of the hepatic compartment to acute leptin treatment (Metlakunta et al., 2017). Treatment of mice with leptin was shown to sensitize Kupffer cells to lipopolysaccharide, in part via upregulation of CD14 (Imajo et al., 2012). Our transcriptomic profiling of the four major hepatic cell types reveals that only LSECs and Kupffer cells express leptin, so any response of hepatocytes to leptin signaling is likely mediated in part by these two cell types. How Kupffer cell responses to leptin signaling influence hepatic metabolism is an intriguing area of future research. Finally, leptin is also an important circadian hormone whose levels cycle throughout the day and are highest between ZT12 and ZT24. The disruption of circadian rhythms has been shown to lead to metabolic syndrome, which is associated with the development of NAFLD and NASH. Furthermore, a large fraction of the Kupffer cell transcriptome has been shown to vary in a circadian fashion. It is intriguing to

speculate that leptin is involved in establishing Kupffer cell circadian rhythms, and that disruption of this pathway could be involved in the development and progression of NAFLD.

Overall, we believe this approach could provide significant utility in the study of tissue macrophages by providing a simple, tractable way to perturb the cellular niche. Furthermore, a niche-focused analysis of genetic variation would only require the collection of transcriptional data for the cell of interest and the surrounding niche. While the cell of interest would benefit from the preparation of a deeply sequenced transcriptional library, the niche could be approximated using bulk tissue or profiled using single cell RNA-sequencing. NicheNet has already been shown to be useful in the analysis of single cell RNA-seq data.

Collectively, the work described in this thesis reveals complex interactions between *cis* regulatory genetic variation and *trans* regulatory differences in the activity of intracellular and extracellular signaling networks. Deeper profiling of the epigenomes of the strains studied in this work using transcription factor ChIP-seq will help elucidate underlying mechanisms of cis variation and the regulatory pathways controlling the specification of *mixed* loci in F1 intercrosses. The relatively close relationship of the three strains used in this study is a limitation of the work described in this thesis. SPRET/EiJ and CAST/EiJ mice contain roughly 10-fold more mutations compared to C57BL/6J as BALB/cJ or A/J (Keane et al., 2011). Studying such wild-derived strains of mice is likely to yield even more insight into the transcriptional regulation of Kupffer cells. However, we show that even the amount of genetic variation present between closely related mouse strains (C57BL6/J, BALB/cJ, and A/J) provides sufficient resolution to detect differential pathway activation. This bodes well for extension of the approaches outlined in this paper to human studies, as the mice used in this study carry the same level of genetic variation as the average human individual does from the reference genome. Extension of this

approach to human studies will be challenged by the lack of independent biologic replicates with matched genomic backgrounds, but this could be potentially overcome by using study designs that leverage shared genetic information, such as the study of parents and their offspring.

Supplementary Information:

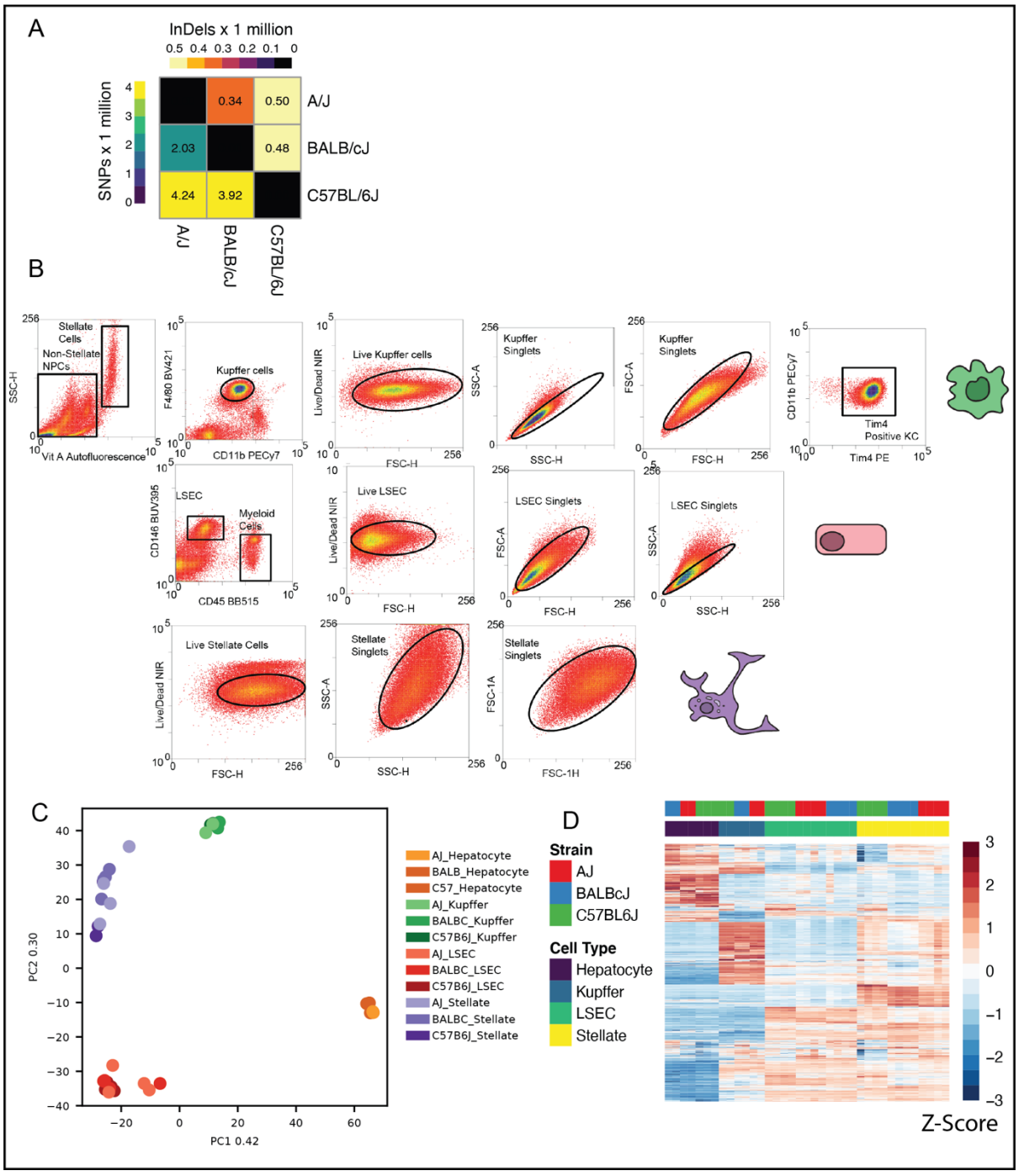

Supplemental Figure 2.1: Sample acquisition and purity. (A) Degree of natural genetic variation between the three inbred strains used in this study. (B) Sorting strategy used to isolate hepatic cell types by FACS. (C) Principal component analysis of transcriptomes of four hepatic cell types across the inbred strains. (D) Total amount of genetic variation observed between all pairwise comparisons of transcriptional data.

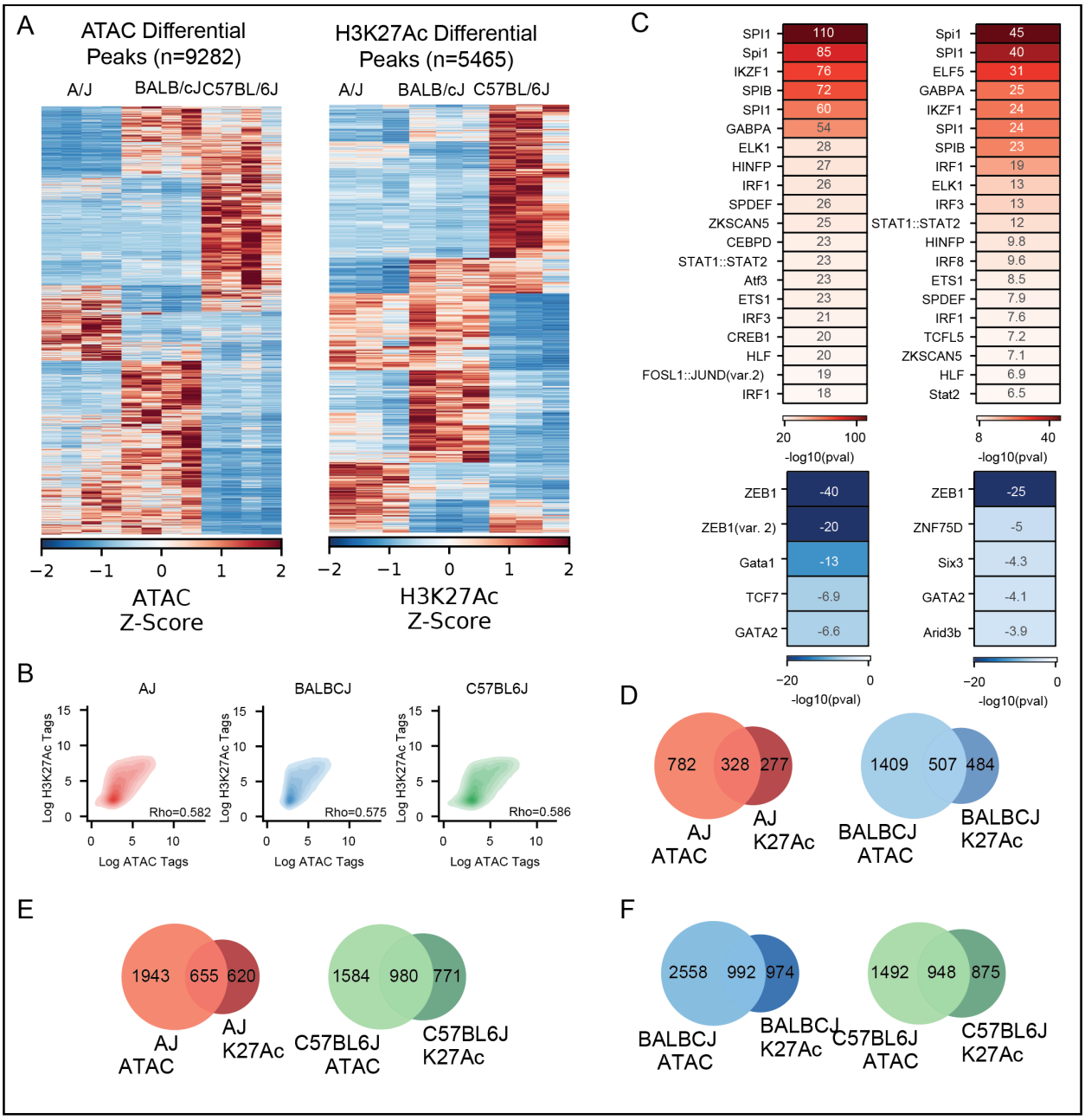

Supplemental Figure 2.2: Correlation of H3K27Ac ChIP-seq and ATAC-seq signals. (A) All pairwise differential peaks for ATAC-seq and H3K27Ac ChIP-seq data. (B) Correlation of H3K27Ac and ATAC-seq data within a strain, correlation calculated using Spearman's Rho. (C) Motifs positively (red) or negatively (blue) associated with accessible chromatin or active chromatin. Correlation p value determined using MAGGIE. (D-F) amount of overlap between pairwise significant H3K27Ac and ATAC peaks for each possible pairwise comparison of the inbred strains. N=3 independent replicates for ChIP-seq studies, N=4 independent replicates for ATAC-seq studies.

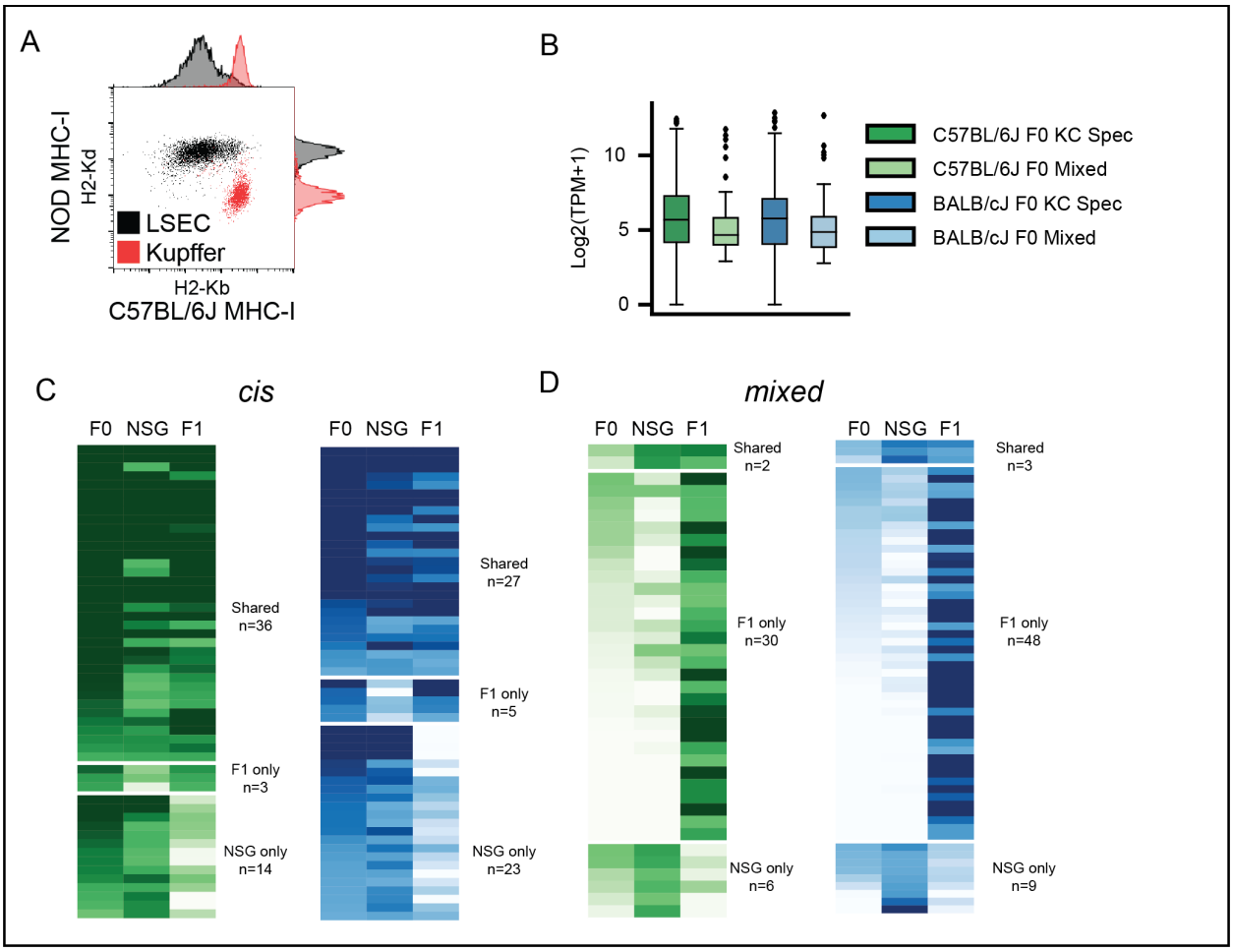

Supplemental Figure 2.3: Characterization of cis and mixed gene sets. (A) Scatter plot showing fraction of chimerism in NSG chimeras. Following bone marrow ablation busulfan, NSG mice were transplanted with C57BL/6J or BALB/cJ bone marrow. Busulfan treatment also depleted hepatic Kupffer cells, allowing for repopulation with C57BL/6J or BALB/cJ monocyte derived Kupffer cells. (B) Expression of mixed genes in F0, mixed genes displaying allele specific bias in the F1 are also expressed in F0 mice, as a comparison we include the expression of the Kupffer cell specific gene list from Lavin et al. (C, D) Degree of overlap between cis and mixed regulated genes between the F1 and NSG model systems.

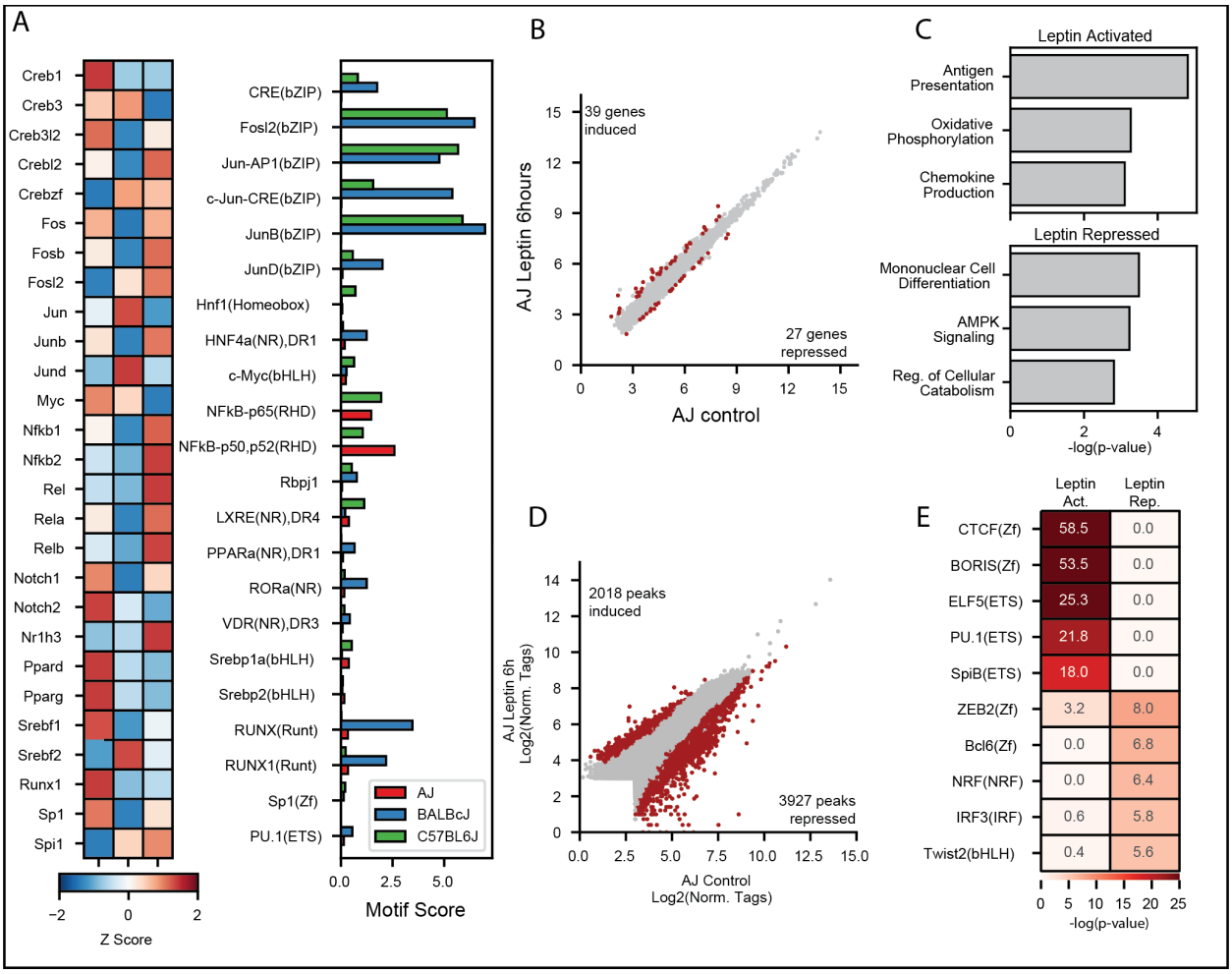

Supplemental Figure 2.4: Motif enrichment downstream of NicheNet ligands. (A) Expression and motif enrichment scores of transcription factors predicted to be downstream of top NicheNet ligands. (B) Scatter plot of leptin effect on A/J gene transcription. Colored genes are significant at Fold Change > 1.5 and adjusted p value < 0.05. (C) Functional enrichment of leptin sensitive A/J genes performed using Metascape. (D) Effect of leptin treatment on open chromatin in A/J Kupffer cells. Colored peaks are significant at Fold Change > 2 and adjusted p value < 0.05. (E) HOMER known enrichment in leptin repressed and induced peaks

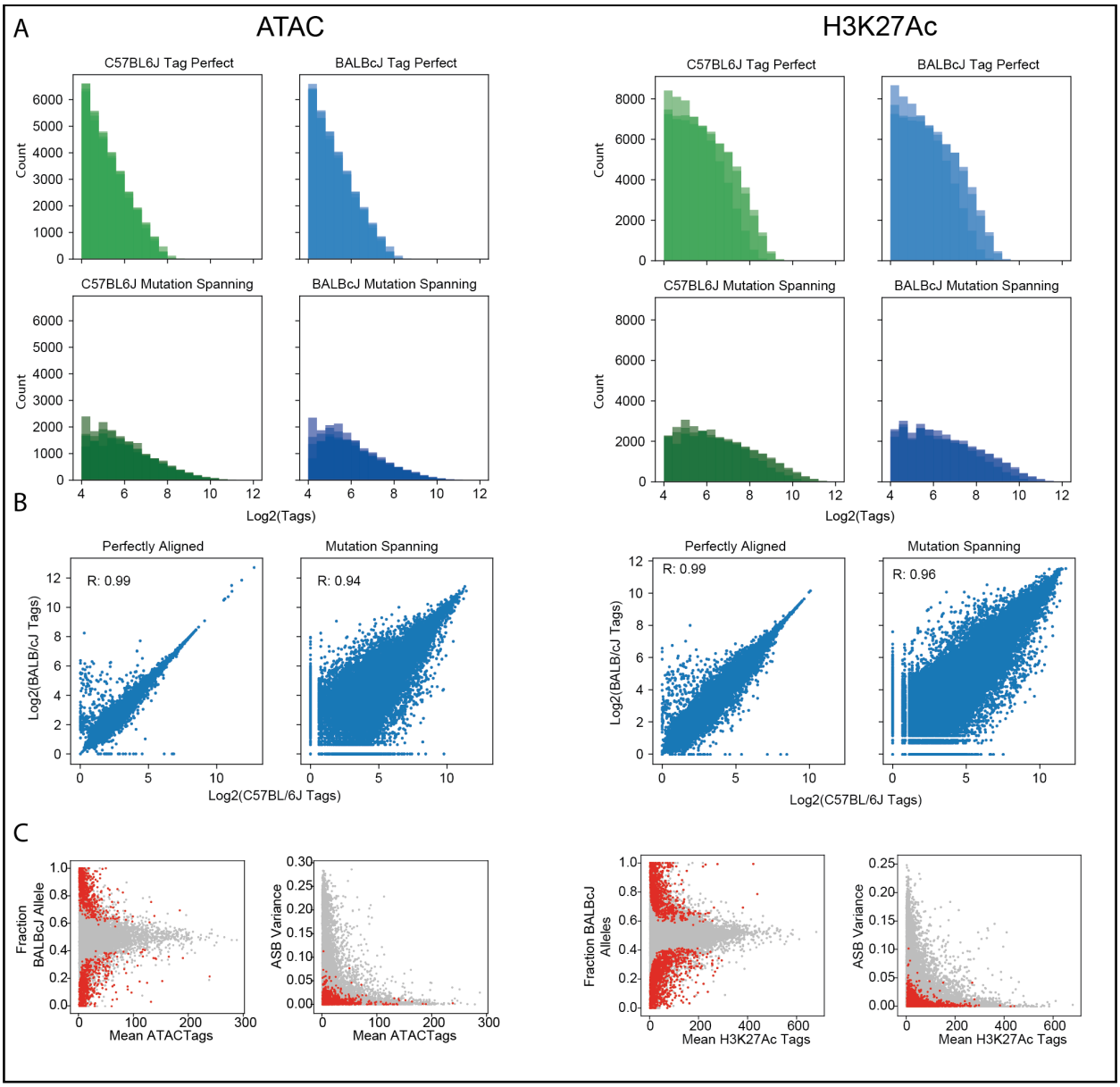

Supplemental Figure 2.5: Distributions of perfectly aligned and mutation spanning ChIP-seq and ATAC-seq reads. (A) Distribution of tag counts at all genomic loci using perfectly mapped reads (upper panels) or perfectly mapped reads spanning a mutation. (B) Scatter plots demonstrating strain specific tag counts for perfectly mapped reads (left panels) or perfectly mapped reads spanning a mutation (right panels). (C) DESeq2 assessment of allelic bias identified instances of allelic bias at genetic loci with low variance. Relationship of tag count and allelic imbalance is shown on right, relationship of tag count and sample variance is shown on left panels.

Acknowledgements:

These studies were supported by NIH grants DK091183, HL088083, DK063491, and GM085764 and Fondation Leducq grant 16CVD01. HB was supported by the NIH Predoctoral training grant T32DK007202 and F30DK124980.

Chapter 2, in full, is a reprint of material being prepared for submission as: Bennett H, Troutman TD, Seidman JS, Nickl C, Mummey H, Shen Z, Spann NJ, Link VM, Guzman C, Prohaska T, Zhou E, Pasillas M, Bruni CB, Vu B, Hosseini M, Glass CK. Predicting Transcriptional Mechanisms in Kupffer Cells Using Natural Genetic Variation. The dissertation author was one of the primary investigators and authors of this paper.

References:

Adams, C. C. & Workman, J. L. (1995). Binding of disparate transcriptional activators to nucleosomal DNA is inherently cooperative. *Molecular and Cellular Biology*, *15*(3), 1405–1421. https://doi.org/10.1128/mcb.15.3.1405

A-Gonzalez, N., Guillen, J. A., Gallardo, G., Díaz, M., Rosa, J. V. de la, Hernandez, I. H., Casanova-Acebes, M., Lopez, F., Tabraue, C., Beceiro, S., Hong, C., Lara, P. C., Andujar, M., Arai, S., Miyazaki, T., Li, S., Corbi, A. L., Tontonoz, P., Hidalgo, A. & Castrillo, A. (2013). The nuclear receptor LXRα controls the functional specialization of splenic macrophages. *Nature Immunology*, *14*(8), 831–839. https://doi.org/10.1038/ni.2622

Alipanahi, B., Delong, A., Weirauch, M. T. & Frey, B. J. (2015). Predicting the sequence specificities of DNA- and RNA-binding proteins by deep learning. *Nature Biotechnology*, *33*(8), 831–838. https://doi.org/10.1038/nbt.3300

An, P., Wei, L.-L., Zhao, S., Sverdlov, D. Y., Vaid, K. A., Miyamoto, M., Kuramitsu, K., Lai, M. & Popov, Y. V. (2020). Hepatocyte mitochondria-derived danger signals directly activate hepatic stellate cells and drive progression of liver fibrosis. *Nature Communications*, *11*(1), 2362. https://doi.org/10.1038/s41467-020-16092-0

Angulo, P., Kleiner, D. E., Dam-Larsen, S., Adams, L. A., Bjornsson, E. S., Charatcharoenwitthaya, P., Mills, P. R., Keach, J. C., Lafferty, H. D., Stahler, A., Haflidadottir, S. & Bendtsen, F. (2015). Liver Fibrosis, but No Other Histologic Features, Is Associated With Long-term Outcomes of Patients With Nonalcoholic Fatty Liver Disease. *Gastroenterology*, *149*(2), 389-397.e10. https://doi.org/10.1053/j.gastro.2015.04.043

Ara, A. I., Xia, M., Ramani, K., Mato, J. M. & Lu, S. C. (2008). S-adenosylmethionine inhibits lipopolysaccharide-induced gene expression via modulation of histone methylation. *Hepatology*, *47*(5), 1655–1666. https://doi.org/10.1002/hep.22231

Atanasovska, B., Rensen, S. S., Sijde, M. R., Marsman, G., Kumar, V., Jonkers, I., Withoff, S., Shiri-Sverdlov, R., Greve, J. W. M., Faber, K. N., Moshage, H., Wijmenga, C., Sluis, B. van de, Hofker, M. H. & Fu, J. (2017). A liver-specific long noncoding RNA with a role in cell viability is elevated in human nonalcoholic steatohepatitis. *Hepatology*, *66*(3), 794–808. https://doi.org/10.1002/hep.29034

Auton, A., Abecasis, G. R., Altshuler, D. M., Durbin, R. M., Abecasis, G. R., Bentley, D. R., Chakravarti, A., Clark, A. G., Donnelly, P., Eichler, E. E., Flicek, P., Gabriel, S. B., Gibbs, R. A., Green, E. D., Hurles, M. E., Knoppers, B. M., Korbel, J. O., Lander, E. S., Lee, C., … Abecasis, G. R. (2015). A global reference for human genetic variation. *Nature*, *526*(7571), 68–74. https://doi.org/10.1038/nature15393

Bala, S., Csak, T., Kodys, K., Catalano, D., Ambade, A., Furi, I., Lowe, P., Cho, Y., Iracheta-Vellve, A. & Szabo, G. (2017). Alcohol-induced miR-155 and HDAC11 inhibit negative regulators of the TLR4 pathway and lead to increased LPS responsiveness of Kupffer cells in

alcoholic liver disease. *Journal of Leukocyte Biology*, *102*(2), 487–498. https://doi.org/10.1189/jlb.3a0716-310r

Bannister, A. J. & Kouzarides, T. (2011). Regulation of chromatin by histone modifications. *Cell Research*, *21*(3), 381–395. https://doi.org/10.1038/cr.2011.22

Beceiro, S., Radin, J. N., Chatuvedi, R., Piazuelo, M. B., Horvarth, D. J., Cortado, H., Gu, Y., Dixon, B., Gu, C., Lange, I., Koomoa, D.-L., Wilson, K. T., Algood, H. M. S. & Partida-Sánchez, S. (2017). TRPM2 ion channels regulate macrophage polarization and gastric inflammation during Helicobacter pylori infection. *Mucosal Immunology*, *10*(2), 493–507. https://doi.org/10.1038/mi.2016.60

Belkina, A. C. & Denis, G. V. (2012). BET domain co-regulators in obesity, inflammation and cancer. *Nature Reviews Cancer*, *12*(7), 465–477. https://doi.org/10.1038/nrc3256

Bieghs, V., Hendrikx, T., Gorp, P. J. van, Verheyen, F., Guichot, Y. D., Walenbergh, S. M. A., Jeurissen, M. L. J., Gijbels, M., Rensen, S. S., Bast, A., Plat, J., Kalhan, S. C., Koek, G. H., Leitersdorf, E., Hofker, M. H., Lütjohann, D. & Sverdlov, R. S. (2013). The cholesterol derivative 27-hydroxycholesterol reduces steatohepatitis in mice. *Gastroenterology*, *144*(1), 167-178.e1. https://doi.org/10.1053/j.gastro.2012.09.062

Blériot, C., Chakarov, S. & Ginhoux, F. (2020). Determinants of Resident Tissue Macrophage Identity and Function. *Immunity*, *52*(6), 957–970. https://doi.org/10.1016/j.immuni.2020.05.014

Blériot, C., Dupuis, T., Jouvion, G., Eberl, G., Disson, O. & Lecuit, M. (2015). Liver-Resident Macrophage Necroptosis Orchestrates Type 1 Microbicidal Inflammation and Type-2-Mediated Tissue Repair during Bacterial Infection. *Immunity*, *42*(1), 145–158. https://doi.org/10.1016/j.immuni.2014.12.020

Bonnardel, J., T'Jonck, W., Gaublomme, D., Browaeys, R., Scott, C. L., Martens, L., Vanneste, B., Prijck, S. D., Nedospasov, S. A., Kremer, A., Hamme, E. V., Borghgraef, P., Toussaint, W., Bleser, P. D., Mannaerts, I., Beschin, A., Grunsven, L. A. van, Lambrecht, B. N., Taghon, T., … Guilliams, M. (2019). Stellate Cells, Hepatocytes, and Endothelial Cells Imprint the Kupffer Cell Identity on Monocytes Colonizing the Liver Macrophage Niche. *Immunity*, *51*(4), 638-654.e9. https://doi.org/10.1016/j.immuni.2019.08.017

Bouhlel, M. A., Derudas, B., Rigamonti, E., Dièvart, R., Brozek, J., Haulon, S., Zawadzki, C., Jude, B., Torpier, G., Marx, N., Staels, B. & Chinetti-Gbaguidi, G. (2007). PPARγ Activation Primes Human Monocytes into Alternative M2 Macrophages with Anti-inflammatory Properties. *Cell Metabolism*, *6*(2), 137–143. https://doi.org/10.1016/j.cmet.2007.06.010

Boyes, J. & Felsenfeld, G. (1996). Tissue-specific factors additively increase the probability of the all-or-none formation of a hypersensitive site. *The EMBO Journal*, *15*(10), 2496–2507. https://doi.org/10.1002/j.1460-2075.1996.tb00607.x

Brawand, D., Soumillon, M., Necsulea, A., Julien, P., Csárdi, G., Harrigan, P., Weier, M., Liechti, A., Aximu-Petri, A., Kircher, M., Albert, F. W., Zeller, U., Khaitovich, P., Grützner, F., Bergmann, S., Nielsen, R., Pääbo, S. & Kaessmann, H. (2011). The evolution of gene expression levels in mammalian organs. *Nature*, *478*(7369), 343–348. https://doi.org/10.1038/nature10532

Browaeys, R., Saelens, W. & Saeys, Y. (2020). NicheNet: modeling intercellular communication by linking ligands to target genes. *Nature Methods*, *17*(2), 159–162. https://doi.org/10.1038/s41592-019-0667-5

Brown, M. S. & Goldstein, J. L. (1997). The SREBP pathway: regulation of cholesterol metabolism by proteolysis of a membrane-bound transcription factor. *Cell*, *89*(3), 331–340.

Bryois, J., Buil, A., Evans, D. M., Kemp, J. P., Montgomery, S. B., Conrad, D. F., Ho, K. M., Ring, S., Hurles, M., Deloukas, P., Smith, G. D. & Dermitzakis, E. T. (2014). Cis and Trans Effects of Human Genomic Variants on Gene Expression. *PLoS Genetics*, *10*(7), e1004461. https://doi.org/10.1371/journal.pgen.1004461

Buenrostro, J. D., Giresi, P. G., Zaba, L. C., Chang, H. Y. & Greenleaf, W. J. (2013). Transposition of native chromatin for fast and sensitive epigenomic profiling of open chromatin, DNA-binding proteins and nucleosome position. *Nature Methods*, *10*(12), 1213–1218. https://doi.org/10.1038/nmeth.2688

Carpentier, K. S., Davenport, B. J., Haist, K. C., McCarthy, M. K., May, N. A., Robison, A., Ruckert, C., Ebel, G. D. & Morrison, T. E. (2019). Discrete viral E2 lysine residues and scavenger receptor MARCO are required for clearance of circulating alphaviruses. *ELife*, *8*, e49163. https://doi.org/10.7554/elife.49163

Carpino, G., Ben, M. D., Pastori, D., Carnevale, R., Baratta, F., Overi, D., Francis, H., Cardinale, V., Onori, P., Safarikia, S., Cammisotto, V., Alvaro, D., Svegliati-Baroni, G., Angelico, F., Gaudio, E. & Violi, F. (2019). Increased liver localization of lipopolysaccharides in human and experimental non-alcoholic fatty liver disease. *Hepatology*. https://doi.org/10.1002/hep.31056

Chakrabarti, R., Celià-Terrassa, T., Kumar, S., Hang, X., Wei, Y., Choudhury, A., Hwang, J., Peng, J., Nixon, B., Grady, J. J., DeCoste, C., Gao, J., Es, J. H. van, Li, M. O., Aifantis, I., Clevers, H. & Kang, Y. (2018). Notch ligand Dll1 mediates cross-talk between mammary stem cells and the macrophageal niche. *Science*, *360*(6396), eaan4153. https://doi.org/10.1126/science.aan4153

Chawla, A., Boisvert, W. A., Lee, C. H., Laffitte, B. A., Barak, Y., Joseph, S. B., Liao, D., Nagy, L., Edwards, P. A., Curtiss, L. K., Evans, R. M. & Tontonoz, P. (2001). A PPAR gamma-LXR-ABCA1 pathway in macrophages is involved in cholesterol efflux and atherogenesis. *Molecular Cell*, *7*(1), 161–171. https://doi.org/10.1016/s1097-2765(01)00164-2

Chen, W., Chen, G., Head, D. L., Mangelsdorf, D. J. & Russell, D. W. (2007). Enzymatic reduction of oxysterols impairs LXR signaling in cultured cells and the livers of mice. *Cell Metabolism*, *5*(1), 73–79. https://doi.org/10.1016/j.cmet.2006.11.012

Chiou, J., Geusz, R. J., Okino, M.-L., Han, J. Y., Miller, M., Melton, R., Beebe, E., Benaglio, P., Huang, S., Korgaonkar, K., Heller, S., Kleger, A., Preissl, S., Gorkin, D. U., Sander, M. & Gaulton, K. J. (2021). Interpreting type 1 diabetes risk with genetics and single-cell epigenomics. *Nature*, 1–5. https://doi.org/10.1038/s41586-021-03552-w

Csak, T., Bala, S., Lippai, D., Kodys, K., Catalano, D., Iracheta-Vellve, A. & Szabo, G. (2015). MicroRNA-155 Deficiency Attenuates Liver Steatosis and Fibrosis without Reducing Inflammation in a Mouse Model of Steatohepatitis. *PLOS ONE*, *10*(6), e0129251. https://doi.org/10.1371/journal.pone.0129251

Cserép, C., Pósfai, B., Lénárt, N., Fekete, R., László, Z. I., Lele, Z., Orsolits, B., Molnár, G., Heindl, S., Schwarcz, A. D., Ujvári, K., Környei, Z., Tóth, K., Szabadits, E., Sperlágh, B., Baranyi, M., Csiba, L., Hortobágyi, T., Maglóczky, Z., … Dénes, Á. (2019). Microglia monitor and protect neuronal function through specialized somatic purinergic junctions. *Science*, *367*(6477), 528–537. https://doi.org/10.1126/science.aax6752

Dai, Z., Ramesh, V. & Locasale, J. W. (2020). The evolving metabolic landscape of chromatin biology and epigenetics. *Nature Reviews Genetics*, *21*(12), 737–753. https://doi.org/10.1038/s41576-020-0270-8

Deaton, A. M., Webb, S., Kerr, A. R. W., Illingworth, R. S., Guy, J., Andrews, R. & Bird, A. (2011). Cell type–specific DNA methylation at intragenic CpG islands in the immune system. *Genome Research*, *21*(7), 1074–1086. https://doi.org/10.1101/gr.118703.110

Devisscher, L., Scott, C. L., Lefere, S., Raevens, S., Bogaerts, E., Paridaens, A., Verhelst, X., Geerts, A., Guilliams, M. & Vlierberghe, H. V. (2017). Non-alcoholic steatohepatitis induces transient changes within the liver macrophage pool. *Cellular Immunology*, *322*, 74–83. https://doi.org/10.1016/j.cellimm.2017.10.006

Dinarello, C. A., Novick, D., Kim, S. & Kaplanski, G. (2013). Interleukin-18 and IL-18 Binding Protein. *Frontiers in Immunology*, *4*, 289. https://doi.org/10.3389/fimmu.2013.00289

Di Paolo, N. C., Doronin, K., Baldwin, L. K., Papayannopoulou, T. & Shayakhmetov, D. M. (2013). The Transcription Factor IRF3 Triggers "Defensive Suicide" Necrosis in Response to Viral and Bacterial Pathogens. *Cell Reports*, *3*(6), 1840–1846. https://doi.org/10.1016/j.celrep.2013.05.025

Dobin, A., Davis, C. A., Schlesinger, F., Drenkow, J., Zaleski, C., Jha, S., Batut, P., Chaisson, M. & Gingeras, T. R. (2013). STAR: ultrafast universal RNA-seq aligner. *Bioinformatics*, *29*(1), 15–21. https://doi.org/10.1093/bioinformatics/bts635

Dong, B., Zhou, Y., Wang, W., Scott, J., Kim, K., Sun, Z., Guo, Q., Lu, Y., Gonzales, N. M., Wu, H., Hartig, S. M., York, R. B., Yang, F. & Moore, D. D. (2020). Vitamin D Receptor Activation in Liver Macrophages Ameliorates Hepatic Inflammation, Steatosis, and Insulin Resistance in Mice. *Hepatology*, *71*(5), 1559–1574. https://doi.org/10.1002/hep.30937

Duewell, P., Kono, H., Rayner, K. J., Sirois, C. M., Vladimer, G., Bauernfeind, F. G., Abela, G. S., Franchi, L., Nuñez, G., Schnurr, M., Espevik, T., Lien, E., Fitzgerald, K. A., Rock, K. L.,

Moore, K. J., Wright, S. D., Hornung, V. & Latz, E. (2010). NLRP3 inflammasomes are required for atherogenesis and activated by cholesterol crystals. *Nature*, *464*(7293), 1357–1361. https://doi.org/10.1038/nature08938

Eichenfield, D. Z., Troutman, T. D., Link, V. M., Lam, M. T., Cho, H., Gosselin, D., Spann, N. J., Lesch, H. P., Tao, J., Muto, J., Gallo, R. L., Evans, R. M. & Glass, C. K. (2016). Tissue damage drives co-localization of NF-κB, Smad3, and Nrf2 to direct Rev-erb sensitive wound repair in mouse macrophages. *ELife*, *5*, 554. https://doi.org/10.7554/elife.13024

Emerson, J. J. & Li, W.-H. (2010). The genetic basis of evolutionary change in gene expression levels. *Philosophical Transactions of the Royal Society B: Biological Sciences*, *365*(1552), 2581–2590. https://doi.org/10.1098/rstb.2010.0005

Endo-Umeda, K., Nakashima, H., Umeda, N., Seki, S. & Makishima, M. (2018). Dysregulation of Kupffer Cells/ Macrophages and Natural Killer T Cells in Steatohepatitis in LXRα Knockout Male Mice. *Endocrinology*. https://doi.org/10.1210/en.2017-03141

Estes, C., Razavi, H., Loomba, R., Younossi, Z. & Sanyal, A. J. (2018). Modeling the epidemic of nonalcoholic fatty liver disease demonstrates an exponential increase in burden of disease. *Hepatology*, *67*(1), 123–133. https://doi.org/10.1002/hep.29466

Farrell, G. C., Mridha, A. R., Yeh, M. M., Arsov, T., Rooyen, D. M. V., Brooling, J., Nguyen, T., Heydet, D., Delghingaro-Augusto, V., Nolan, C. J., Shackel, N. A., McLennan, S. V., Teoh, N. C. & Larter, C. Z. (2014). Strain dependence of diet-induced NASH and liver fibrosis in obese mice is linked to diabetes and inflammatory phenotype. *Liver International*, *34*(7), 1084–1093. https://doi.org/10.1111/liv.12335

Fasolino, M., Goldman, N., Wang, W., Cattau, B., Zhou, Y., Petrovic, J., Link, V. M., Cote, A., Chandra, A., Silverman, M., Joyce, E. F., Little, S. C., Consortium, T. H., Kaestner, K. H., Naji, A., Raj, A., Henao-Mejia, J., Faryabi, R. B. & Vahedi, G. (2020). Genetic Variation in Type 1 Diabetes Reconfigures the 3D Chromatin Organization of T Cells and Alters Gene Expression. *Immunity*, *52*(2), 257-274.e11. https://doi.org/10.1016/j.immuni.2020.01.003

Fernandes-Alnemri, T., Kang, S., Anderson, C., Sagara, J., Fitzgerald, K. A. & Alnemri, E. S. (2013). Cutting Edge: TLR Signaling Licenses IRAK1 for Rapid Activation of the NLRP3 Inflammasome. *The Journal of Immunology*, *191*(8), 3995–3999. https://doi.org/10.4049/jimmunol.1301681

Filippakopoulos, P. & Knapp, S. (2014). Targeting bromodomains: epigenetic readers of lysine acetylation. *Nature Reviews Drug Discovery*, *13*(5), 337–356. https://doi.org/10.1038/nrd4286

Fonseca, G. J., Tao, J., Westin, E. M., Duttke, S. H., Spann, N. J., Strid, T., Shen, Z., Stender, J. D., Sakai, M., Link, V. M., Benner, C. & Glass, C. K. (2019). Diverse motif ensembles specify non-redundant DNA binding activities of AP-1 family members in macrophages. *Nature Communications*, *10*(1), 414. https://doi.org/10.1038/s41467-018-08236-0

Franklin, R. A., Liao, W., Sarkar, A., Kim, M. V., Bivona, M. R., Liu, K., Pamer, E. G. & Li, M. O. (2014). The cellular and molecular origin of tumor-associated macrophages. *Science*, *344*(6186), 921–925. https://doi.org/10.1126/science.1252510

Goncalves, A., Leigh-Brown, S., Thybert, D., Stefflova, K., Turro, E., Flicek, P., Brazma, A., Odom, D. T. & Marioni, J. C. (2012). Extensive compensatory cis-trans regulation in the evolution of mouse gene expression. *Genome Research*, *22*(12), 2376–2384. https://doi.org/10.1101/gr.142281.112

Gosselin, D., Link, V. M., Romanoski, C. E., Fonseca, G. J., Eichenfield, D. Z., Spann, N. J., Stender, J. D., Chun, H. B., Garner, H., Geissmann, F. & Glass, C. K. (2014). Environment drives selection and function of enhancers controlling tissue-specific macrophage identities. *Cell*, *159*(6), 1327–1340. https://doi.org/10.1016/j.cell.2014.11.023

Gosselin, D., Skola, D., Coufal, N. G., Holtman, I. R., Schlachetzki, J. C. M., Sajti, E., Jaeger, B. N., O'Connor, C., Fitzpatrick, C., Pasillas, M. P., Pena, M., Adair, A., Gonda, D. D., Levy, M. L., Ransohoff, R. M., Gage, F. H. & Glass, C. K. (2017). An environment-dependent transcriptional network specifies human microglia identity. *Science*, *356*(6344), eaal3222. https://doi.org/10.1126/science.aal3222

Haldar, M., Kohyama, M., So, A. Y.-L., Kc, W., Wu, X., Briseño, C. G., Satpathy, A. T., Kretzer, N. M., Arase, H., Rajasekaran, N. S., Wang, L., Egawa, T., Igarashi, K., Baltimore, D., Murphy, T. L. & Murphy, K. M. (2014). Heme-mediated SPI-C induction promotes monocyte differentiation into iron-recycling macrophages. *Cell*, *156*(6), 1223–1234. https://doi.org/10.1016/j.cell.2014.01.069

Hanna, R. N., Carlin, L. M., Hubbeling, H. G., Nackiewicz, D., Green, A. M., Punt, J. A., Geissmann, F. & Hedrick, C. C. (2011). The transcription factor NR4A1 (Nur77) controls bone marrow differentiation and the survival of Ly6C− monocytes. *Nature Immunology*, *12*(8), 778–785. https://doi.org/10.1038/ni.2063

Hanna, R. N., Shaked, I., Hubbeling, H. G., Punt, J. A., Wu, R., Herrley, E., Zaugg, C., Pei, H., Geissmann, F., Ley, K. & Hedrick, C. C. (2012). NR4A1 (Nur77) Deletion Polarizes Macrophages Toward an Inflammatory Phenotype and Increases Atherosclerosis. *Circulation Research*, *110*(3), 416–427. https://doi.org/10.1161/circresaha.111.253377

He, K., Dai, Z.-Y., Li, P.-Z., Zhu, X.-W. & Gong, J.-P. (2015). Association between liver X receptor-α and neuron-derived orphan nuclear receptor-1 in Kupffer cells of C57BL/6 mice during inflammation. *Molecular Medicine Reports*, *12*(4), 6098–6104. https://doi.org/10.3892/mmr.2015.4155

Heinz, S., Romanoski, C. E., Benner, C., Allison, K. A., Kaikkonen, M. U., Orozco, L. D. & Glass, C. K. (2013). Effect of natural genetic variation on enhancer selection and function. *Nature*, *503*(7477), 487–492. https://doi.org/10.1038/nature12615

Heinz, Sven, Benner, C., Spann, N., Bertolino, E., Lin, Y. C., Laslo, P., Cheng, J. X., Murre, C., Singh, H. & Glass, C. K. (2010). Simple combinations of lineage-determining transcription

factors prime cis-regulatory elements required for macrophage and B cell identities. *Molecular Cell*, *38*(4), 576–589. https://doi.org/10.1016/j.molcel.2010.05.004

Heinz, Sven, Romanoski, C. E., Benner, C. & Glass, C. K. (2015). The selection and function of cell type-specific enhancers. *Nature Reviews Molecular Cell Biology*, *16*(3), 144–154. https://doi.org/10.1038/nrm3949

Helmy, K. Y., Jr., K. J. K., Gorgani, N. N., Kljavin, N. M., Elliott, J. M., Diehl, L., Scales, S. J., Ghilardi, N. & Campagne, M. van L. (2006). CRIg: A Macrophage Complement Receptor Required for Phagocytosis of Circulating Pathogens. *Cell*, *124*(5), 915–927. https://doi.org/10.1016/j.cell.2005.12.039

Hendrikx, T., Jeurissen, M. L. J., Bieghs, V., Walenbergh, S. M. A., Gorp, P. J. van, Verheyen, F., Houben, T., Guichot, Y. D., Gijbels, M. J. J., Leitersdorf, E., Hofker, M. H., Lütjohann, D. & Sverdlov, R. S. (2015). Hematopoietic overexpression of Cyp27a1 reduces hepatic inflammation independently of 27-hydroxycholesterol levels in Ldlr(-/-) mice. *Journal of Hepatology*, *62*(2), 430–436. https://doi.org/10.1016/j.jhep.2014.09.027

Hernandez, G., Luo, T., Javed, T. A., Wen, L., Kalwat, M. A., Vale, K., Ammouri, F., Husain, S. Z., Kliewer, S. A. & Mangelsdorf, D. J. (2020). Pancreatitis is an FGF21-deficient state that is corrected by replacement therapy. *Science Translational Medicine*, *12*(525), eaay5186. https://doi.org/10.1126/scitranslmed.aay5186

Heymann, F., Peusquens, J., Ludwig-Portugall, I., Kohlhepp, M., Ergen, C., Niemietz, P., Martin, C., Rooijen, N. van, Ochando, J. C., Randolph, G. J., Luedde, T., Ginhoux, F., Kurts, C., Trautwein, C. & Tacke, F. (2015). Liver inflammation abrogates immunological tolerance induced by Kupffer cells. *Hepatology*, *62*(1), 279–291. https://doi.org/10.1002/hep.27793

Heymann, F. & Tacke, F. (2016). Immunology in the liver--from homeostasis to disease. *Nature Reviews. Gastroenterology & Hepatology*, *13*(2), 88–110. https://doi.org/10.1038/nrgastro.2015.200

Hindorff, L. A., Sethupathy, P., Junkins, H. A., Ramos, E. M., Mehta, J. P., Collins, F. S. & Manolio, T. A. (2009). Potential etiologic and functional implications of genome-wide association loci for human diseases and traits. *Proceedings of the National Academy of Sciences*, *106*(23), 9362–9367. https://doi.org/10.1073/pnas.0903103106

Hoeksema, M. A., Shen, Z., Holtman, I. R., Zheng, A., Spann, N. J., Cobo, I., Gymrek, M. & Glass, C. K. (2021). Mechanisms underlying divergent responses of genetically distinct macrophages to IL-4. *Science Advances*, *7*(25), eabf9808. https://doi.org/10.1126/sciadv.abf9808

Horvath, S. & Raj, K. (2018). DNA methylation-based biomarkers and the epigenetic clock theory of ageing. *Nature Reviews Genetics*, *19*(6), 371–384. https://doi.org/10.1038/s41576-018-0004-3

Hotamisligil, G. S. (2010). Endoplasmic reticulum stress and atherosclerosis. *Nature Medicine*, *16*(4), 396–399. https://doi.org/10.1038/nm0410-396

Huang, W., Metlakunta, A., Dedousis, N., Zhang, P., Sipula, I., Dube, J. J., Scott, D. K. & O'Doherty, R. M. (2010). Depletion of liver Kupffer cells prevents the development of diet-induced hepatic steatosis and insulin resistance. *Diabetes*, *59*(2), 347–357. https://doi.org/10.2337/db09-0016

Hui, S. T., Parks, B. W., Org, E., Norheim, F., Che, N., Pan, C., Castellani, L. W., Charugundla, S., Dirks, D. L., Psychogios, N., Neuhaus, I., Gerszten, R. E., Kirchgessner, T., Gargalovic, P. S. & Lusis, A. J. (2015). The genetic architecture of NAFLD among inbred strains of mice. *ELife*, *4*, e05607. https://doi.org/10.7554/elife.05607

Imajo, K., Fujita, K., Yoneda, M., Nozaki, Y., Ogawa, Y., Shinohara, Y., Kato, S., Mawatari, H., Shibata, W., Kitani, H., Ikejima, K., Kirikoshi, H., Nakajima, N., Saito, S., Maeyama, S., Watanabe, S., Wada, K. & Nakajima, A. (2012). Hyperresponsivity to low-dose endotoxin during progression to nonalcoholic steatohepatitis is regulated by leptin-mediated signaling. *Cell Metabolism*, *16*(1), 44–54. https://doi.org/10.1016/j.cmet.2012.05.012

Ioannou, G. N. (2016). The Role of Cholesterol in the Pathogenesis of NASH. *Trends in Endocrinology and Metabolism: TEM*, *27*(2), 84–95. https://doi.org/10.1016/j.tem.2015.11.008

Ioannou, G. N., Subramanian, S., Chait, A., Haigh, W. G., Yeh, M. M., Farrell, G. C., Lee, S. P. & Savard, C. (2017). Cholesterol crystallization within hepatocyte lipid droplets and its role in murine NASH. *Journal of Lipid Research*, *58*(6), 1067–1079. https://doi.org/10.1194/jlr.m072454

Ito, A., Hong, C., Rong, X., Zhu, X., Tarling, E. J., Hedde, P. N., Gratton, E., Parks, J. & Tontonoz, P. (2015). LXRs link metabolism to inflammation through Abca1-dependent regulation of membrane composition and TLR signaling. *ELife*, *4*, e08009. https://doi.org/10.7554/elife.08009

Jaitin, D. A., Adlung, L., Thaiss, C. A., Weiner, A., Li, B., Descamps, H., Lundgren, P., Bleriot, C., Liu, Z., Deczkowska, A., Keren-Shaul, H., David, E., Zmora, N., Eldar, S. M., Lubezky, N., Shibolet, O., Hill, D. A., Lazar, M. A., Colonna, M., … Amit, I. (2019). Lipid-Associated Macrophages Control Metabolic Homeostasis in a Trem2-Dependent Manner. *Cell*, *178*(3), 686-698.e14. https://doi.org/10.1016/j.cell.2019.05.054

Janowski, B. A., Willy, P. J., Devi, T. R., Falck, J. R. & Mangelsdorf, D. J. (1996). An oxysterol signalling pathway mediated by the nuclear receptor LXR alpha. *Nature …*, *383*(6602), 728–731. https://doi.org/10.1038/383728a0

Joseph, S. B., Bradley, M. N., Castrillo, A., Bruhn, K. W., Mak, P. A., Pei, L., Hogenesch, J., O'connell, R. M., Cheng, G., Saez, E., Miller, J. F. & Tontonoz, P. (2004). LXR-dependent gene expression is important for macrophage survival and the innate immune response. *Cell*, *119*(2), 299–309. https://doi.org/10.1016/j.cell.2004.09.032

Joseph, S. B., Laffitte, B. A., Patel, P. H., Watson, M. A., Matsukuma, K. E., Walczak, R., Collins, J. L., Osborne, T. F. & Tontonoz, P. (2002). Direct and indirect mechanisms for regulation of fatty acid synthase gene expression by liver X receptors. *The Journal of Biological Chemistry*, *277*(13), 11019–11025. https://doi.org/10.1074/jbc.m111041200

Kaikkonen, M. U., Spann, N. J., Heinz, S., Romanoski, C. E., Allison, K. A., Stender, J. D., Chun, H. B., Tough, D. F., Prinjha, R. K., Benner, C. & Glass, C. K. (2013). Remodeling of the enhancer landscape during macrophage activation is coupled to enhancer transcription. *Molecular Cell*, *51*(3), 310–325. https://doi.org/10.1016/j.molcel.2013.07.010

Kawai, T. & Akira, S. (2010). The role of pattern-recognition receptors in innate immunity: update on Toll-like receptors. *Nature Immunology*, *11*(5), 373–384. https://doi.org/10.1038/ni.1863

Keane, T. M., Goodstadt, L., Danecek, P., White, M. A., Wong, K., Yalcin, B., Heger, A., Agam, A., Slater, G., Goodson, M., Furlotte, N. A., Eskin, E., Nellåker, C., Whitley, H., Cleak, J., Janowitz, D., Hernandez-Pliego, P., Edwards, A., Belgard, T. G., … Adams, D. J. (2011). Mouse genomic variation and its effect on phenotypes and gene regulation. *Nature …*, *477*(7364), 289–294. https://doi.org/10.1038/nature10413

Kent, W. J., Sugnet, C. W., Furey, T. S., Roskin, K. M., Pringle, T. H., Zahler, A. M. & Haussler, and D. (2002). The Human Genome Browser at UCSC. *Genome Research*, *12*(6), 996–1006. https://doi.org/10.1101/gr.229102

Keren-Shaul, H., Spinrad, A., Weiner, A., Matcovitch-Natan, O., Dvir-Szternfeld, R., Ulland, T. K., David, E., Baruch, K., Lara-Astaiso, D., Toth, B., Itzkovitz, S., Colonna, M., Schwartz, M. & Amit, I. (2017). A Unique Microglia Type Associated with Restricting Development of Alzheimer's Disease. *Cell*, *169*(7), 1276-1290.e17. https://doi.org/10.1016/j.cell.2017.05.018

Kiguchi, N., Maeda, T., Kobayashi, Y., Fukazawa, Y. & Kishioka, S. (2009). Leptin enhances CC-chemokine ligand expression in cultured murine macrophage. *Biochemical and Biophysical Research Communications*, *384*(3), 311–315. https://doi.org/10.1016/j.bbrc.2009.04.121

Kleiner, D. E., Brunt, E. M., Natta, M. V., Behling, C., Contos, M. J., Cummings, O. W., Ferrell, L. D., Liu, Y.-C., Torbenson, M. S., Unalp-Arida, A., Yeh, M., McCullough, A. J., Sanyal, A. J. & Network, N. S. C. R. (2005). Design and validation of a histological scoring system for nonalcoholic fatty liver disease. *Hepatology*, *41*(6), 1313–1321. https://doi.org/10.1002/hep.20701

Kobayashi, K., Hernandez, L. D., Galán, J. E., Janeway, C. A., Medzhitov, R. & Flavell, R. A. (2002). IRAK-M Is a Negative Regulator of Toll-like Receptor Signaling. *Cell*, *110*(2), 191–202. https://doi.org/10.1016/s0092-8674(02)00827-9

Krenkel, O., Hundertmark, J., Abdallah, A. T., Kohlhepp, M., Puengel, T., Roth, T., Branco, D. P. P., Mossanen, J. C., Luedde, T., Trautwein, C., Costa, I. G. & Tacke, F. (2019). Myeloid cells in liver and bone marrow acquire a functionally distinct inflammatory phenotype during

obesity-related steatohepatitis. *Gut*, gutjnl-2019-318382. https://doi.org/10.1136/gutjnl-2019-318382

Krenkel, O. & Tacke, F. (2017). Liver macrophages in tissue homeostasis and disease. *Nature Reviews Immunology*, *17*(5), 306–321. https://doi.org/10.1038/nri.2017.11

Kupffer, C. v. (1899). Ueber die sogenannten Sternzellen der Säugethierleber. *Archiv Für Mikroskopische Anatomie*, *54*(2), 254. https://doi.org/10.1007/bf02976809

Kusnadi, A., Park, S. H., Yuan, R., Pannellini, T., Giannopoulou, E., Oliver, D., Lu, T., Park-Min, K.-H. & Ivashkiv, L. B. (2019). The Cytokine TNF Promotes Transcription Factor SREBP Activity and Binding to Inflammatory Genes to Activate Macrophages and Limit Tissue Repair. *Immunity*, *51*(2), 241-257.e9. https://doi.org/10.1016/j.immuni.2019.06.005

Laffitte, B. A., Joseph, S. B., Walczak, R., Pei, L., Wilpitz, D. C., Collins, J. L. & Tontonoz, P. (2001). Autoregulation of the human liver X receptor alpha promoter. *Molecular and Cellular Biology*, *21*(22), 7558–7568. https://doi.org/10.1128/mcb.21.22.7558-7568.2001

Langmead, B. & Salzberg, S. L. (2012). Fast gapped-read alignment with Bowtie 2. *Nature Methods*, *9*(4), 357–359. https://doi.org/10.1038/nmeth.1923

Lanthier, N., Molendi-Coste, O., Horsmans, Y., Rooijen, N. van, Cani, P. D. & Leclercq, I. A. (2010). Kupffer cell activation is a causal factor for hepatic insulin resistance. *American Journal of Physiology. Gastrointestinal and Liver Physiology*, *298*(1), G107-16. https://doi.org/10.1152/ajpgi.00391.2009

Lavin, Y., Winter, D., Blecher-Gonen, R., David, E., Keren-Shaul, H., Merad, M., Jung, S. & Amit, I. (2014). Tissue-Resident Macrophage Enhancer Landscapes Are Shaped by the Local Microenvironment. *Cell*, *159*(6), 1312–1326. https://doi.org/10.1016/j.cell.2014.11.018

Lee, S. H., Chaves, M. M., Kamenyeva, O., Gazzinelli-Guimaraes, P. H., Kang, B., Pessenda, G., Passelli, K., Tacchini-Cottier, F., Kabat, J., Jacobsen, E. A., Nutman, T. B. & Sacks, D. L. (2020). M2-like, dermal macrophages are maintained via IL-4/CCL24–mediated cooperative interaction with eosinophils in cutaneous leishmaniasis. *Science Immunology*, *5*(46), eaaz4415. https://doi.org/10.1126/sciimmunol.aaz4415

Lefebvre, E., Moyle, G., Reshef, R., Richman, L. P., Thompson, M., Hong, F., Chou, H., Hashiguchi, T., Plato, C., Poulin, D., Richards, T., Yoneyama, H., Jenkins, H., Wolfgang, G. & Friedman, S. L. (2016). Antifibrotic Effects of the Dual CCR2/CCR5 Antagonist Cenicriviroc in Animal Models of Liver and Kidney Fibrosis. *PLoS ONE*, *11*(6), e0158156. https://doi.org/10.1371/journal.pone.0158156

Leroux, A., Ferrere, G., Godie, V., Cailleux, F., Renoud, M.-L., Gaudin, F., Naveau, S., Prévot, S., Makhzami, S., Perlemuter, G. & Cassard-Doulcier, A.-M. (2012). Toxic lipids stored by Kupffer cells correlates with their pro-inflammatory phenotype at an early stage of steatohepatitis. *Journal of Hepatology*, *57*(1), 141–149. https://doi.org/10.1016/j.jhep.2012.02.028

Leti, F., Legendre, C., Still, C. D., Chu, X., Petrick, A., Gerhard, G. S. & DiStefano, J. K. (2017). Altered expression of MALAT1 lncRNA in nonalcoholic steatohepatitis fibrosis regulates CXCL5 in hepatic stellate cells. *Translational Research*, *190*, 25-39.e21. https://doi.org/10.1016/j.trsl.2017.09.001

Li, C., Lu, L., Feng, B., Zhang, K., Han, S., Hou, D., Chen, L., Chu, X. & Wang, R. (2017). The lincRNA-ROR/miR-145 axis promotes invasion and metastasis in hepatocellular carcinoma via induction of epithelial-mesenchymal transition by targeting ZEB2. *Scientific Reports*, *7*(1), 4637. https://doi.org/10.1038/s41598-017-04113-w

Li, Q., Brown, J. B., Huang, H. & Bickel, P. J. (2011). Measuring reproducibility of high-throughput experiments. *The Annals of Applied Statistics*, *5*(3), 1752–1779. https://doi.org/10.1214/11-aoas466

Li, Y., Schwalie, P. C., Bast-Habersbrunner, A., Mocek, S., Russeil, J., Fromme, T., Deplancke, B. & Klingenspor, M. (2019). Systems-Genetics-Based Inference of a Core Regulatory Network Underlying White Fat Browning. *Cell Reports*, *29*(12), 4099-4113.e5. https://doi.org/10.1016/j.celrep.2019.11.053

Lin, H.-Y., Yang, Y.-L., Wang, P.-W., Wang, F.-S. & Huang, Y.-H. (2020). The Emerging Role of MicroRNAs in NAFLD: Highlight of MicroRNA-29a in Modulating Oxidative Stress, Inflammation, and Beyond. *Cells*, *9*(4), 1041. https://doi.org/10.3390/cells9041041

Lin, K.-M., Hu, W., Troutman, T. D., Jennings, M., Brewer, T., Li, X., Nanda, S., Cohen, P., Thomas, J. A. & Pasare, C. (2014). IRAK-1 bypasses priming and directly links TLRs to rapid NLRP3 inflammasome activation. *Proceedings of the National Academy of Sciences*, *111*(2), 775–780. https://doi.org/10.1073/pnas.1320294111

Link, V. M., Duttke, S. H., Chun, H. B., Holtman, I. R., Westin, E., Hoeksema, M. A., Abe, Y., Skola, D., Romanoski, C. E., Tao, J., Fonseca, G. J., Troutman, T. D., Spann, N. J., Strid, T., Sakai, M., Yu, M., Hu, R., Fang, R., Metzler, D., … Glass, C. K. (2018). Analysis of Genetically Diverse Macrophages Reveals Local and Domain-wide Mechanisms that Control Transcription Factor Binding and Function. *Cell*, *173*(7), 1796-1809.e17. https://doi.org/10.1016/j.cell.2018.04.018

Link, V. M., Romanoski, C. E., Metzler, D. & Glass, C. K. (2018). MMARGE: Motif Mutation Analysis for Regulatory Genomic Elements. *Nucleic Acids Research*, *46*(14), gky491-. https://doi.org/10.1093/nar/gky491

Liu, G., Fu, Y., Yosri, M., Chen, Y., Sun, P., Xu, J., Zhang, M., Sun, D., Strickland, A. B., Mackey, Z. B. & Shi, M. (2019). CRIg plays an essential role in intravascular clearance of bloodborne parasites by interacting with complement. *Proceedings of the National Academy of Sciences*, *116*(48), 24214–24220. https://doi.org/10.1073/pnas.1913443116

Loomba, R., Gindin, Y., Jiang, Z., Lawitz, E., Caldwell, S., Djedjos, C. S., Xu, R., Chung, C., Myers, R. P., Subramanian, G. M., Goodman, Z., Charlton, M., Afdhal, N. H. & Diehl, A. M. (2018). DNA methylation signatures reflect aging in patients with nonalcoholic steatohepatitis. *JCI Insight*, *3*(2), e96685. https://doi.org/10.1172/jci.insight.96685

Love, M. I., Huber, W. & Anders, S. (2014). Moderated estimation of fold change and dispersion for RNA-seq data with DESeq2. *Genome Biology*, *15*(12), 550. https://doi.org/10.1186/s13059-014-0550-8

Luo, W., Xu, Q., Wang, Q., Wu, H. & Hua, J. (2017). Effect of modulation of PPAR-γ activity on Kupffer cells M1/M2 polarization in the development of non-alcoholic fatty liver disease. *Scientific Reports*, *7*(1), 44612. https://doi.org/10.1038/srep44612

Maeda, T., Kiguchi, N., Kobayashi, Y., Ikuta, T., Ozaki, M. & Kishioka, S. (2009). Leptin derived from adipocytes in injured peripheral nerves facilitates development of neuropathic pain via macrophage stimulation. *Proceedings of the National Academy of Sciences*, *106*(31), 13076–13081. https://doi.org/10.1073/pnas.0903524106

Mahady, S. E., Webster, A. C., Walker, S., Sanyal, A. & George, J. (2011). The role of thiazolidinediones in non-alcoholic steatohepatitis - a systematic review and meta analysis. *Journal of Hepatology*, *55*(6), 1383–1390. https://doi.org/10.1016/j.jhep.2011.03.016

Maistrenko, O. M., Mende, D. R., Luetge, M., Hildebrand, F., Schmidt, T. S. B., Li, S. S., Rodrigues, J. F. M., Mering, C. von, Coelho, L. P., Huerta-Cepas, J., Sunagawa, S. & Bork, P. (2020). Disentangling the impact of environmental and phylogenetic constraints on prokaryotic within-species diversity. *The ISME Journal*, *14*(5), 1247–1259. https://doi.org/10.1038/s41396-020-0600-z

Mak, P. A., Laffitte, B. A., Desrumaux, C., Joseph, S. B., Curtiss, L. K., Mangelsdorf, D. J., Tontonoz, P. & Edwards, P. A. (2002). Regulated expression of the apolipoprotein E/C-I/C-IV/C-II gene cluster in murine and human macrophages. A critical role for nuclear liver X receptors alpha and beta. *The Journal of Biological Chemistry*, *277*(35), 31900–31908. https://doi.org/10.1074/jbc.m202993200

Mass, E., Ballesteros, I., Farlik, M., Halbritter, F., Günther, P., Crozet, L., Jacome-Galarza, C. E., Händler, K., Klughammer, J., Kobayashi, Y., Gomez-Perdiguero, E., Schultze, J. L., Beyer, M., Bock, C. & Geissmann, F. (2016). Specification of tissue-resident macrophages during organogenesis. *Science*, *353*(6304), aaf4238–aaf4238. https://doi.org/10.1126/science.aaf4238

Mass, E., Jacome-Galarza, C. E., Blank, T., Lazarov, T., Durham, B. H., Ozkaya, N., Pastore, A., Schwabenland, M., Chung, Y. R., Rosenblum, M. K., Prinz, M., Abdel-Wahab, O. & Geissmann, F. (2017). A somatic mutation in erythro-myeloid progenitors causes neurodegenerative disease. *Nature …*, *549*(7672), 389–393. https://doi.org/10.1038/nature23672

McDaniel, K., Herrera, L., Zhou, T., Francis, H., Han, Y., Levine, P., Lin, E., Glaser, S., Alpini, G. & Meng, F. (2014). The functional role of microRNAs in alcoholic liver injury. *Journal of Cellular and Molecular Medicine*, *18*(2), 197–207. https://doi.org/10.1111/jcmm.12223

McGettigan, B., McMahan, R., Orlicky, D., Burchill, M., Danhorn, T., Francis, P., Cheng, L. L., Mason, L. G., Jakubzick, C. V. & Rosen, H. R. (2019). Dietary Lipids Differentially Shape

Nonalcoholic Steatohepatitis Progression and the Transcriptome of Kupffer Cells and Infiltrating Macrophages. *Hepatology*, *70*(1), 67–83. https://doi.org/10.1002/hep.30401

Mercer, E. M., Lin, Y. C., Benner, C., Jhunjhunwala, S., Dutkowski, J., Flores, M., Sigvardsson, M., Ideker, T., Glass, C. K. & Murre, C. (2011). Multilineage priming of enhancer repertoires precedes commitment to the B and myeloid cell lineages in hematopoietic progenitors. *Immunity*, *35*(3), 413–425. https://doi.org/10.1016/j.immuni.2011.06.013

Metlakunta, A., Huang, W., Stefanovic-Racic, M., Dedousis, N., Sipula, I. & O'Doherty, R. M. (2017). Kupffer cells facilitate the acute effects of leptin on hepatic lipid metabolism. *American Journal of Physiology-Endocrinology and Metabolism*, *312*(1), E11–E18. https://doi.org/10.1152/ajpendo.00250.2016

Mets, D. G. & Brainard, M. S. (2018). Genetic variation interacts with experience to determine interindividual differences in learned song. *Proceedings of the National Academy of Sciences*, *115*(2), 421–426. https://doi.org/10.1073/pnas.1713031115

Metschnikoff, E. (1883). Untersuchungen über die mesodermalen Phagocyten einiger Wirbeltiere. *Biologisches Centralblatt*.

Metschnikoff, E. (1891). Lecture on Phagocytosis and Immunity. *British Medical Journal*, *1*(1570), 213. https://doi.org/10.1136/bmj.1.1570.213

Meuleman, W., Muratov, A., Rynes, E., Halow, J., Lee, K., Bates, D., Diegel, M., Dunn, D., Neri, F., Teodosiadis, A., Reynolds, A., Haugen, E., Nelson, J., Johnson, A., Frerker, M., Buckley, M., Sandstrom, R., Vierstra, J., Kaul, R. & Stamatoyannopoulos, J. (2020). Index and biological spectrum of human DNase I hypersensitive sites. *Nature*, *584*(7820), 244–251. https://doi.org/10.1038/s41586-020-2559-3

Miao, C.-M., He, K., Li, P.-Z., Liu, Z.-J., Zhu, X.-W., Ou, Z.-B., Ruan, X.-Z., Gong, J.-P. & Liu, C.-A. (2016). LXRα represses LPS-induced inflammatory responses by competing with IRF3 for GRIP1 in Kupffer cells. *International Immunopharmacology*, *35*, 272–279. https://doi.org/10.1016/j.intimp.2016.04.009

Miura, K., Yang, L., Rooijen, N. van, Ohnishi, H. & Seki, E. (2012). Hepatic recruitment of macrophages promotes nonalcoholic steatohepatitis through CCR2. *American Journal of Physiology. Gastrointestinal and Liver Physiology*, *302*(11), G1310-21. https://doi.org/10.1152/ajpgi.00365.2011

Momen-Heravi, F., Bala, S., Kodys, K. & Szabo, G. (2015). Exosomes derived from alcohol-treated hepatocytes horizontally transfer liver specific miRNA-122 and sensitize monocytes to LPS. *Scientific Reports*, *5*(1), 9991. https://doi.org/10.1038/srep09991

Mossanen, J. C., Krenkel, O., Ergen, C., Govaere, O., Liepelt, A., Puengel, T., Heymann, F., Kalthoff, S., Lefebvre, E., Eulberg, D., Luedde, T., Marx, G., Strassburg, C. P., Roskams, T., Trautwein, C. & Tacke, F. (2016). Chemokine (C-C motif) receptor 2-positive monocytes aggravate the early phase of acetaminophen-induced acute liver injury. *Hepatology*, *64*(5), 1667–1682. https://doi.org/10.1002/hep.28682

Mouries, J., Brescia, P., Silvestri, A., Spadoni, I., Sorribas, M., Wiest, R., Mileti, E., Galbiati, M., Invernizzi, P., Adorini, L., Penna, G. & Rescigno, M. (2019). Microbiota-driven gut vascular barrier disruption is a prerequisite for non-alcoholic steatohepatitis development. *Journal of Hepatology*. https://doi.org/10.1016/j.jhep.2019.08.005

Mridha, A. R., Wree, A., Robertson, A. A. B., Yeh, M. M., Johnson, C. D., Rooyen, D. M. V., Haczeyni, F., Teoh, N. C.-H., Savard, C., Ioannou, G. N., Masters, S. L., Schroder, K., Cooper, M. A., Feldstein, A. E. & Farrell, G. C. (2017). NLRP3 inflammasome blockade reduces liver inflammation and fibrosis in experimental NASH in mice. *Journal of Hepatology*, *66*(5), 1037–1046. https://doi.org/10.1016/j.jhep.2017.01.022

Muse, E. D., Yu, S., Edillor, C. R., Tao, J., Spann, N. J., Troutman, T. D., Seidman, J. S., Henke, A., Roland, J. T., Ozeki, K. A., Thompson, B. M., McDonald, J. G., Bahadorani, J., Tsimikas, S., Grossman, T. R., Tremblay, M. S. & Glass, C. K. (2018). Cell-specific discrimination of desmosterol and desmosterol mimetics confers selective regulation of LXR and SREBP in macrophages. *Proceedings of the National Academy of Sciences of the United States of America*, *115*(20), E4680–E4689. https://doi.org/10.1073/pnas.1714518115

Nairz, M., Theurl, I., Swirski, F. K. & Weiss, G. (2017). "Pumping iron"—how macrophages handle iron at the systemic, microenvironmental, and cellular levels. *Pflügers Archiv - European Journal of Physiology*, *469*(3–4), 397–418. https://doi.org/10.1007/s00424-017-1944-8

Nandagopal, N., Santat, L. A., LeBon, L., Sprinzak, D., Bronner, M. E. & Elowitz, M. B. (2018). Dynamic Ligand Discrimination in the Notch Signaling Pathway. *Cell*, *172*(4), 869-880.e19. https://doi.org/10.1016/j.cell.2018.01.002

Neyrinck, A. M., Cani, P. D., Dewulf, E. M., Backer, F. D., Bindels, L. B. & Delzenne, N. M. (2009). Critical role of Kupffer cells in the management of diet-induced diabetes and obesity. *Biochemical and Biophysical Research Communications*, *385*(3), 351–356. https://doi.org/10.1016/j.bbrc.2009.05.070

Nicodeme, E., Jeffrey, K. L., Schaefer, U., Beinke, S., Dewell, S., Chung, C., Chandwani, R., Marazzi, I., Wilson, P., Coste, H., White, J., Kirilovsky, J., Rice, C. M., Lora, J. M., Prinjha, R. K., Lee, K. & Tarakhovsky, A. (2010). Suppression of inflammation by a synthetic histone mimic. *Nature*, *468*(7327), 1119–1123. https://doi.org/10.1038/nature09589

Nicolás-Ávila, J. A., Lechuga-Vieco, A. V., Esteban-Martínez, L., Sánchez-Díaz, M., Díaz-García, E., Santiago, D. J., Rubio-Ponce, A., Li, J. L., Balachander, A., Quintana, J. A., Martínez-de-Mena, R., Castejón-Vega, B., Pun-García, A., Través, P. G., Bonzón-Kulichenko, E., García-Marqués, F., Cussó, L., A-González, N., González-Guerra, A., … Hidalgo, A. (2020). A Network of Macrophages Supports Mitochondrial Homeostasis in the Heart. *Cell*. https://doi.org/10.1016/j.cell.2020.08.031

Nott, A., Holtman, I. R., Coufal, N. G., Schlachetzki, J. C. M., Yu, M., Hu, R., Han, C. Z., Pena, M., Xiao, J., Wu, Y., Keulen, Z., Pasillas, M. P., O'Connor, C., Nickl, C. K., Schafer, S. T., Shen, Z., Rissman, R. A., Brewer, J. B., Gosselin, D., … Glass, C. K. (2019). Brain cell

type–specific enhancer–promoter interactome maps and disease-risk association. *Science*, *366*(6469), 1134–1139. https://doi.org/10.1126/science.aay0793

O'Connell, R. M., Chaudhuri, A. A., Rao, D. S. & Baltimore, D. (2009). Inositol phosphatase SHIP1 is a primary target of miR-155. *Proceedings of the National Academy of Sciences*, *106*(17), 7113–7118. https://doi.org/10.1073/pnas.0902636106

O'Connell, R. M., Rao, D. S. & Baltimore, D. (2012). microRNA Regulation of Inflammatory Responses. *Annual Review of Immunology*, *30*(1), 295–312. https://doi.org/10.1146/annurev-immunol-020711-075013

Odegaard, J. I., Ricardo-Gonzalez, R. R., Eagle, A. R., Vats, D., Morel, C. R., Goforth, M. H., Subramanian, V., Mukundan, L., Ferrante, A. W. & Chawla, A. (2008). Alternative M2 activation of Kupffer cells by PPARdelta ameliorates obesity-induced insulin resistance. *Cell Metabolism*, *7*(6), 496–507. https://doi.org/10.1016/j.cmet.2008.04.003

Odegaard, J. I., Ricardo-Gonzalez, R. R., Goforth, M. H., Morel, C. R., Subramanian, V., Mukundan, L., Eagle, A. R., Vats, D., Brombacher, F., Ferrante, A. W. & Chawla, A. (2007). Macrophage-specific PPARgamma controls alternative activation and improves insulin resistance. *Nature …*, *447*(7148), 1116–1120. https://doi.org/10.1038/nature05894

Oishi, Y., Spann, N. J., Link, V. M., Muse, E. D., Strid, T., Edillor, C., Kolar, M. J., Matsuzaka, T., Hayakawa, S., Tao, J., Kaikkonen, M. U., Carlin, A. F., Lam, M. T., Manabe, I., Shimano, H., Saghatelian, A. & Glass, C. K. (2017). SREBP1 Contributes to Resolution of Pro-inflammatory TLR4 Signaling by Reprogramming Fatty Acid Metabolism. *Cell Metabolism*, *25*(2), 412–427. https://doi.org/10.1016/j.cmet.2016.11.009

Org, E., Parks, B. W., Joo, J. W. J., Emert, B., Schwartzman, W., Kang, E. Y., Mehrabian, M., Pan, C., Knight, R., Gunsalus, R., Drake, T. A., Eskin, E. & Lusis, A. J. (2015). Genetic and environmental control of host-gut microbiota interactions. *Genome Research*, *25*(10), 1558–1569. https://doi.org/10.1101/gr.194118.115

Ozcan, L., Ergin, A. S., Lu, A., Chung, J., Sarkar, S., Nie, D., Myers, M. G. & Ozcan, U. (2009). Endoplasmic Reticulum Stress Plays a Central Role in Development of Leptin Resistance. *Cell Metabolism*, *9*(1), 35–51. https://doi.org/10.1016/j.cmet.2008.12.004

Pamir, N., Pan, C., Plubell, D. L., Hutchins, P. M., Tang, C., Wimberger, J., Irwin, A., Vallim, T. Q. de A., Heinecke, J. W. & Lusis, A. J. (2019). Genetic control of the mouse HDL proteome defines HDL traits, function, and heterogeneity[S]. *Journal of Lipid Research*, *60*(3), 594–608. https://doi.org/10.1194/jlr.m090555

Park, H., Shima, T., Yamaguchi, K., Mitsuyoshi, H., Minami, M., Yasui, K., Itoh, Y., Yoshikawa, T., Fukui, M., Hasegawa, G., Nakamura, N., Ohta, M., Obayashi, H. & Okanoue, T. (2011). Efficacy of long-term ezetimibe therapy in patients with nonalcoholic fatty liver disease. *Journal of Gastroenterology*, *46*(1), 101–107. https://doi.org/10.1007/s00535-010-0291-8

Parrow, N. L. & Fleming, R. E. (2017). Liver sinusoidal endothelial cells as iron sensors. *Blood*, *129*(4), 397–398. https://doi.org/10.1182/blood-2016-12-754499

Peake, K., Manning, J., Lewis, C.-A., Barr, C., Rossi, F. & Krieger, C. (2015). Busulfan as a Myelosuppressive Agent for Generating Stable High-level Bone Marrow Chimerism in Mice. *Journal of Visualized Experiments*, *98*, e52553. https://doi.org/10.3791/52553

Peet, D. J., Turley, S. D., Ma, W., Janowski, B. A., Lobaccaro, J. M., Hammer, R. E. & Mangelsdorf, D. J. (1998). Cholesterol and bile acid metabolism are impaired in mice lacking the nuclear oxysterol receptor LXR alpha. *Cell*, *93*(5), 693–704.

Perdiguero, E. G., Klapproth, K., Schulz, C., Busch, K., Azzoni, E., Crozet, L., Garner, H., Trouillet, C., Bruijn, M. F. de, Geissmann, F. & Rodewald, H.-R. (2015). Tissue-resident macrophages originate from yolk-sac-derived erythro-myeloid progenitors. *Nature*, *518*(7540), 547–551. https://doi.org/10.1038/nature13989

Pham, T.-H., Minderjahn, J., Schmidl, C., Hoffmeister, H., Schmidhofer, S., Chen, W., Längst, G., Benner, C. & Rehli, M. (2013). Mechanisms of in vivo binding site selection of the hematopoietic master transcription factor PU.1. *Nucleic Acids Research*, *41*(13), 6391–6402. https://doi.org/10.1093/nar/gkt355

Ramachandran, P., Dobie, R., Wilson-Kanamori, J. R., Dora, E. F., Henderson, B. E. P., Luu, N. T., Portman, J. R., Matchett, K. P., Brice, M., Marwick, J. A., Taylor, R. S., Efremova, M., Vento-Tormo, R., Carragher, N. O., Kendall, T. J., Fallowfield, J. A., Harrison, E. M., Mole, D. J., Wigmore, S. J., … Henderson, N. C. (2019). Resolving the fibrotic niche of human liver cirrhosis at single-cell level. *Nature …*, 1–1. https://doi.org/10.1038/s41586-019-1631-3

Ramón-Vázquez, A., Rosa, J. V. de la, Tabraue, C., Lopez, F., Díaz-Chico, B. N., Bosca, L., Tontonoz, P., Alemany, S. & Castrillo, A. (2019). Common and Differential Transcriptional Actions of Nuclear Receptors LXRα and LXRβ in macrophages. *Molecular and Cellular Biology*, 1–36. https://doi.org/10.1128/mcb.00376-18

Reid, D. T., Reyes, J. L., McDonald, B. A., Vo, T., Reimer, R. A. & Eksteen, B. (2016). Kupffer Cells Undergo Fundamental Changes during the Development of Experimental NASH and Are Critical in Initiating Liver Damage and Inflammation. *PLoS ONE*, *11*(7), e0159524. https://doi.org/10.1371/journal.pone.0159524

Remmerie, A., Martens, L., Thoné, T., Castoldi, A., Seurinck, R., Pavie, B., Roels, J., Vanneste, B., Prijck, S. D., Vanhockerhout, M., Latib, M. B. A., Devisscher, L., Hoorens, A., Bonnardel, J., Vandamme, N., Kremer, A., Borghgraef, P., Vlierberghe, H. V., Lippens, S., … Scott, C. L. (2020). Osteopontin Expression Identifies a Subset of Recruited Macrophages Distinct from Kupffer Cells in the Fatty Liver. *Immunity*. https://doi.org/10.1016/j.immuni.2020.08.004

Repa, J. J., Liang, G., Ou, J., Bashmakov, Y., Lobaccaro, J. M., Shimomura, I., Shan, B., Brown, M. S., Goldstein, J. L. & Mangelsdorf, D. J. (2000). Regulation of mouse sterol regulatory element-binding protein-1c gene (SREBP-1c) by oxysterol receptors, LXRalpha and LXRbeta. *Genes & Development*, *14*(22), 2819–2830. https://doi.org/10.1101/gad.844900

Repa, J. J., Turley, S. D., Lobaccaro, J. M. A., Medina, J., Li, L., Lustig, K., Shan, B., Heyman, R. A., Dietschy, J. M. & Mangelsdorf, D. J. (2000). Regulation of Absorption and ABC1-Mediated Efflux of Cholesterol by RXR Heterodimers. *Science*, *289*(5484), 1524–1529. https://doi.org/10.1126/science.289.5484.1524

Ricote, M., Li, A. C., Willson, T. M., Kelly, C. J. & Glass, C. K. (1998). The peroxisome proliferator-activated receptor-gamma is a negative regulator of macrophage activation. *Nature …*, *391*(6662), 79–82. https://doi.org/10.1038/34178

Riek, A. E., Oh, J., Sprague, J. E., Timpson, A., Fuentes, L. de las, Bernal-Mizrachi, L., Schechtman, K. B. & Bernal-Mizrachi, C. (2012). Vitamin D Suppression of Endoplasmic Reticulum Stress Promotes an Antiatherogenic Monocyte/Macrophage Phenotype in Type 2 Diabetic Patients. *Journal of Biological Chemistry*, *287*(46), 38482–38494. https://doi.org/10.1074/jbc.m112.386912

Rong, X., Albert, C. J., Hong, C., Duerr, M. A., Chamberlain, B. T., Tarling, E. J., Ito, A., Gao, J., Wang, B., Edwards, P. A., Jung, M. E., Ford, D. A. & Tontonoz, P. (2013). LXRs regulate ER stress and inflammation through dynamic modulation of membrane phospholipid composition. *Cell Metabolism*, *18*(5), 685–697. https://doi.org/10.1016/j.cmet.2013.10.002

Sakai, M., Matsumoto, M., Tujimura, T., Yongheng, C., Noguchi, T., Inagaki, K., Inoue, H., Hosooka, T., Takazawa, K., Kido, Y., Yasuda, K., Hiramatsu, R., Matsuki, Y. & Kasuga, M. (2012). CITED2 links hormonal signaling to PGC-1α acetylation in the regulation of gluconeogenesis. *Nature Medicine*, *18*(4), 612–617. https://doi.org/10.1038/nm.2691

Sakai, M., Troutman, T. D., Seidman, J. S., Ouyang, Z., Spann, N. J., Abe, Y., Ego, K. M., Bruni, C. M., Deng, Z., Schlachetzki, J. C. M., Nott, A., Bennett, H., Chang, J., Vu, B. T., Pasillas, M. P., Link, V. M., Texari, L., Heinz, S., Thompson, B. M., … Glass, C. K. (2019). Liver-Derived Signals Sequentially Reprogram Myeloid Enhancers to Initiate and Maintain Kupffer Cell Identity. *Immunity*, *51*(4), 655-670.e8. https://doi.org/10.1016/j.immuni.2019.09.002

Sallam, T., Jones, M., Thomas, B. J., Wu, X., Gilliland, T., Qian, K., Eskin, A., Casero, D., Zhang, Z., Sandhu, J., Salisbury, D., Rajbhandari, P., Civelek, M., Hong, C., Ito, A., Liu, X., Daniel, B., Lusis, A. J., Whitelegge, J., … Tontonoz, P. (2018). Transcriptional regulation of macrophage cholesterol efflux and atherogenesis by a long noncoding RNA. *Nature Medicine*. https://doi.org/10.1038/nm.4479

Sanyal, A. J., Chalasani, N., Kowdley, K. V., McCullough, A., Diehl, A. M., Bass, N. M., Neuschwander-Tetri, B. A., Lavine, J. E., Tonascia, J., Unalp, A., Natta, M. V., Clark, J., Brunt, E. M., Kleiner, D. E., Hoofnagle, J. H. & Robuck, P. R. (2010). Pioglitazone, Vitamin E, or Placebo for Nonalcoholic Steatohepatitis. *The New England Journal of Medicine*, *362*(18), 1675–1685. https://doi.org/10.1056/nejmoa0907929

Sanyal, A. J., Harrison, S. A., Ratziu, V., Abdelmalek, M. F., Diehl, A. M., Caldwell, S., Shiffman, M. L., Schall, R. A., Jia, C., McColgan, B., Djedjos, C. S., McHutchison, J. G., Subramanian, G. M., Myers, R. P., Younossi, Z., Muir, A. J., Afdhal, N. H., Bosch, J. & Goodman, Z. (2019). The Natural History of Advanced Fibrosis Due to Nonalcoholic

Steatohepatitis: Data From the Simtuzumab Trials. *Hepatology*, *70*(6), 1913–1927. https://doi.org/10.1002/hep.30664

Schnabl, B. (2013). Linking intestinal homeostasis and liver disease. *Current Opinion in Gastroenterology*, *29*(3), 264–270. https://doi.org/10.1097/mog.0b013e32835ff948

Scott, C. L. & Guilliams, M. (2018). The role of Kupffer cells in hepatic iron and lipid metabolism. *Journal of Hepatology*, *69*(5), 1197–1199. https://doi.org/10.1016/j.jhep.2018.02.013

Scott, C. L., T'Jonck, W., Martens, L., Todorov, H., Sichien, D., Soen, B., Bonnardel, J., Prijck, S. D., Vandamme, N., Cannoodt, R., Saelens, W., Vanneste, B., Toussaint, W., Bleser, P. D., Takahashi, N., Vandenabeele, P., Henri, S., Pridans, C., Hume, D. A., … Guilliams, M. (2018). The Transcription Factor ZEB2 Is Required to Maintain the Tissue-Specific Identities of Macrophages. *Immunity*, *49*(2), 312-325.e5. https://doi.org/10.1016/j.immuni.2018.07.004

Scott, C. L., Zheng, F., Baetselier, P. D., Martens, L., Saeys, Y., Prijck, S. D., Lippens, S., Abels, C., Schoonooghe, S., Raes, G., Devoogdt, N., Lambrecht, B. N., Beschin, A. & Guilliams, M. (2016). Bone marrow-derived monocytes give rise to self-renewing and fully differentiated Kupffer cells. *Nature Communications*, *7*(1), 10321. https://doi.org/10.1038/ncomms10321

Seidman, J. S., Troutman, T. D., Sakai, M., Gola, A., Spann, N. J., Bennett, H., Bruni, C. M., Ouyang, Z., Li, R. Z., Sun, X., Vu, B. T., Pasillas, M. P., Ego, K. M., Gosselin, D., Link, V. M., Chong, L.-W., Evans, R. M., Thompson, B. M., McDonald, J. G., … Glass, C. K. (2020). Niche-Specific Reprogramming of Epigenetic Landscapes Drives Myeloid Cell Diversity in Nonalcoholic Steatohepatitis. *Immunity*. https://doi.org/10.1016/j.immuni.2020.04.001

Shen, Z., Hoeksema, M. A., Ouyang, Z., Benner, C. & Glass, C. K. (2020). MAGGIE: leveraging genetic variation to identify DNA sequence motifs mediating transcription factor binding and function. *Bioinformatics*, *36*(Supplement_1), i84–i92. https://doi.org/10.1093/bioinformatics/btaa476

Shrikumar, A., Greenside, P. & Kundaje, A. (2017). Learning Important Features Through Propagating Activation Differences. *ArXiv*.

Signor, S. A. & Nuzhdin, S. V. (2018). The Evolution of Gene Expression in cis and trans. *Trends in Genetics*, *34*(7), 532–544. https://doi.org/10.1016/j.tig.2018.03.007

Smale, S. T., Tarakhovsky, A. & Natoli, G. (2014). Chromatin Contributions to the Regulation of Innate Immunity. *Annual Review of Immunology*, *32*(1), 489–511. https://doi.org/10.1146/annurev-immunol-031210-101303

Soccio, R. E., Chen, E. R., Rajapurkar, S. R., Safabakhsh, P., Marinis, J. M., Dispirito, J. R., Emmett, M. J., Briggs, E. R., Fang, B., Everett, L. J., Lim, H.-W., Won, K.-J., Steger, D. J., Wu, Y., Civelek, M., Voight, B. F. & Lazar, M. A. (2015). Genetic Variation Determines

PPARγ Function and Anti-diabetic Drug Response In Vivo. *Cell*, *162*(1), 33–44. https://doi.org/10.1016/j.cell.2015.06.025

Song, K., Kwon, H., Han, C., Chen, W., Zhang, J., Ma, W., Dash, S., Gandhi, C. R. & Wu, T. (2019). YAP in Kupffer cells enhances the production of pro-inflammatory cytokines and promotes the development of non-alcoholic steatohepatitis. *Hepatology*. https://doi.org/10.1002/hep.30990

Spann, N. J., Garmire, L. X., McDonald, J. G., Myers, D. S., Milne, S. B., Shibata, N., Reichart, D., Fox, J. N., Shaked, I., Heudobler, D., Raetz, C. R. H., Wang, E. W., Kelly, S. L., Sullards, M. C., Murphy, R. C., Jr., A. H. M., Brown, H. A., Dennis, E. A., Li, A. C., … Glass, C. K. (2012). Regulated Accumulation of Desmosterol Integrates Macrophage Lipid Metabolism and Inflammatory Responses. *Cell*, *151*(1), 138–152. https://doi.org/10.1016/j.cell.2012.06.054

Stienstra, R., Saudale, F., Duval, C., Keshtkar, S., Groener, J. E. M., Rooijen, N. van, Staels, B., Kersten, S. & Müller, M. (2010). Kupffer cells promote hepatic steatosis via interleukin-1beta-dependent suppression of peroxisome proliferator-activated receptor alpha activity. *Hepatology*, *51*(2), 511–522. https://doi.org/10.1002/hep.23337

Sun, C., Liu, X., Yi, Z., Xiao, X., Yang, M., Hu, G., Liu, H., Liao, L. & Huang, F. (2015). Genome-wide analysis of long noncoding RNA expression profiles in patients with non-alcoholic fatty liver disease. *IUBMB Life*, *67*(11), 847–852. https://doi.org/10.1002/iub.1442

Sun, D., Sun, P., Li, H., Zhang, M., Liu, G., Strickland, A. B., Chen, Y., Fu, Y., Xu, J., Yosri, M., Nan, Y., Zhou, H., Zhang, X. & Shi, M. (2019). Fungal dissemination is limited by liver macrophage filtration of the blood. *Nature Communications*, *10*(1), 4566. https://doi.org/10.1038/s41467-019-12381-5

Szabo, G. & Satishchandran, A. (2015). MicroRNAs in Alcoholic Liver Disease. *Seminars in Liver Disease*, *35*(01), 036–042. https://doi.org/10.1055/s-0034-1397347

Szyf, M. (2009). Epigenetics, DNA Methylation, and Chromatin Modifying Drugs. *Annual Review of Pharmacology and Toxicology*, *49*(1), 243–263. https://doi.org/10.1146/annurev-pharmtox-061008-103102

Takeshita, Y., Takamura, T., Honda, M., Kita, Y., Zen, Y., Kato, K., Misu, H., Ota, T., Nakamura, M., Yamada, K., Sunagozaka, H., Arai, K., Yamashita, T., Mizukoshi, E. & Kaneko, S. (2014). The effects of ezetimibe on non-alcoholic fatty liver disease and glucose metabolism: a randomised controlled trial. *Diabetologia*, *57*(5), 878–890. https://doi.org/10.1007/s00125-013-3149-9

Tall, A. R. & Yvan-Charvet, L. (2015). Cholesterol, inflammation and innate immunity. *Nature Reviews Immunology*, *15*(2), 104–116. https://doi.org/10.1038/nri3793

Texari, L., Spann, N. J., Troutman, T. D., Sakai, M., Seidman, J. S. & Heinz, S. (2021). An optimized protocol for rapid, sensitive and robust on-bead ChIP-seq from primary cells. *STAR Protocols*, *2*(1), 100358. https://doi.org/10.1016/j.xpro.2021.100358

Theurl, I., Hilgendorf, I., Nairz, M., Tymoszuk, P., Haschka, D., Asshoff, M., He, S., Gerhardt, L. M. S., Holderried, T. A. W., Seifert, M., Sopper, S., Fenn, A. M., Anzai, A., Rattik, S., McAlpine, C., Theurl, M., Wieghofer, P., Iwamoto, Y., Weber, G. F., … Swirski, F. K. (2016). On-demand erythrocyte disposal and iron recycling requires transient macrophages in the liver. *Nature Medicine*, *22*(8), 945–951. https://doi.org/10.1038/nm.4146

Thomas, G. D., Hanna, R. N., Vasudevan, N. T., Hamers, A. A., Romanoski, C. E., McArdle, S., Ross, K. D., Blatchley, A., Yoakum, D., Hamilton, B. A., Mikulski, Z., Jain, M. K., Glass, C. K. & Hedrick, C. C. (2016). Deleting an Nr4a1 Super-Enhancer Subdomain Ablates Ly6Clow Monocytes while Preserving Macrophage Gene Function. *Immunity*, *45*(5), 975–987. https://doi.org/10.1016/j.immuni.2016.10.011

Tirosh, I., Reikhav, S., Levy, A. A. & Barkai, N. (2009). A Yeast Hybrid Provides Insight into the Evolution of Gene Expression Regulation. *Science*, *324*(5927), 659–662. https://doi.org/10.1126/science.1169766

Tosello-Trampont, A.-C., Landes, S. G., Nguyen, V., Novobrantseva, T. I. & Hahn, Y. S. (2012). Kuppfer cells trigger nonalcoholic steatohepatitis development in diet-induced mouse model through tumor necrosis factor-α production. *The Journal of Biological Chemistry*, *287*(48), 40161–40172. https://doi.org/10.1074/jbc.m112.417014

Tran, S., Baba, I., Poupel, L., Dussaud, S., Moreau, M., Gélineau, A., Marcelin, G., Magréau-Davy, E., Ouhachi, M., Lesnik, P., Boissonnas, A., Goff, W. L., Clausen, B. E., Yvan-Charvet, L., Sennlaub, F., Huby, T. & Gautier, E. L. (2020). Impaired Kupffer Cell Self-Renewal Alters the Liver Response to Lipid Overload during Non-alcoholic Steatohepatitis. *Immunity*. https://doi.org/10.1016/j.immuni.2020.06.003

Troutman, T. D., Bennett, H., Sakai, M., Seidman, J. S., Heinz, S. & Glass, C. K. (2021). Purification of mouse hepatic non-parenchymal cells or nuclei for use in ChIP-seq and other next-generation sequencing approaches. *STAR Protocols*, *2*(1), 100363. https://doi.org/10.1016/j.xpro.2021.100363

Veeken, J. van der, Glasner, A., Zhong, Y., Hu, W., Wang, Z.-M., Bou-Puerto, R., Charbonnier, L.-M., Chatila, T. A., Leslie, C. S. & Rudensky, A. Y. (2020). The Transcription Factor Foxp3 Shapes Regulatory T Cell Identity by Tuning the Activity of trans-Acting Intermediaries. *Immunity*, *53*(5), 971-984.e5. https://doi.org/10.1016/j.immuni.2020.10.010

Veeken, J. van der, Zhong, Y., Sharma, R., Mazutis, L., Dao, P., Pe'er, D., Leslie, C. S. & Rudensky, A. Y. (2019). Natural Genetic Variation Reveals Key Features of Epigenetic and Transcriptional Memory in Virus-Specific CD8 T Cells. *Immunity*, *50*(5), 1202-1217.e7. https://doi.org/10.1016/j.immuni.2019.03.031

Venkateswaran, A., Laffitte, B. A., Joseph, S. B., Mak, P. A., Wilpitz, D. C., Edwards, P. A. & Tontonoz, P. (2000). Control of cellular cholesterol efflux by the nuclear oxysterol receptor LXR alpha. *Proceedings of the National Academy of Sciences*, *97*(22), 12097–12102. https://doi.org/10.1073/pnas.200367697

Vierbuchen, T., Ling, E., Cowley, C. J., Couch, C. H., Wang, X., Harmin, D. A., Roberts, C. W. M. & Greenberg, M. E. (2017). AP-1 Transcription Factors and the BAF Complex Mediate Signal-Dependent Enhancer Selection. *Molecular Cell*, *68*(6), 1067-1082.e12. https://doi.org/10.1016/j.molcel.2017.11.026

Wang, K. C. & Chang, H. Y. (2011). Molecular Mechanisms of Long Noncoding RNAs. *Molecular Cell*, *43*(6), 904–914. https://doi.org/10.1016/j.molcel.2011.08.018

Wang, Xiaobo, Cai, B., Yang, X., Sonubi, O. O., Zheng, Z., Ramakrishnan, R., Shi, H., Valenti, L., Pajvani, U. B., Sandhu, J., Infante, R. E., Radhakrishnan, A., Covey, D. F., Guan, K.-L., Buck, J., Levin, L. R., Tontonoz, P., Schwabe, R. F. & Tabas, I. (2020). Cholesterol Stabilizes TAZ in Hepatocytes to Promote Experimental Non-alcoholic Steatohepatitis. *Cell Metabolism*. https://doi.org/10.1016/j.cmet.2020.03.010

Wang, Xiaobo, Zheng, Z., Caviglia, J. M., Corey, K. E., Herfel, T. M., Cai, B., Masia, R., Chung, R. T., Lefkowitch, J. H., Schwabe, R. F. & Tabas, I. (2016). Hepatocyte TAZ/WWTR1 Promotes Inflammation and Fibrosis in Nonalcoholic Steatohepatitis. *Cell Metabolism*, *24*(6), 848–862. https://doi.org/10.1016/j.cmet.2016.09.016

Wang, Xue, Sun, W., Shen, W., Xia, M., Chen, C., Xiang, D., Ning, B., Cui, X., Li, H., Li, X., Ding, J. & Wang, H. (2016). Long non-coding RNA DILC regulates liver cancer stem cells via IL-6/STAT3 axis. *Journal of Hepatology*, *64*(6), 1283–1294. https://doi.org/10.1016/j.jhep.2016.01.019

Wang, Y. Y., Dahle, M. K., Steffensen, K. R., Reinholt, F. P., Collins, J. L., Thiemermann, C., Aasen, A. O., Gustafsson, J.-Å. & Wang, J. E. (2009). LIVER X RECEPTOR AGONIST GW3965 DOSE-DEPENDENTLY REGULATES LPS-MEDIATED LIVER INJURY AND MODULATES POSTTRANSCRIPTIONAL TNF-&agr; PRODUCTION AND P38 MITOGEN-ACTIVATED PROTEIN KINASE ACTIVATION IN LIVER MACROPHAGES. *Shock*, *32*(5), 548–553. https://doi.org/10.1097/shk.0b013e3181a47f85

Wankhade, U. D., Zhong, Y., Kang, P., Alfaro, M., Chintapalli, S. V., Thakali, K. M. & Shankar, K. (2017). Enhanced offspring predisposition to steatohepatitis with maternal high-fat diet is associated with epigenetic and microbiome alterations. *PLOS ONE*, *12*(4), e0175675. https://doi.org/10.1371/journal.pone.0175675

Watanabe, H., Numata, K., Ito, T., Takagi, K. & Matsukawa, A. (2004). Innate immune response in Th1- and Th2-dominant mouse strains. *Shock*, *22*(5), 460–466. https://doi.org/10.1097/01.shk.0000142249.08135.e9

Willy, P. J., Umesono, K., Ong, E. S., Evans, R. M., Heyman, R. A. & Mangelsdorf, D. J. (1995). LXR, a nuclear receptor that defines a distinct retinoid response pathway. *Genes & Development*, *9*(9), 1033–1045.

Xiong, X., Kuang, H., Ansari, S., Liu, T., Gong, J., Wang, S., Zhao, X.-Y., Ji, Y., Li, C., Guo, L., Zhou, L., Chen, Z., Leon-Mimila, P., Chung, M. T., Kurabayashi, K., Opp, J., Campos-Pérez, F., Villamil-Ramírez, H., Canizales-Quinteros, S., … Lin, J. D. (2019). Landscape of

Intercellular Crosstalk in Healthy and NASH Liver Revealed by Single-Cell Secretome Gene Analysis. *Molecular Cell*, *75*(3), 644-660.e5. https://doi.org/10.1016/j.molcel.2019.07.028

Yamanishi, K., Maeda, S., Kuwahara-Otani, S., Watanabe, Y., Yoshida, M., Ikubo, K., Okuzaki, D., El-Darawish, Y., Li, W., Nakasho, K., Nojima, H., Yamanishi, H., Hayakawa, T., Okamura, H. & Matsunaga, H. (2016). Interleukin-18–deficient mice develop dyslipidemia resulting in nonalcoholic fatty liver disease and steatohepatitis. *Translational Research*, *173*, 101-114.e7. https://doi.org/10.1016/j.trsl.2016.03.010

Yáñez-Cuna, J. O., Dinh, H. Q., Kvon, E. Z., Shlyueva, D. & Stark, A. (2012). Uncovering cis-regulatory sequence requirements for context-specific transcription factor binding. *Genome Research*, *22*(10), 2018–2030. https://doi.org/10.1101/gr.132811.111

Yang, C., McDonald, J. G., Patel, A., Zhang, Y., Umetani, M., Xu, F., Westover, E. J., Covey, D. F., Mangelsdorf, D. J., Cohen, J. C. & Hobbs, H. H. (2006). Sterol intermediates from cholesterol biosynthetic pathway as liver X receptor ligands. *The Journal of Biological Chemistry*, *281*(38), 27816–27826. https://doi.org/10.1074/jbc.m603781200

Yang, H. S., Onos, K. D., Choi, K., Keezer, K. J., Skelly, D. A., Carter, G. W. & Howell, G. R. (2021). Natural genetic variation determines microglia heterogeneity in wild-derived mouse models of Alzheimer's disease. *Cell Reports*, *34*(6), 108739. https://doi.org/10.1016/j.celrep.2021.108739

Yu, S., Li, S., Henke, A., Muse, E. D., Cheng, B., Welzel, G., Chatterjee, A. K., Wang, D., Roland, J., Glass, C. K. & Tremblay, M. (2016). Dissociated sterol-based liver X receptor agonists as therapeutics for chronic inflammatory diseases. *FASEB Journal : Official Publication of the Federation of American Societies for Experimental Biology*, *30*(7), 2570–2579. https://doi.org/10.1096/fj.201600244r

Zhang, Y., Leung, D. Y. M., Richers, B. N., Liu, Y., Remigio, L. K., Riches, D. W. & Goleva, E. (2012). Vitamin D Inhibits Monocyte/Macrophage Proinflammatory Cytokine Production by Targeting MAPK Phosphatase-1. *The Journal of Immunology*, *188*(5), 2127–2135. https://doi.org/10.4049/jimmunol.1102412

Zheng, A., Lamkin, M., Wu, C., Su, H. & Gymrek, M. (2020). Deep neural networks identify context-specific determinants of transcription factor binding affinity. *BioRxiv*, 2020.02.26.965343. https://doi.org/10.1101/2020.02.26.965343

Zhou, J. & Troyanskaya, O. G. (2015). Predicting effects of noncoding variants with deep learning-based sequence model. *Nature Methods*, *12*(10), 931–934. https://doi.org/10.1038/nmeth.3547

Zhou, T., Sun, Y., Li, M., Ding, Y., Yin, R., Li, Z., Xie, Q., Bao, S. & Cai, W. (2018). Enhancer of zeste homolog 2-catalysed H3K27 trimethylation plays a key role in acute-on-chronic liver failure via TNF-mediated pathway. *Cell Death & Disease*, *9*(6), 590. https://doi.org/10.1038/s41419-018-0670-2

Zhou, V. W., Goren, A. & Bernstein, B. E. (2011). Charting histone modifications and the functional organization of mammalian genomes. *Nature Reviews Genetics*, *12*(1), 7–18. https://doi.org/10.1038/nrg2905

Zhou, Ying, Dong, B., Kim, K. H., Choi, S., Sun, Z., Wu, N., Wu, Y., Scott, J. & Moore, D. D. (2019). Vitamin D receptor activation in liver macrophages protects against hepatic endoplasmic reticulum stress in mice. *Hepatology*, hep.30887. https://doi.org/10.1002/hep.30887

Zhou, Yingyao, Zhou, B., Pache, L., Chang, M., Khodabakhshi, A. H., Tanaseichuk, O., Benner, C. & Chanda, S. K. (2019). Metascape provides a biologist-oriented resource for the analysis of systems-level datasets. *Nature Communications*, *10*(1), 1523. https://doi.org/10.1038/s41467-019-09234-6